

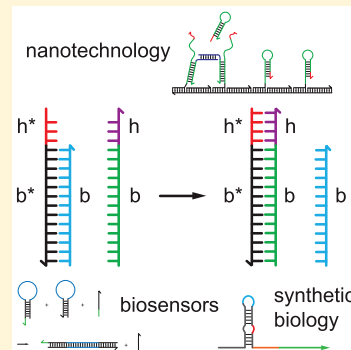
Principles and Applications of Nucleic Acid Strand Displacement Reactions

Friedrich C. Simmel,^{*,†} Bernard Yurke,^{*,‡} and Hari R. Singh[†]

[†]Physics Department, TU München, 85748 Garching, Germany

[‡]Micron School of Materials Science and Engineering, Boise State University, Boise, ID 83725, United States

ABSTRACT: Dynamic DNA nanotechnology, a subfield of DNA nanotechnology, is concerned with the study and application of nucleic acid strand-displacement reactions. Strand-displacement reactions generally proceed by three-way or four-way branch migration and initially were investigated for their relevance to genetic recombination. Through the use of toeholds, which are single-stranded segments of DNA to which an invader strand can bind to initiate branch migration, the rate with which strand displacement reactions proceed can be varied by more than 6 orders of magnitude. In addition, the use of toeholds enables the construction of enzyme-free DNA reaction networks exhibiting complex dynamical behavior. A demonstration of this was provided in the year 2000, in which strand displacement reactions were employed to drive a DNA-based nanomachine (Yurke, B.; et al. *Nature* **2000**, *406*, 605–608). Since then, toehold-mediated strand displacement reactions have been used with ever increasing sophistication and the field of dynamic DNA nanotechnology has grown exponentially. Besides molecular machines, the field has produced enzyme-free catalytic systems, all DNA chemical oscillators and the most complex molecular computers yet devised. Enzyme-free catalytic systems can function as chemical amplifiers and as such have received considerable attention for sensing and detection applications in chemistry and medical diagnostics. Strand-displacement reactions have been combined with other enzymatically driven processes and have also been employed within living cells (Groves, B.; et al. *Nat. Nanotechnol.* **2015**, *11*, 287–294). Strand-displacement principles have also been applied in synthetic biology to enable artificial gene regulation and computation in bacteria. Given the enormous progress of dynamic DNA nanotechnology over the past years, the field now seems poised for practical application.



CONTENTS

1. Introduction
2. Physical Chemistry of Strand Displacement Reactions
 - 2.1. Hybridization Reactions
 - 2.2. Toehold-Mediated Strand-Displacement Reactions
 - 2.2.1. Spontaneous Strand-Displacement Reactions
 - 2.2.2. Toehold-Mediated Strand-Displacement Reactions with Three-Way Branch Migration
 - 2.2.3. Toehold-Mediated Strand-Displacement Reactions with Four-Way Branch Migration
 - 2.3. Thermodynamic Driving Forces
 - 2.3.1. Configuration-Entropy Driven Reactions
 - 2.3.2. Concentration Imbalance Driven Reactions
 - 2.4. Finite-State Machines and Hybridization Motors
 - 2.5. DNA Hybridization Mechanochemistry
3. Catalytic Processes Based on Strand Displacement
 - 3.1. Hybridization Catalysts

B	3.2. Hairpin Toeholds <ol style="list-style-type: none"> 3.2.1. Hybridization Chain Reaction and Hybridization Polymerization 3.2.2. Hairpin Fuels and Catalytic Hairpin Assembly 	I
C	3.3. Other Tools within the Dynamic DNA Toolbox	K
D	4. Applications in DNA Nanotechnology <ol style="list-style-type: none"> 4.1. DNA Fuel for Nanomachines <ol style="list-style-type: none"> 4.1.1. DNA-Based Molecular Switches and Devices 4.1.2. Molecular Walkers 4.1.3. Mechanically Interlocked Molecules 4.2. Switchable and Reconfigurable Assembly of Nanomaterials <ol style="list-style-type: none"> 4.2.1. Reconfigurable Assembly of DNA Nanostructures 4.2.2. Reversible Assembly of Metallic Nanoparticles 4.2.3. Reversible Assembly of Biomolecules 4.2.4. DNA Switchable Gels 	K
E		L
F		N
G		O
H		O
		P
		Q

Special Issue: Nucleic Acid Nanotechnology

Received: September 21, 2018

4.2.5. Control of Chemical Synthesis	R
4.2.6. Other Reconfigurable Structures	R
4.3. Origami-Based Nanomechanical Devices	R
4.4. Switchable Cages and Containers	S
4.4.1. Actuation of Origami Containers via Strand Displacement	T
4.4.2. Other Types of DNA Containers	T
4.5. Localized Strand Displacement Cascades on DNA Origami Platforms	T
4.6. Patterning and Lithography	V
4.6.1. Biocompatible Lithography Using DNA Strand Displacement	V
4.6.2. Pattern Formation	V
4.7. Super-Resolution Imaging and DNA-PAINT	W
4.8. Challenges and Future Directions for Dynamic DNA Nanotechnology	W
4.8.1. Speed	W
4.8.2. DNA as a Fuel	W
4.8.3. Future Directions	X
5. Applications in Sensing, Diagnostics, and Therapeutics	X
5.1. Sensing Based on the Hybridization Chain Reaction	X
5.1.1. In Situ Detection of mRNA Using HCR	X
5.1.2. Other Bioanalytical Applications of HCR	Y
5.2. Biosensors Based on Catalytic Hairpin Assembly	Y
5.2.1. Reaction Cascades and Networks Based on Catalytic Hairpin Assembly	Z
5.3. Other Sensor Schemes Based on Toehold-Mediated Strand Displacement	Z
5.3.1. DNA and RNA Detection	Z
5.3.2. Protein Detection	AA
5.3.3. Sensing of Small Molecules and Ions	AA
5.4. Autonomous Diagnosis and Therapy	AB
5.5. Challenges and Future Directions for Biosensors Based on Strand Displacement	AC
6. Applications in Synthetic Biology	AC
6.1. Synthetic Riboregulators	AC
6.1.1. First Generation Riboregulators	AD
6.1.2. Toehold Riboregulators	AD
6.1.3. Translational Inhibitors and the YUNR Motif	AE
6.2. Combining Strand Invasion with CRISPR Mechanisms	AF
6.3. Molecular Assembly and Computing via Strand Displacement in Mammalian Cells	AF
6.4. Future Applications at the Interface of Dynamic DNA Nanotechnology and Synthetic Biology	AG
7. Conclusion	AG
Author Information	AG
Corresponding Authors	AG
ORCID	AG
Notes	AG
Biographies	AG
Acknowledgments	AG
References	AG

1. INTRODUCTION

In biological organisms, DNA's chief function is to serve as a read-only memory whose information content is transcribed

into RNA before this information is used to orchestrate life's functions through the synthesis of protein and RNA-based molecular machines. During cell division a specialized subset of these molecular machines manufacture copies of the DNA through template replication, thereby enabling each of the daughter cells to possess a copy of the read-only memory. In spite of its specialized function in biological organisms as an information storage medium, like wood, hide, and bone, DNA has proven to be a versatile biomaterial with which humans can fashion objects of utility, but now at the nanometer scale. The field in which DNA is used in such an artificial manner is referred to as DNA nanotechnology,^{3–7} but as the term is commonly understood, also includes the construction of nanodevices and systems out of RNA and synthetic nucleic acid analogues.

Several physical properties of DNA contribute to its utility as a construction material. DNA's linear structure, its large combinatorial base sequence space,⁸ and Watson–Crick base-pairing enable the design of sets of oligomers that in aqueous solution spontaneously self-assemble into target structures. The stiffness of duplex DNA enables the assembly of rigid two- and three-dimensional structures.⁵ The nearly two-order-of-magnitude difference in stiffness between duplex DNA and single-stranded DNA facilitates the construction of nanodevices with movable parts¹ in which single-strand DNA functions as hinges or flexible tether between rigid elements. It also enables the construction of tensegrity structures in which single-stranded DNA functions as guy wires.⁹ The relative weakness of the supramolecular interactions involved in base-pairing enables hybridization and strand-displacement reactions, thereby providing a means to animate DNA nanostructures.¹

Automated synthesis of oligomers with a variety of modifications that include fluorescent labels and chemically reactive groups greatly facilitates the use of DNA as a construction material, as does the variety of biological or biologically derived enzymes that operate on DNA in specific ways.

DNA nanotechnology can be divided into several subdisciplines.¹⁰ One is structural DNA nanotechnology⁵ which is concerned primarily with the construction of static structures such as DNA origami and DNA brick structures. Another is dynamic DNA nanotechnology¹⁰ which is concerned with the construction of nanostructures that can be animated and with reaction networks based on DNA hybridization.

The focus of this review is on dynamic DNA nanotechnology, with an emphasis on “all-DNA systems” which are driven by hybridization and strand invasion reactions alone. However, there are other means by which motion can be induced in DNA systems. The first dynamic DNA device was driven by the B-Z transition of duplex DNA induced via a change of buffer composition.¹¹ Light-driven nanodevices have been created which employ photochromic molecules to induce conformational changes.¹² DNA systems have also been animated by employing protein¹³ or nucleic acid based¹⁴ enzymes to make or break covalent chemical bonds.

A synopsis of the history of dynamic DNA nanotechnology is provided here. Early work on DNA strand displacement reactions^{15–19} addressed physical chemistry aspects of these processes and their biological relevance, especially to genetic recombination. Interest in DNA strand displacement reactions greatly increased in 2000 with the publication by Yurke et al.,¹ demonstrating that toehold-mediated strand displacement

reactions could be used to cycle DNA nanostructures through a sequence of differing conformational states. This early work sought to emulate the function of biological motors in a polymer (i.e., DNA) that differed from that employed by biological organisms (i.e., protein) and thereby open a pathway for the construction of artificial molecular motors. The initial devices functioned more like stepper motors^{20–24} rather than autonomous motors such as kinesin, myosin, or dynein. To more closely emulate these biological molecular motors, metastable DNA nanostructures were devised that, in principle, could serve as fuel for autonomous DNA nanomachines in which the nanomachine, in the process of catalytically releasing the energy stored in the metastable fuel, performs work.^{25,26} With the demonstration of DNA systems in which metastable fuel is catalytically consumed, work in dynamic DNA nanotechnology¹⁰ diverged into three major directions: (i) the construction of DNA nanodevices^{27–29} and DNA responsive materials^{30–38} (ii) the construction of hybridization networks that could function as detector or sensor systems,^{39–44} and (iii) the construction of chemical reaction networks that can carry out analog or digital computation.^{45–48} This work has stimulated theoretical and computational efforts to better understand DNA hybridization and strand-displacement reactions^{49–51} and to develop design tools to aid in the design of dynamic DNA systems.^{46,47,52–56} DNA hybridization and strand displacement networks are often plagued by undesired leak reactions that limit system performance. A considerable amount of experimental and theoretical work has been devoted to finding means to eliminate or mitigate against these reactions.^{26,45,57–66} Dynamic DNA nanotechnology has seen the greatest amount of activity in research directed to the practical application in medical diagnostics^{67,68} and therapeutics,^{69–71} an area that appears especially attractive due to the biocompatibility and the ease with which nucleic acid based devices and systems can be interfaced with biological DNA and RNA. DNA hybridization networks, functioning as nucleic acid detectors, achieving attomolar^{72–75} and even subattomolar DNA detection sensitivity^{76–78} have recently been reported.

Here are listed a few of the other highlights of the field to convey a sense of what has been accomplished since the year 2000: (i) DNA walkers that walk on DNA substrates much as myosin motors walk on actin,^{78,80} (ii) nanofactories,^{81–83} (iii) oscillatory DNA reaction networks,⁴⁷ (iv) a DNA polymerization motor⁸⁴ that emulates the actin polymerization motor of *Listeria* bacteria, (v) polymerization reaction networks for biological labeling⁸⁵ and analyte detection,⁴⁰ (vi) strand-displacement systems operating in living cells,² and also (vii) chemical reaction networks, consisting of hundreds of DNA strands that carry out computational tasks.⁴⁸

Dynamic DNA nanotechnology has grown exponentially over the past years. For this reason, the authors of this article have found the task of reviewing the field quite daunting, and we certainly cannot claim that it is complete in any sense. We say little about logic gates and computing-network architectures. An early review providing insight into the development of the field has been given by Zhang and Seelig in 2011.¹⁰ More recent work in enzyme-free nucleic acid dynamical systems has been discussed by Srinivas et al.,⁴⁷ whereas the review by Bi, Yue, and Zhang⁴⁰ focuses on hybridization chain reactions and their application to biosensing, bioimaging, and biomedicine. A recent review focusing on the design of enzyme-free DNA reaction networks that carry out computation has been given by George and Singh.⁸⁶

We now proceed with a discussion of the physical chemistry of strand displacement reactions in order to describe the elemental reaction mechanisms employed in all-DNA dynamic DNA systems. Since sometimes the purpose of these reactions is to perform mechanical work, the mechanochemistry of DNA hybridization is also discussed. Then illustrations are presented of the assembly of these elemental processes into complex DNA-reaction networks including catalytic networks. This is followed by a survey of the major applications of dynamic DNA processes in nanotechnology, sensing, and synthetic biology.

2. PHYSICAL CHEMISTRY OF STRAND DISPLACEMENT REACTIONS

Three primitives for the construction of all-DNA reaction networks are hybridization reactions in which complementary sequences form duplex DNA, three-way branch migration reactions in which a DNA strand displaces one member of a DNA duplex, and four-way branch migration reactions in which two duplexes exchange DNA strands. Toeholds are typically short sections of single-stranded DNA that through a hybridization reaction initiates branch migration. Toeholds thereby provide a means to control the kinetics of strand displacement reactions. These primitives along with the thermodynamic forces that can be employed to drive reactions in the desired direction are now discussed.

2.1. Hybridization Reactions

Figure 1 is a schematic of a DNA hybridization reaction. The left-hand side shows two complementary DNA oligomers *S*

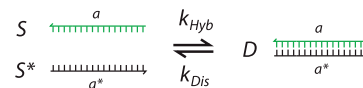


Figure 1. DNA hybridization and dissociation. In the hybridization reaction the complementary oligomers *S* and *S** having the base sequences *a* and *a** combine to form the duplex *D*. The forward and reverse rate constants are *k*_{hyb} and *k*_{dis}, respectively.

and *S**. The right-hand side shows the duplex *D* formed by hybridization. Such systems are often adequately modeled as a two state system where the DNA strands are either fully associated or fully dissociated. In this case, the forward reaction is second order and its rate constant is denoted *k*_{hyb}. The reverse reaction in which the duplex *D* spontaneously dissociates is first order, and its rate constant is denoted by *k*_{dis}. The equilibrium concentration of reactants and reaction products is determined by the equilibrium constant *K* given by

$$K = \frac{k_{\text{hyb}}}{k_{\text{dis}}} = \frac{[D]}{[S][S^*]} \quad (1)$$

which is related to the standard Gibbs free energy change ΔG° of the reaction via

$$K\Gamma = e^{-\Delta G^\circ/RT} \quad (2)$$

where Γ has the numerical value of 1 with units that make the left-hand side of the equation dimensionless. The free energy ΔG° and other thermodynamic quantities can be adequately calculated for a duplex of any base sequence using a nearest-neighbor model.⁸⁷ Due to the propensity for single-stranded DNA to form secondary structure the rate constants *k*_{hyb} and *k*_{dis} are much more difficult to predict. The rate constant *k*_{hyb}

can vary by orders of magnitude⁸⁸ and depends on temperature and buffer composition, but a value of $3 \times 10^6 \text{ M}^{-1} \text{ s}^{-1}$ is representative for oligomers with lengths of a few tens of nucleotides in commonly used hybridization buffers.^{89,90} For an oligomer concentration of 10 nM, which is typical of that employed in DNA nanotechnology, this rate constant yields an experimentally convenient time-to-half completion of ≈ 30 s. Recently a weighted neighbor voting prediction algorithm has been developed that is able to predict the hybridization rate constant k_{hyb} to within a factor of 3 with $\approx 91\%$ accuracy.⁸⁸ An intuitive sense of the value of k_{dis} and therefore a sense of the stability of duplex DNA for short oligomers is provided by data reported by Morrison and Stols.¹⁸ For the 10-mer they studied, k_{dis} was measured to be at $1.1 \times 10^{-2} \text{ s}^{-1}$ at 30.5°C in a 1 M NaCl/10 mM NaH₂PO₄ buffer. Extrapolating the data for their 20-mer to the same buffer conditions one finds for k_{dis} a value of $1 \times 10^{-10} \text{ s}^{-1}$. That is, the half-life for dissociation of the 10mer duplex is about a minute, while that of the 20-mer is about 300 years. Thus, with oligomers a few tens of bases long, DNA nanostructures can be assembled via DNA hybridization that are stable against dissociation on the time scale of a human lifetime.

2.2. Toehold-Mediated Strand-Displacement Reactions

2.2.1. Spontaneous Strand-Displacement Reactions.

Figure 2 illustrates a DNA exchange reaction in which one

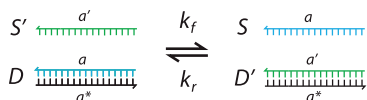


Figure 2. DNA strand-displacement reaction in which, in the forward reaction, strand S' displaces from the duplex D the member a which becomes the free strand S. Base sequences *a* and *a'* are identical but have been denoted differently to aid visualization of the exchange process. Base sequence *a** is complementary to *a*.

member of a duplex strand *D* trades partners *S* and *S'*. Although the base sequences of *S* and *S'* are identical in this example, the DNA strands could carry labels allowing them to be distinguished. Access of *S'* to the complementary strand in *D* is blocked by the complementary partner *S*. As a consequence, the forward reaction is inhibited, as is the reverse reaction. However, the reaction rates will not be zero since, as already discussed, *D* can spontaneously dissociate. In addition, breathing of the duplex strand or end fraying can make bases of sequence *a** available for binding with *S'* to initiate the exchange. An experimental study of the system of Figure 2 has been carried out by Reynaldo et al.,⁹¹ who showed that spontaneous dissociation dominates near the melting temperature of the duplex while fraying-initiated three-way branch migration occurs at low temperatures.

2.2.2. Toehold-Mediated Strand-Displacement Reactions with Three-Way Branch Migration. Toeholds provide a means to increase the rate of strand displacement by increasing the attempt frequency for three-way branch migration. The process is illustrated in Figure 3. In the overall reaction from (A) to (F), strand *Y* (having sequence *b*), also referred to as the incumbent, is displaced from the substrate strand *h***b** of duplex *S* by the invader strand *X* to produce the duplex strand *L*. The toehold is the single-stranded extension *h** on the duplex *S*. The displacement reaction is initiated when domain *h* of the invader strand hybridizes to the toehold

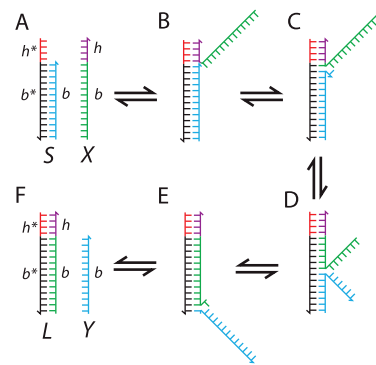


Figure 3. Toehold-mediated strand displacement via three-way branch migration. (A) The toehold consists of the single-stranded overhang *h** on the duplex strand *S*. The invader strand *X* displaces the incumbent strand *b*, also denoted as *Y* to form the duplex *L* in (F). (B–E) Intermediate steps in the branch migration process.

as shown in (B). End fraying of *Y* then allows the invader strand *X* to initiate a three-way branch migration process (Figure 3C). The first step of this process consists of the dissociation of a base of the incumbent strand from the substrate strand which enables the invader strand to bind with the substrate strand via one more base. This is the initial step of a random walk process in which the invader strand competes with the incumbent strand for binding with the substrate strand (Figure 3D). The mean step time for a one-base step of the branch point in this branch migration process^{16,92} is $12\text{--}20 \mu\text{s}$. Shown in Figure 3E is the configuration in which the branch point is at a position where the invader is one base short of having displaced the incumbent. Finally, the incumbent strand will be completely displaced and the invader and substrate are fully hybridized, forming the duplex *L* (Figure 3F). Due to the lack of a toehold with which the incumbent *Y* can bind, the rate constant for the reaction going from (F) to (E) will be small compared to the association reaction going from (A) to (B). The toehold thus drives the system from (A) to (F). When all the oligomers are present at the same concentration, the ratio of the concentrations of the complexes *L* and *S* is given by

$$\frac{[L]}{[S]} = \sqrt{\frac{k_f}{k_r}} = e^{-\Delta G^\circ/2RT} \quad (3)$$

where k_f is the overall or pseudo rate constant for $S + X \rightarrow L + Y$, k_r is the corresponding rate constant for the reverse reaction, and ΔG° is the standard free energy of hybridization of *h* with *h**. As ΔG° becomes more negative for longer toeholds, the equilibrium is pushed more strongly toward the configuration in Figure 3F.

Experimentally measured forward reaction rates as a function of toehold length are shown in Figure 4. The data conform qualitatively with expectations. For short toeholds, the probability that the invader strand will remain attached to the toehold long enough to displace the incumbent strand is small due to the high dissociation rate and also due to the multiple returns the branch point makes to the end of the substrate proximate to the toehold. With a sufficiently long toehold the probability of dissociation will be small compared to the probability that the random walk of the branch point completes a first passage to the distal end of the substrate strand and displaces the incumbent. One thus expects the rate

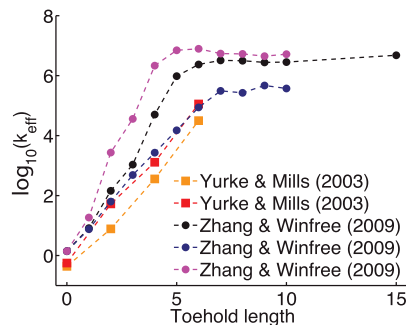


Figure 4. Effective rate constant k_{eff} as a function of toehold length for several experimental systems (the data of Yurke and Mills (2003) are from ref 90 and the data of Zhang and Winfree (2009) are from ref 93). Reprinted with permission from ref 51. Copyright 2013 Oxford University Press.

constant to increase with toehold length for short toeholds and then to saturate once the toehold has become sufficiently long. Srinivas et al.⁵¹ carried out extensive energy landscape modeling and coarse-grained molecular dynamics simulations in order to obtain a quantitative understanding of the rate with which toehold-mediated strand displacement reactions occur. Two key findings of this work were (1) that the rate with which a single step of the branch migration process occurs is significantly slower than the fraying of a single base pair and (2) that the initiation of branch migration incurs a thermodynamic penalty due to the additional overhang it engenders at the junction. Molecular dynamics simulations carried out with oxDNA^{49,50,94} suggest that the greater structural rearrangements required to advance the branch point by one step account for the slower rate of this process compared with base pair fraying. Further, the branch migration initiation penalty results from partial disruption of the base stacking and reduction of conformational freedom as the two single-stranded extensions at the branch point (after the first step) are forced to bend away from each other.

Studies of the strand exchange process have been carried out in vitro and in vivo using plasmon rulers,⁹⁵ a technique that does not suffer from photobleaching and blinking. Li, Tian, and Mao⁹⁶ showed that toehold-mediated strand displacement could proceed even if the incumbent and substrate strand were engaged in triplex binding with a third strand but proceeds at a much slower rate. Kabza, Young, and Szczepanski⁹⁷ showed that also PNA, an oligonucleotide analogue in which the sugar-phosphate backbone is replaced with uncharged *N*-(2-aminoethyl)glycine units, can function as an incumbent strand or an invader strand for systems in which the other members of the strand exchange system are either composed of natural DNA consisting of D-deoxynucleotides or the corresponding L-DNA enantiomers. The achiral molecule PNA is thus able to couple D-DNA reaction networks with L-DNA reaction networks.

2.2.3. Toehold-Mediated Strand-Displacement Reactions with Four-Way Branch Migration. Four-way branch migration, a process in which the branch point consists of a mobile Holliday junction, has found use in all-DNA reaction networks.^{26,64} Toehold initiated four-way branch migration is illustrated in Figure 5. In (A) are shown two duplex strands with the one on the left possessing toeholds *b* and *c*^{*}, while the one on the right possesses the complementary toeholds *b*^{*} and *c*. Four-strand branch migration is initiated when domains *b* and *c*^{*} hybridize with the corresponding complementary

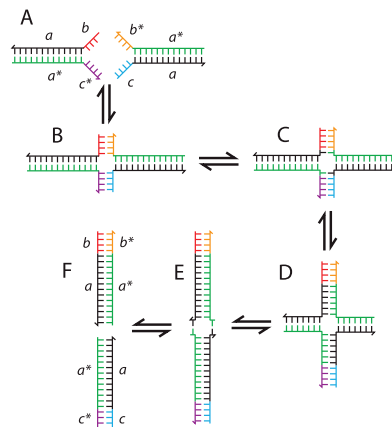


Figure 5. Toehold-mediated strand displacement via four-way branch migration. (A) Two complementary DNA constructs each possessing a pair of single-stranded overhangs that serve as toeholds. (B) The two constructs combine into a Holliday junction through hybridization of complementary toeholds. (C–E) depict the random walk executed by the branch point through four-way branch migration, which results in two new duplex strands (F) having a greater number of base pairs.

toeholds to form the Holliday junction shown in Figure 5B. Through rearrangement of base pairing in the junction core, the branch point excites a random walk where, in a given step, two opposite arms shorten while the other two lengthen by a base pair. Representative configurations as the random walk progresses are shown in Figure 5, panels C–E. Upon making a first passage of the branch point from the end distal to the toeholds, the complex dissociates into two duplex strands having a greater number of base pairs, as shown in Figure 5F. As with the system employing three strand branch migration, the energy of hybridization of the toeholds pushes the equilibrium toward the configuration shown in Figure 5F. Four-way branch migration occurs at a slower rate than three-way branch migration. The rate is strongly dependent on the valency of the salt cation of the buffer and rapidly decreases with lower temperature.¹⁹ The mean step time was measured to be 0.3 s at 37 °C in the buffer containing Mg²⁺, while in the buffer containing only Na⁺ the step time was measured to be 1000 times shorter.¹⁹

2.3. Thermodynamic Driving Forces

In the examples of toehold-mediated strand exchange presented so far, the change in the free energy resulting from the hybridization of a toehold with its complement has been used to drive the strand exchange reaction forward. Configuration entropy differences and concentration disequilibria provide alternative means by which toehold-mediated strand exchange reactions can be driven in a desired direction. These alternative thermodynamic driving forces have been used to great advantage in the construction of complex reaction networks.^{48,98}

2.3.1. Configuration-Entropy Driven Reactions. A reaction can be driven in the forward direction if the number of products is greater than the number of reactants, due to the increase in configuration entropy. As examples, consider the systems shown in Figure 6 where the number of constituents increases from two to three in the overall reaction. On the right side of Figure 6A is shown one strand of single-stranded DNA *X* having base sequence *ba* and a duplex strand consisting of two DNA strands with sequences *a* and *b* hybridized to a strand

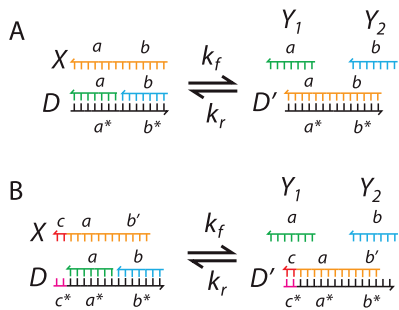


Figure 6. DNA reaction systems driven in the forward direction by an increase in configurational entropy due to an increase in the number of constituents. In particular, in these systems two reactants give rise to three products, but the number of base pairs remains the same. The system in (A) lacks a toehold, and relaxation to equilibrium will proceed slowly. The system in (B) has a toehold (domain c^* of strand D). This provides an attachment site for X , which possesses the domain c that is complementary to the toehold, thereby increasing the rate of the reaction.

with sequence a^*b^* . On the left is shown two strands of single-stranded DNA Y_1 and Y_2 having base sequences a and b , respectively, and a duplex consisting of the strand X hybridized with the strand having sequence a^*b^* . The system on the right has the same base pairs as the system on the left. Hence, there is no gain or loss in free energy due to a change in the number of base pairs to drive the reaction one way or the other. However, since the system on the left consists of two entities while the system on the right consists of three, the configurational entropy is greater on the right. This entropy difference will push the equilibrium concentration in the forward direction. The strength of this thermodynamic driving force can be estimated as follows: the system on the left can be regarded as the same as that on the right except that the 5' end of Y_1 is forced to be colocalized with the 3' end of Y_2 . Let this colocalization volume be denoted as V_1 . Now consider the case when all oligomers X , Y_1 , Y_2 , and a^*b^* are present at equal concentrations ρ . Then the volume the 5' end of Y_1 occupies when it is not forced to colocalize with the 3' end of Y_2 is $V_2 = 1/\rho$. The change in entropy going from the system on the left to that on the right is $\Delta S = k_B \ln(V_2/V_1)$, corresponding to a free energy change of

$$\Delta G_S = -T\Delta S = -k_B T \ln(V_2/V_1) \quad (4)$$

A reasonable estimate of the colocalization volume V_1 is 1 \AA^3 . Considering the case when all the oligomers in the system are present at 100 nM concentration, V_2 is $1.67 \times 10^{10} \text{ \AA}^3$. Taking T to be 300 K, eq 4 yields $\Delta G_S = -0.6 \text{ eV}$. As the average free energy of hybridization is $\approx 0.073 \text{ eV}$ per base pair,¹ the entropic driving force in this example is equivalent to the formation of eight base pairs, which actually is quite comparable to that inferred by the experiment.⁹⁸ The reactions of Figure 6A will proceed slowly since all the bases in duplex structures D and D' participate in base pairing with a complementary base. Figure 6B shows that toeholds can increase the reaction rate without additional base pairing to push the reaction in the forward direction. This is accomplished by attaching a toehold domain c^* as an overhang to the a^*b^* strand of the duplex D and a corresponding complementary domain c to X . In addition, the domain b of X has been truncated at the end distal from the toehold by the same number of bases that are in the toehold so that the total

length of X remains unchanged. Thus, the driving force remains the change in entropy due to the increase in the number of components that are free to diffuse throughout the solution. Given the estimate that the driving force is equivalent to the binding of 8 bp at 100 nM concentration, b' could be truncated by an additional 8 bp before the configuration on the left side would be thermodynamically favored over that of the right.

An advantage of employing configuration entropy as a driving force in DNA reaction networks is that it is insensitive to temperature, pH, and buffer composition. Entropy-driving has been successfully used to implement cascade networks and catalytic and autocatalytic networks.⁹⁸

2.3.2. Concentration Imbalance Driven Reactions.

Concentration imbalances have been used to drive reactions forward in the most complex hybridization reaction networks devised to date.^{48,58,99,100} To illustrate the use of this principle, consider the system shown in Figure 7, in which reactants X

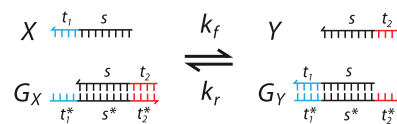


Figure 7. A toehold-mediated strand exchange system driven by concentration imbalance. In the forward reaction invader X reacts with G_X to produce Y and G_Y . When the toeholds t_1^* and t_2^* have the same free energy of hybridization with their complements, there is no change in hybridization free energy. A change in the concentration of one of the reactants will cause the system to readjust the concentration of all the constituents to a new equilibrium.

and G_X react to form the products Y and G_Y . The reactant G_X consists of duplex DNA with a short toehold t_1^* . The reactant X functions as an invader that binds to the toehold and by three-way branch migration displaces the incumbent strand Y to form the duplex strand G_Y with the short toehold t_2^* . This second toehold results in an appreciable reaction rate for the reverse reaction. For the case when t_1 and t_2 are the same, there is no change in the number of base-pairs between the left and right configuration of this reaction, and thus no change in hybridization energy to drive the system in one direction or another. However, if a concentration imbalance is introduced, the system will adjust to a new set of equilibrium concentrations through the toehold-mediated strand exchange reactions. For instance, when the forward and backward rate constants are the same and the initial concentrations $[Y]_0$ and $[G_Y]_0$ are zero, the equilibrium concentrations for the components of the system are given by

$$[X]_\infty = \frac{[X]_0^2}{[X]_0 + [G_X]_0}, \quad [G_X]_\infty = \frac{[G_X]_0^2}{[X]_0 + [G_X]_0} \quad (5)$$

and

$$[Y]_\infty = [G_Y]_\infty = \frac{[X]_0[G_X]_0}{[X]_0 + [G_X]_0} \quad (6)$$

If $[X]_0 = [G_X]_0$, the system settles to an equilibrium in which each component of the system is present at a concentration of $[X]_0/2$. In contrast, when $[X]_0$ is in large excess over $[G_X]$, that is $[X]_0 \gg [G_X]$, the equilibrium concentrations of the constituents are $[X]_\infty \simeq [X]_0$, $[G_X]_\infty \simeq 0$, and $[Y]_\infty = [G_Y]_\infty \simeq [G_X]_0$. Hence, a high concentration of X provides a

concentration-disequilibrium force that drives the effective reaction $X + G_X \rightarrow Y + G_Y$ forward.

Employing elemental reactions of the form depicted in Figure 7, Qian and Winfree^{58,99,100} have developed a practical scheme for the synthesis of large scale DNA reaction networks that can carry out digital and analog computation. Due to the back-and-forth nature of the dynamics of the system of Figure 7, the DNA-based gates employed by Qian and Winfree^{58,99,100} are referred to as “seesaw gates”.

2.4. Finite-State Machines and Hybridization Motors

DNA strand-displacement reactions have already been studied for about a half century due to their biological relevance in DNA recombination reactions. However, interest in these reactions greatly increased with the insight that they can also be used as a means to drive nanomachines constructed out of DNA.¹ Through the addition of a specific sequence of invader strands, these machines can be cycled through a corresponding sequence of states; in other words, these devices function as biomolecular “finite state machines”. These machines can also function as DNA-hybridization motors and perform mechanical work.

Perhaps the simplest such system is shown in Figure 8. Here, a DNA strand M_1 is successively cycled between a state in

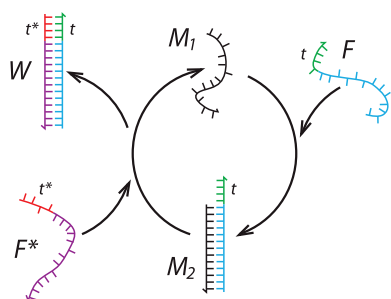


Figure 8. A prototypical finite state machine driven by the free energy of hybridization of the fuel strand F with its complement F^* . The finite state machine consists of the DNA oligomer M_1 that is cycled between the single-stranded state and the state in which it is a member of the duplex M_2 formed by hybridization with a complementary domain in F . The toehold domain of F is labeled t . The fuel complement F^* releases M_1 from the duplex through toehold-mediated strand displacement and in the process forms waste product W .

which it is single-stranded and a state in which it is a member of the duplex M_2 . The transition from the single-stranded state to the member-of-a-duplex state is induced by the introduction of a strand F , which has a domain that is complementary to M_1 . F has a toehold domain t at one of its ends which becomes an overhang when M_1 and F are hybridized. The reverse transition from the member-of-a-duplex strand to the single-stranded state is induced by the introduction of a strand F^* complementary to F . This strand binds with the toehold on M_2 and then displaces the incumbent M_1 . A waste product W consisting of F hybridized with F^* is formed each time the cycle is completed.

In the free state, M_1 is a flexible linear oligomer having a persistence length of ~ 1 nm. As a member of a duplex strand, M_1 is an ordered helix in which the duplex is a stiff linear structure having a persistence length of ~ 50 nm. These changes of state can be used to induce mechanical changes in structures coupled to M_1 . The strand M_1 can thus also be

viewed as a prototypical motor that operates on the free energy of hybridization of F with F^* . Strands F and F^* are referred to as the set and reset strands, respectively.²²

To emphasize the analogy with an internal combustion engine in which a chemical fuel is reacted with oxygen to produce mechanical work, F is also often referred to as the fuel strand and F^* as the removal strand or fuel complement.¹ In the initial demonstration of toehold-mediated strand displacement to drive DNA-based finite state machines,¹ the DNA device driven was a pair of tweezers composed of two long single-stranded overhangs extending off of the tips of the tweezers. The fuel strand had domains complementary to both overhangs and, upon hybridization with the overhangs, would close the tweezers. The fuel complement would restore the tweezers to the open configuration. In contrast to autonomous motors, this motor functions like a stepper motor since it is the successive application of F and F^* that cycles the motor through its states.

2.5. DNA Hybridization Mechanochemistry

DNA nanomachines powered by DNA hybridization motors can exert forces and perform mechanical work. An early demonstration of this was the use of a hybridization motor to pull an aptamer from a thrombin molecule.¹⁰¹ A DNA tweezer-like device has also been used to actuate the activity of an enzyme/cofactor pair.¹⁰² Given the potential of DNA hybridization motors as tools for mechanochemical investigation, it is worth considering the magnitude of the forces that such motors could develop. The mechanical force depends on the mechanical advantage with which the structural changes induced by base pairing are coupled to the structural changes of the nanodevice. Figure 9 depicts two Gedanken experiments in which DNA hybridization is used to lift a weight against the pull of gravity.

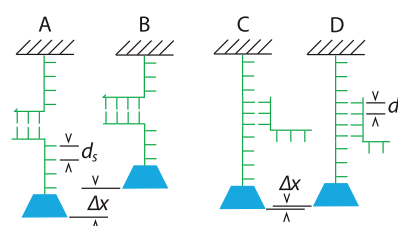


Figure 9. Gedanken experiments in which DNA hybridization is used to lift weights against gravity. In the experiments of A and B, the weight moves up a distance that is twice the spacing between bases in single-stranded DNA when a base pair is formed. In the experiment of C and D, the weight moves up a distance that is the difference between the spacing between bases in single-stranded DNA and double-stranded DNA when a base pair is formed. Δx is the distance the weight travels. d_s and d_d are the spacing between bases on single-stranded DNA and between successive base pairs on double-stranded DNA, respectively. Because the displacement Δx is smaller for the system on the right, it will develop a greater stall force.

If the weight is small, hybridization will proceed, but as the weight is made heavier, a point will be reached where DNA hybridization will no longer proceed. The force exerted by the weight at this point is referred to as the stall force F_{stall} , which is given by

$$F_{\text{stall}} = \frac{\Delta G}{\Delta x} \quad (7)$$

where ΔG is the change in free energy upon forming a base pair and Δx is the displacement of the weight that results from the formation of that base pair. In the Gedanken experiment shown in Figure 9, panels A and B, when a base pair is formed, the weight is lifted by twice the distance d_s between bases in single-stranded DNA, that is $\Delta x = 2d_s$. Assuming $d_s = 0.43$ nm and taking the average free energy for formation of a base pair to be 1.2×10^{-20} J yields a stall force of ≈ 14 pN, which is in line with the experimentally measured force required to pull apart duplex DNA.^{103,104} In the experiment of Figure 9, panels C and D, upon forming a base pair, the weight is lifted by a distance that is the difference between the distance d_s of bases on single-stranded DNA and the distance $d_d = 0.34$ nm between base pairs in duplex DNA (i.e., $\Delta x = d_s - d_d \approx 0.09$ nm). However, not the full free energy of base pair formation is available to lift the weight since some of it is used to twist the DNA. Therefore, in this case, the right side of eq 7 has to be multiplied by the additional mechanical advantage factor $d_d/D\theta$ where D is the diameter of the DNA and θ is the angle of twist between successive base pairs. Using $D = 2$ nm and $\theta = \pi/5$ (since there are ≈ 5 base pairs per half turn of the helix), one obtains an estimated stall force of 78 pN which is comparable to the measured overstretching force for duplex DNA.^{104,105} Hence, in principle, a DNA hybridization engine consisting of single-stranded DNA could develop a force comparable to the DNA overstretching force along the duplex axis when a complement hybridizes with it.

3. CATALYTIC PROCESSES BASED ON STRAND DISPLACEMENT

Free-running biological molecular motors such as kinesin, myosin, and dynein are catalysts, ATPase enzymes that break down the high energy fuel molecule adenosine triphosphate (ATP) into adenosine diphosphate and a phosphate ion. Inspired by these biological examples, the initial impetus for devising enzyme-free DNA reaction networks displaying catalytic behavior was to make artificial systems that behave like free-running motors rather than the stepped DNA motors briefly discussed above.²⁵ Since catalytic systems can function as chemical amplifiers,⁹⁸ the application of enzyme free DNA-based catalytic networks as sensor and detector systems later became a major driving force in the development of these systems.^{78,106–109}

3.1. Hybridization Catalysts

Initial work on hybridization catalysts focused on the construction of metastable DNA complexes, analogues of ATP, whose collapse to a lower energy configuration could be triggered by strand invasion by a catalyst strand. During the decay of the metastable complex, the catalyst strand is released and can thus catalyze the decay of the next complex.

Figure 10A illustrates the first such enzyme-free catalytic system devised by Turberfield et al.²⁵ In this reaction system, a single-stranded DNA catalyst C^* operates on a metastable mixture of DNA strands composed of the loop complex LS^* and the single-stranded oligomer L^* which is complementary to L . LS^* and L^* can react with each other to form the single-stranded product S^* and the duplex LL^* , which is energetically favored by the additional base pairs that are formed in the loop region of L . In the absence of the catalyst C^* , this reaction is sterically hindered due to the difficulty of threading L^* through

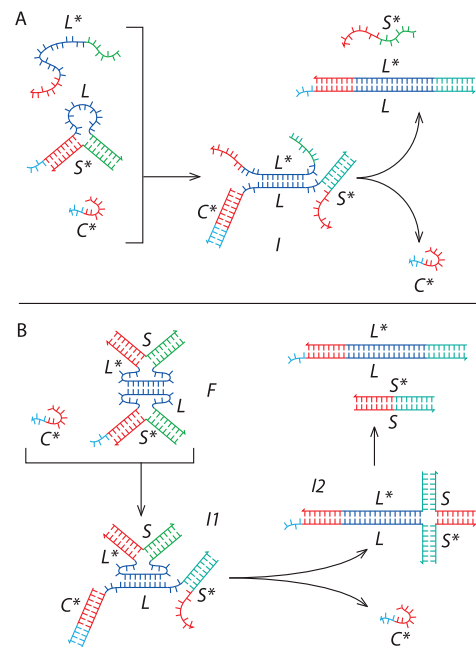


Figure 10. Early enzyme free catalytic DNA systems. (A) Scheme of Turberfield et al.²⁵ In this scheme, the catalyst C^* facilitates the reaction of L^* with the loop structure LS^* to form the products S^* and LL^* . (B) A reaction intermediate I is shown. Scheme of Seelig et al.²⁶ In this scheme, the catalyst C^* facilitates the decay of the metastable structure F , consisting of two complementary loop structures held together by a kissing interaction, into the products LL^* and SS^* . Two reaction intermediates $I1$ and $I2$ are shown. In both systems, the catalyst strand C^* increases the reaction rate by opening a loop through toehold initiated strand invasion.

the loop of LS^* . The catalyst increases the rate of the reaction by opening up the loop via toehold-initiated strand displacement, thereby releasing the steric constraint (cf. the intermediate complex in the figure). When the toehold of C^* is short, the catalyst is released through dissociation at the toehold upon strand displacement of C^* by L^* . The catalyst is thus not consumed in the overall reaction.

Figure 10B illustrates a modification of the catalytic system of Figure 10A, first investigated by Seelig et al.,²⁶ which exhibits a marked improvement in performance. Here the L^* of the metastable system of Figure 10A has been replaced by the loop L^*S which is complementary to the loop LS^* , absent the toehold. It was found that these two loops formed a metastable complex F through the kissing interaction between the loops. This structure was remarkably stable; it could be gel purified and stored on the time scale of a week without serious decay into the products LL^* and SS^* . The catalyst operates by opening the LS^* loop, thereby forming the intermediate complex I . The catalyst is released by strand invasion of the L^* strand of the SL^* loop. In the process, a Holliday junction is formed that via four-way branch migration decays into the products LL^* and SS^* . The catalyst of this system exhibited a total turnover of 40. From the experiment, it was inferred that limited turnover was due to capture of defective oligomers in intermediate complexes.

As with the simple finite state machine of Figure 8, the catalyst C^* of the systems of Figure 10 can be regarded as a prototypical molecular motor since it undergoes a conformational change from single-stranded to duplex DNA, and this motion could in principle be harnessed to drive nanomachines.

In contrast to stepped hybridization motors, this functions as a free running molecular motor in that it autonomously cycles between the two states as long as fuel is present.

Zhang et al.⁹⁸ later devised enzyme-free catalytic systems that employed an increase in configurational entropy to drive the reaction forward, the principles of which have been discussed in connection with Figure 6. Figure 11A illustrates

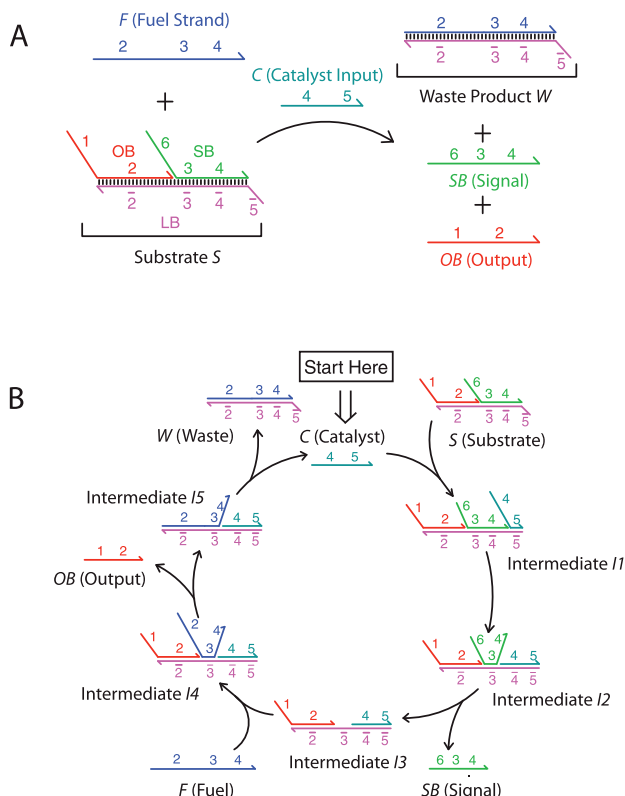


Figure 11. An enzyme free entropy-driven catalytic system.⁹⁸ In (A), the overall reaction is depicted. The reactants consisting of the fuel strand *F* and the substrate *S* are catalyzed by strand *C* to produce the products consisting of waste product *W*, a signal strand *SB*, and an output strand *OB* (i.e., two reactants become three products). In (B), the catalytic cycle is depicted with hypothesized intermediates displayed. Toehold domains 3 and 5 are chosen to be sufficiently short so that the fraction of catalyst bound to the waste product is small and the dissociation of *SB* from intermediate *I*2 is fast. Reprinted with permission from ref 98. Copyright 2007 AAAS.

the overall reaction, in which the substrate complex *S* and the fuel strand *F* react to form the waste product *W* and release the oligomers *SB* and *OB*. The reaction is entropically favored due to the increase in the number of components from two to three. In Figure 11B, the reaction mechanism with hypothesized intermediates is displayed in more detail.

Note that this reaction network employs a hidden toehold $\bar{3}$ that becomes exposed when *SB* is released from intermediate *I*2. This toehold provides an attachment site for the fuel strand *F*, which then drives the reaction to completion by toehold-initiated strand invasion. Another hidden toehold has already been encountered in the system shown in Figure 7; the control of reactions by hidden toeholds has now developed into an important principle for the design of enzyme-free DNA reaction networks.

The catalytic system of Figure 11 can be cascaded with other similar catalytic systems. In particular *SB* and *OB* can serve as catalysts for other catalytic systems by virtue of the freedom available in choosing the base sequences for domains 1 and 2.⁹⁸ Of particular note, the base sequence of the output strand *OB* can be chosen to be identical to that of the catalyst *C*. The resulting system is then autocatalytic, and the number of free catalyst strands is doubled with the completion of each catalytic cycle, resulting in exponential growth of catalyst concentration before substrate depletion.⁹⁸ The catalytic system of Figure 11 also is of interest as a chemical amplifier in enzyme free DNA-based detector applications (cf. section 5).

3.2. Hairpin Toeholds

Another effective way to “hide” toeholds is provided by DNA hairpins. In particular, the single-stranded loop of a hairpin can function as a sequence domain which is, due to steric constraints, unavailable for hybridization until the hairpin is opened. This principle has been employed to construct hybridization polymerization systems [the “hairpin chain reaction” (HCR)],¹¹⁰ catalytic systems [“catalytic hairpin assembly” (CHA)],¹¹¹ and even polymerization motors.⁸⁴ In particular, HCR has found a vast number of applications in dynamic DNA nanotechnology, and both HCR and CHA are used extensively in the context of biosensors, as will be reviewed in detail in sections 4 and 5.

3.2.1. Hybridization Chain Reaction and Hybridization Polymerization. The hybridization chain reaction was first described by Dirks and Pierce in 2004 and is based on toehold-mediated strand invasion into stable hairpin structures with long stem duplexes.¹¹⁰ As shown in Figure 12, the HCR

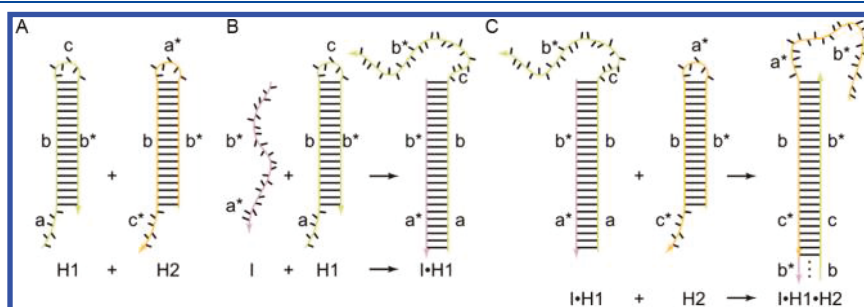


Figure 12. Principle of the hybridization chain reaction (HCR).¹¹⁰ (A) The two hairpins *H*1 and *H*2 metastably coexist. (B) Initiator strand *I* can bind to *H*1 by toehold-mediated strand invasion. (C) The opened *I*-*H*1 complex can invade hairpin *H*2 via the toehold *c*. This process continues by polymerization of the *H*1 and *H*2 hairpins. In a sensor application, the analyte is used as (or somehow transformed into) the initiator strand. Reprinted with permission from ref 110. Copyright 2004 National Academy of Sciences.

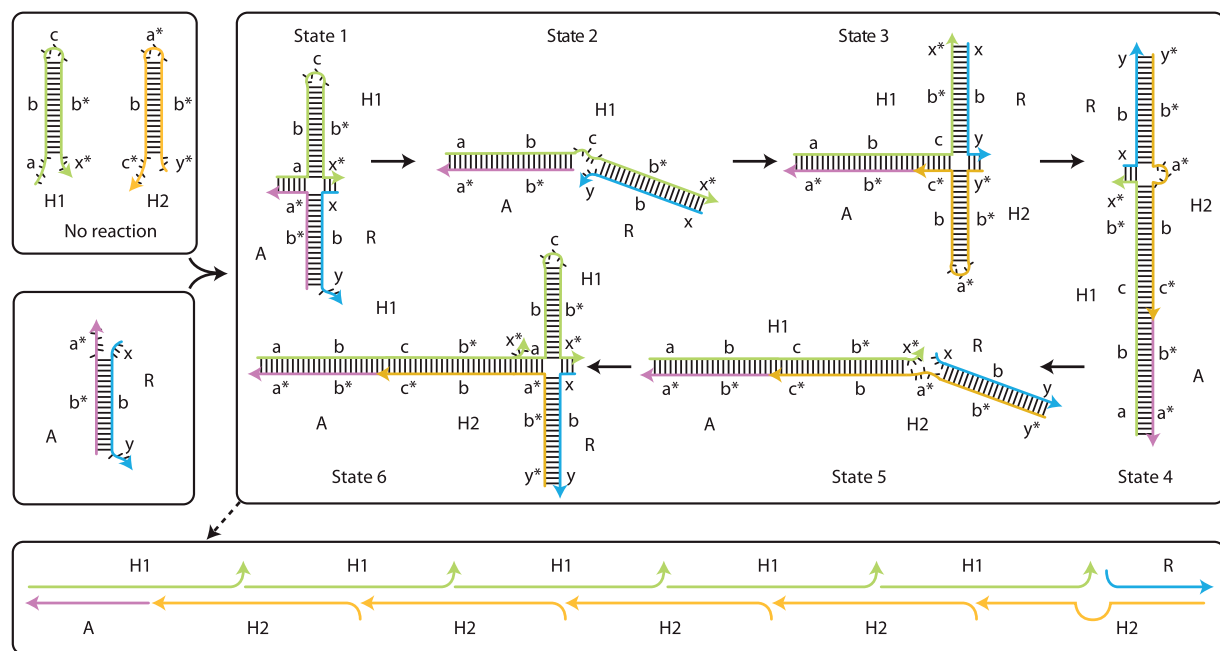


Figure 13. A DNA strand exchange reaction in which strands S and S' having base sequences a and a' , respectively, trade partners with a complementary strand having sequence a^* to form the duplex strand D or D' . The sequences a and a' are identical but have been identified differently to clearly display the exchange process. Reprinted with permission from ref 84. Copyright 2007 Nature Research.

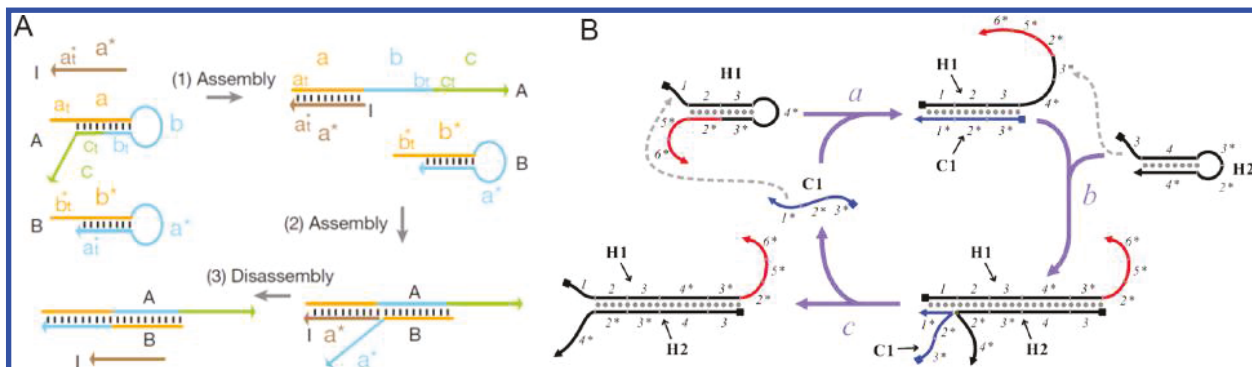


Figure 14. Two implementations of catalytic hairpin assembly (CHA).^{57,111} (A) The initiator I, playing the role of an analyte in sensor applications, catalyzes the reaction of the hairpins A and B into a duplex structure, regenerating strand I after each cycle. Reprinted with permission from ref 57. Copyright 2008 SpringerNature. (B) Similar as in (A), strand C1 catalyzes the hybridization reaction between H1 and H2. Sequence domain 2*, which is exposed in H1·H2 duplexes, can be used to generate a fluorescence output for sensor application. Reprinted with permission from ref 111. Copyright 2011 Oxford University Press.

system is constituted of two types of DNA hairpins H1 and H2, which possess single-stranded toehold extensions at their 5' and 3' ends, respectively. Ingeniously, the loop region of H1 contains the complement of the H2 toehold, whereas the H2 loop is complementary to the H1 toehold and the double-stranded stems of H1 and H2 are identical. Due to the long double-stranded stem region, the two hairpins metastably coexist. Upon addition of a trigger molecule with appropriate sequence (complementary to the toehold and the adjacent stem sequence), one of the hairpins is opened via toehold-mediated strand invasion, which makes the loop sequence freely accessible. The loop sequence can now attach to the toehold of the other type of hairpin and thereby start a chain reaction, in which multiple H1 and H2 molecules bind to each other to form long double-stranded polymers.

In the original design, the toehold/loop regions were chosen to be 6 nt long, while the stem region had a length of 18 bp. As pointed out by Dirks and Pierce in 2004, the design

considerations for HCR hairpins are actually opposite to those for molecular beacons,¹¹² which are widely used as FRET sensors for nucleic acid sequences. Molecular beacons typically have a relatively short stem of only a few bp and a long loop region required for specific sequence detection. The short stem of a molecular beacon facilitates fast switching in the presence of the nucleic acid analyte. By contrast, in order to ensure metastable coexistence of H1 and H2, the stem duplex has to be rather long (which in fact makes HCR comparatively slow). Furthermore, increasing the size of the loop results in an increase of leaky strand invasion in the absence of a trigger, while decreasing the size of the toehold slows down or even completely diminishes the HCR process. These effects are coupled, as the length of the loop region and their complementary toehold are the same. Thermodynamically, each step of the HCR process is driven by the enthalpic contribution of additional base-pairing and base stacking and an entropic contribution from loop opening.

A variant of HCR employing four-way branch migration has been utilized for the construction of hybridization polymerization systems (Figure 13).⁸⁴ In this case, the reaction between H1 and H2 is initiated by the introduction of the DNA complex AR. The overhangs a^* and x of this complex bind with the complementary overhangs a and x^* of hairpin H1 to produce a mobile Holliday junction (state 1 in Figure 13). By four-way branch migration this structure transforms into state 2, in which hairpin H1 has been unfolded to expose the toehold domain c . Toehold domains c and y are now available for hairpin loop H2 to bind to, creating another Holliday junction intermediate (state 3). The configuration relaxes to that of state 4, in which two new domains x and a^* have become available for loop H1 to bind. The sequence of hybridization events now repeats cyclically to produce a long-nicked duplex strand as indicated in the figure. This system has been used to mimic the actin polymerization motor of *Rickettsia* bacteria,⁸⁴ and recently such polymerization motors have also been used to drive the swelling of DNA-cross-linked hydrogels.^{37,38}

3.2.2. Hairpin Fuels and Catalytic Hairpin Assembly.

Rather than catalyzing the formation of polymers as in HCR, systems can be devised in which the catalyst simply catalyzes the formation of a duplex from two hairpins, a concept which was initially introduced by Turberfield and co-workers¹¹³ as a means to fuel autonomous DNA nanomachines (cf. section 4).

Two versions of such “catalytic hairpin assembly” (CHA) by Yin, Pierce, and co-workers⁵⁷ and by Li, Ellington, and Chen¹¹¹ are shown in Figure 14. In contrast to HCR, in a set of hairpin fuels H1 and H2, the loop sequence of each hairpin is partly complementary to the stem regions of the respective other hairpin. As a result, the CHA process does not result in polymeric products but generates DNA duplexes. Li and co-workers¹¹¹ realized that this reaction scheme can be used as an isothermal sensor for DNA and RNA molecules (cf. section 5). To this end, they augmented the hairpins with sequences that could be read out via hybridization to fluorescent probes.

3.3. Other Tools within the Dynamic DNA Toolbox

The dynamic DNA design principles discussed so far do not exhaust the design tools available to the designer of enzyme free DNA reaction networks. In addition to duplex DNA, depending on base sequence or buffer conditions, DNA can exist in a three-stranded form, triplex DNA, or a four-stranded form, the G-quadruplex. Toehold-mediated strand exchange reactions can be implemented also with these structures. For example, an early DNA hybridization motor used toehold-mediated strand exchange to cyclically unfold and refold a G-quadruplex.²³ Triplex binding depends on pH, and this has made possible toehold-mediated strand invasion systems that are pH sensitive.^{114,115}

The toehold examples that have been discussed above consist of toehold domains on the same DNA strand involved in branch migration. We note that also the use of remote toeholds^{116,117} and toeholds that are activated by hybridization between toehold and branch migration domains (associative toeholds)¹¹⁸ have been investigated.

4. APPLICATIONS IN DNA NANOTECHNOLOGY

One of the main benefits of the strand displacement technique is the possibility to reverse a DNA hybridization process at a constant temperature (as opposed to thermal melting of a stable DNA duplex). While, as mentioned, this can be also

achieved by other chemical means (addition of salts, denaturants, a change in pH, etc.), toehold-mediated strand displacement has the advantage of being highly sequence-specific. Thus, addition of a strand displacing oligonucleotide will only affect molecular processes or devices that carry the correct “address”, while it will leave all others essentially unaffected. In the context of DNA nanotechnology, this capability has been utilized in manifold ways. For one, hybridization and strand displacement can be used to reversibly connect separate DNA nanostructures or other nanoscale objects with each other. In a similar way, it can be used to connect and disconnect movable parts of machine-like molecular assemblies and thus drive such devices through their “machine cycle” (cf. section 2.2). Many processes also utilize the fact that double-stranded DNA (with a persistence length of $L_p = 50$ nm) is a much more rigid polymer than single-stranded DNA ($L_p \approx 2-4$ nm). Thus, hybridization and strand displacement can be used directly for mechanical actuation and make parts of a molecular assembly either more rigid or more flexible.

Importantly, the ability to “switch” molecular conformation or processes also supports their characterization; the ability to switch between multiple possible states of a system in a controllable manner helps prove that such well-defined states exist in the first place.

4.1. DNA Fuel for Nanomachines

4.1.1. DNA-Based Molecular Switches and Devices.

Following the development of the DNA tweezers as the first DNA machine driven by strand displacement processes, a large variety of similar switchable devices were developed. Yurke and Simmel described a variation of the tweezers that could stretch, relax, contract, and thus cycle between three distinct mechanical states.^{20,119} In later work, DNA tweezers were modified with various aptamer-based functionalities, which made their opening and closing dependent on the presence of small molecules like adenosine¹²⁰ or proteins such as thrombin^{121,122} or the malaria biomarker PfLDH (*Plasmodium falciparum* lactate dehydrogenase).¹²³

Similarly, light-switchable DNA tweezers were developed using fuel strands containing azobenzene moieties.¹²⁴ As shown by Asanuma and co-workers,^{125,126} azobenzene in the trans conformation fits into DNA double helices and stacks with neighboring base-pairs. Induction of the trans-to-cis conformational change of the photoswitches by irradiation with UV light ($\lambda = 330 - 350$ nm) destabilizes the helix, resulting in helix dissociation, while irradiation with blue light ($\lambda = 440 - 460$ nm) promotes the cis-trans transition and thus hybridization. This principle allows cyclic light-induced switching of DNA nanodevices and represents an alternative to toehold-mediated strand displacement but can be easily combined with it.

A wide variety of DNA devices involving noncanonical base-pairing were developed, mainly involving quadruplex formation^{23,24,101} or pH-dependent i-motif¹²⁷ or triplex switching.¹²⁸ Particularly i-motif switching has been very successfully used for the development of nanomechanical DNA devices that operate inside living organisms as this conformational transition can be used to monitor intracellular pH in endosomes^{129,130} or the trans-Golgi network.¹³¹ These devices do not require, however, the use of strand displacement processes; salt concentrations or pH are more readily available input triggers for DNA nanomechanical devices in the cellular

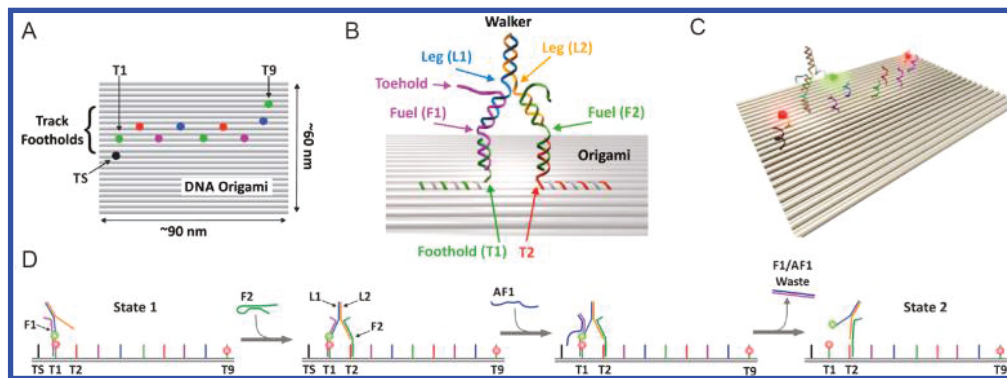


Figure 15. Nonautonomous walker on a DNA origami platform.¹³⁵ (A) Schematic of a standard rectangular origami platform (top view) with indication of foothold positions for the walker. (B) Design of the two-legged walker and its placement on the origami structure. The structure of the walker is identical to that originally conceived by Shin and Pierce.⁸⁰ (C) Movement of the walker can be read out via fluorescence via modification of the start and end site with a FRET acceptor and labeling of the walker with a FRET donor. (D) Operation cycle of the walker for one step. Addition of fuel strand F2 places the leading foot onto its foothold T2. Subsequent addition of antifuel AF1 lifts the lagging foot. In ref 135, Nir and co-workers automated the process of fuel/antifuel addition using a microfluidic device, enabling walker stepping over long distances. Adapted and reprinted with permission from ref 135. Copyright 2017 American Chemical Society.

context, while intracellular RNA (miRNA or mRNA) has been mainly utilized in the context of intracellular computing and biosensing (see sections 5 and 6). Nevertheless, pH-dependent processes and strand displacement can be combined. For instance, Ricci and co-workers demonstrated nanodevices based on pH-controlled DNA strand displacement switching by “clamping” one of the reaction partners of a strand displacement process inside of a pH-dependent DNA triplex.¹¹⁴ Depending on the pH value, the clamp was released and thus strand displacement enabled.

Apart from their basic functionality as molecular switches or motors, applications of DNA-based devices were mainly envisioned for biosensing and biocomputing applications. For an overview of the huge diversity of DNA-based devices developed to date, not exclusively utilizing strand displacement for their operation, and their potential applications the reader may consult dedicated reviews such as refs 132–134.

4.1.2. Molecular Walkers. A major class of DNA devices are the “molecular walkers”, for which a fuel-consuming chemical cycle is coupled to directed movement along a molecular track. As DNA walker systems involve the transfer of the “walker” between specific binding sites on a track, most implementations so far utilized strand displacement reactions in one way or another.

The first DNA walker was developed by Shin and Pierce and involved a double-stranded walker “body” with two single-stranded extensions that served as “feet” (cf. Figure 15B). The latter could be connected to distinct single-stranded foothold periodically spaced along a double-stranded molecular track.⁸⁰ With the use of appropriate fuel and antifuel DNA strands, each foot could be addressably released from its foothold via toehold-mediated strand displacement and then attached to another foothold. A similar principle was applied by Sherman and Seeman who used a more complex double-crossover molecule as the walker structure.⁷⁹

Both of these walker devices were “non-autonomous” (i.e., they had to be driven from one binding site to the next by the external addition of the corresponding fuels). While this automatically provides clocked, synchronized stepping of the walkers, the process is relatively cumbersome and slow. To address these issues, Nir and co-workers came up with several improvements over the original strand displacement schemes.

For one, based on insights gained from single-molecule experiments, they developed optimized fuel strands with more predictable hybridization kinetics without kinetic trapping of the structures.¹³⁶ In order to facilitate fast stepping, high fuel concentrations are desirable; however, this causes undesirable effects such as two fuel strands simultaneously binding to walker and track without connecting them. To overcome this problem, the authors employed hairpin fuels, which connected to the walker first, which then activated binding to the track. They also came up with a technical solution to speed up the clocked addition of fuel strands. Using a microfluidic system, they were able to drive a DNA walker over 32 steps along an origami-based track (Figure 15), which demonstrated the extraordinarily high stepping efficiency achieved.¹³⁵

A number of variations of nonautonomous strand displacement walkers have been demonstrated. Instead of DNA molecules walking along a linear track, Tian and Mao demonstrated two DNA circles rolling against each other, using the same fuel/antifuel approach as Shin and Pierce.¹³⁷ Using a set of three different set/reset strands, Wang et al. created a system they termed a “DNA transporter”.¹³⁸ In this system, a walker module was used to connect the vertex of a DNA three-way junction and reversibly connected to one of its three extensions. The walker/transporter could thus be programmably transferred from one docking position to the other, which was demonstrated using FRET experiments. Turberfield and co-workers showed that walkers can be also “programmed” to navigate a network of tracks, in which the choice to turn left or right at network junctions was controlled by the addition of corresponding hairpin fuels.¹³⁹ One of the most advanced achievements to date was the employment of DNA-clocked molecular walkers for the realization of a DNA-based “assembly line” by Seeman and co-workers.⁸² In this work, a three-legged walker based on a triangular DNA structure could be moved along a series of “pick-up” sites on a DNA origami, where the walker could take up gold nanoparticles to programmably generate a variety of different nanoparticle assemblies.

Using aptamers or photosensitive compounds, the motion of DNA walkers can also be controlled by the addition of molecules (the ligands of the aptamers)^{140,141} or light

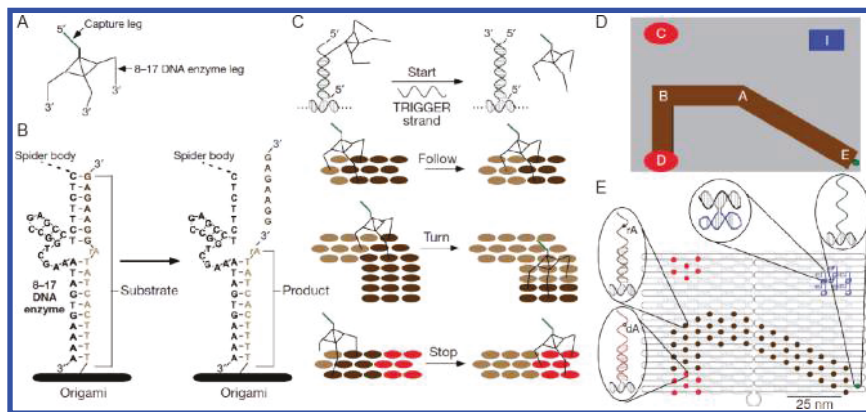


Figure 16. Molecular “spiders” on an origami track.¹⁵¹ (A) Structure of the spiders: a streptavidin “body” is connected to three “legs” containing an RNA-cleaving 8–17 deoxyribozyme. The additional capture leg serves for initial placement of the walker onto the start site of the track. (B) The 8–17 deoxyribozyme cleaves its foothold when bound to a substrate strand. This exposes part of the 8–17 enzyme as a toehold, which facilitates transfer of the leg to a neighboring, uncleaved substrate. (C) The spider is released from its start site by a trigger strand via toehold-mediated strand displacement and then diffusively walks toward regions with uncleaved substrates. (D and E) Substrate track and additional molecular features defined on a standard rectangular origami structure. Reprinted with permission from ref 151. Copyright 2010 Nature Research.

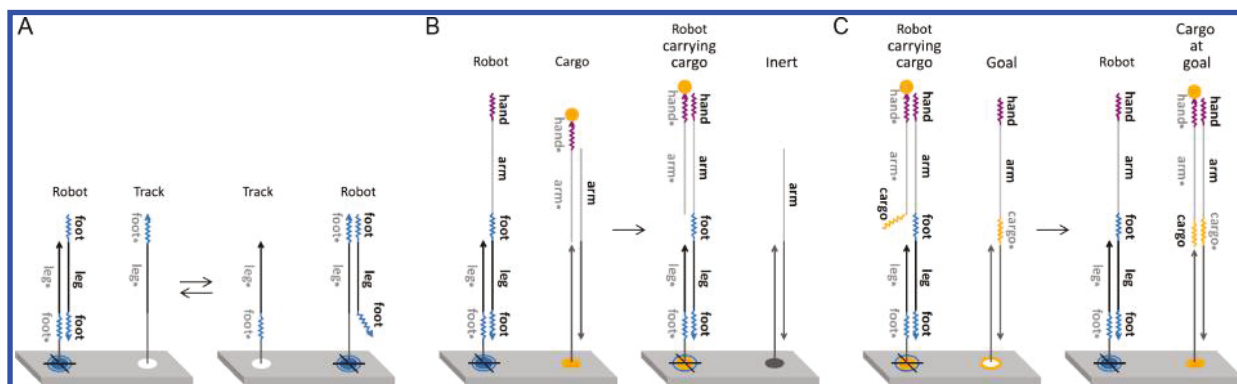


Figure 17. An origami-based strand displacement scheme for diffusive transport of cargo.¹⁵⁹ (A) Similar as in seesawing (cf. Figure 7), the “robot” strand containing two feet (which act as toeholds) can either bind to the track strand on the left or on the right, leading to a diffusive motion of the robot on a track of footholds. (B) With the use of an additional toehold (the “hand”), the robot can pick up cargo from a corresponding storage site. (C) In combination, the robot can diffusively pick up and transport cargo until it is delivered to a thermodynamically stable site (the goal). Reprinted with permission from ref 159. Copyright 2017 AAAS.

irradiation,^{142–147} in an analogous manner to what has been used for the operation of other DNA-based devices (cf. previous section 4.1.1).

Apart from “clocked” molecular walkers, a variety of autonomous schemes for DNA-based molecular motors have been developed, which either utilized the action of DNA-processing enzymes or deoxyribozymes or were based on hybridization catalysis (cf. section 3). The first example of an enzyme-driven “walker” was demonstrated by Yin et al. in 2004.¹³ With the use of an ingenious reaction scheme involving a T4 DNA ligase and two restriction endonucleases (BstAP I and PflM I), a six-nucleotide long DNA fragment could be transferred along a track of anchor sites arranged along a double-stranded DNA scaffold. While this scheme did not involve strand displacement processes, using a similar mechanism based on nicking enzymes (N.BbvC I B) and branch migration, DNA walker systems were developed shortly thereafter, which were capable of moving larger DNA fragments along a track.¹⁴⁸ Nicking enzyme schemes were later employed for various other walker systems. Wickham et al. used AFM to directly observe the motion of such a walker on a track laid out on an origami platform¹⁴⁹ and later also

demonstrated navigation of a walker on a branched network.¹⁵⁰

Instead of nicking enzymes, also RNA-cleaving deoxyribozymes were employed for walking. Tian et al. designed a walker molecule containing the RNA-cleaving 10–23 DNAzyme that could bind to DNA substrate molecules (containing an RNA base at the cleavage site), which were aligned along a linear DNA track.¹⁵² Cleavage of a substrate by the walker exposes a toehold on the walker/docking duplex, which can be used for strand invasion by the substrate molecule on the next site of the track. This progressively and autonomously transfers the walker from one docking site to the next. On the basis of a similar idea, three-legged “molecular spiders” were designed (Figure 16), which were composed of three biotinylated feet (each containing a 8–17 DNAzyme) bound to a streptavidin “body.”¹⁵³ This allows the spiders to autonomously walk on surfaces modified with substrates for the deoxyribozyme; upon cleavage of a substrate, the spider can lift one of its legs and step to a neighboring substrate site. Even though the motion of molecular spiders is essentially diffusive, there is a bias to walk toward regions with intact rather than cleaved substrate molecules. This property was later utilized to direct molecular

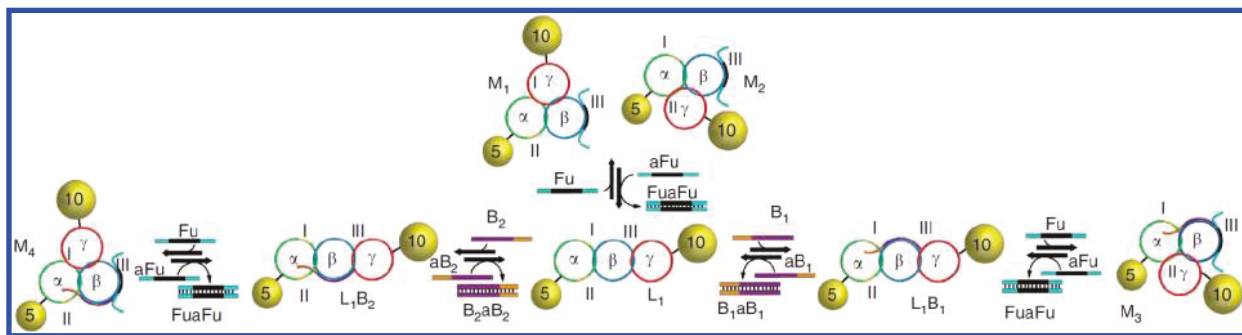


Figure 18. Catenanes made from three interlocked single-stranded DNA circles, which are partially complementary to each other. Two of the rings are labeled with gold nanoparticles with diameters 5 and 10 nm, respectively. Using appropriate sets of fuel and antifuel strands, the three rings can be placed into the different configurations indicated. This also changes the distance between the gold particles, which influences their plasmonic interactions. Reprinted with permission from ref 173. Copyright 2013 Nature Research.

spiders along specific substrate tracks defined on DNA origami platforms.¹⁵¹

An autonomous walking scheme based exclusively on DNA hybridization reactions, not requiring enzymes or deoxyribozymes, was demonstrated by Yin et al. in 2008, in which a bipedal DNA construct stochastically moved along a track of docking sites driven by a hairpin fuel. A scheme for rectifying the motion of such a walker was next presented by Turberfield and co-workers,¹⁵⁴ who developed a bipedal walker whose stepping was coupled to the hybridization of two hairpin fuels, thereby acting as a hybridization catalyst. Using an intricate walker design, the two feet were made to communicate with each other such that only the lagging foot was lifted in the operation cycle and thus the walker could walk unidirectionally. The same scheme was also employed using deoxyribozymes rather than hybridization catalysis.¹⁵⁵ A different scheme for unidirectional motion of a bipedal motor along a DNA track, also involving metastable fuel molecules, was demonstrated by Omabhego, Sha, and Seeman¹⁵⁶ (cf. also the discussion of both systems in ref 157). For a more recent review exclusively focusing on DNA walkers, the reader is referred to the overview by Pan et al.¹⁵⁸

Several origami-based strand displacement schemes similar to walker systems have been demonstrated also in other contexts such as DNA computing and DNA robotics. For example, Thubagere et al. recently demonstrated “cargo-sorting” by a molecular robot on DNA origami.¹⁵⁹ The “robot” was composed of only a single strand of DNA, which diffusively moved between binding sites on the origami in a way similar to the seesaw gate principle (cf. Figure 7). The robot also carried binding sites (“hands”) for cargo DNA, which could be transferred from origami docking sites to the robot and in turn from the robot to target sites on the origami, in each case using toehold-mediated strand displacement (Figure 17). A different approach for a diffusive DNA walker, in which a single DNA strand was transferred from one binding site to another in a “cartwheeling” motion (i.e., changing the strand orientation with respect to the substrate with each step) was studied by Li et al.¹⁶⁰ The steptime for the cartwheeling motion was found to be only on the order of 1 s. Walker-inspired strand transfer processes have been also demonstrated to occur between footholds attached to cell membranes via hydrophobic modifications.¹⁶¹

4.1.3. Mechanically Interlocked Molecules. Already before the development of DNA nanotechnology and DNA-based nanodevices, chemists have attempted to create

machine-like devices based on supramolecular assemblies of organic molecules (efforts for which Sauvage, Stoddart, and Feringa earned the Nobel Prize in Chemistry in 2016¹⁶²). Mechanically interlocked molecules and, concomitantly, mechanical bonds play a central role in the development of molecular machinery as they provide a means to achieve and control motion in molecular systems. Two of the major classes of interlocked molecules are termed catenanes and rotaxanes. Catenanes comprise several interlocked ring molecules, whereas rotaxanes consist of a ring molecule thread onto a linear “axle”, which has two bulky terminal groups acting as “stoppers” that prevent detreading of the ring.

In the past years, several research groups have created large interlocked molecular assemblies also from DNA, which could be switched between the multiple different conformational states accessible to such assemblies, again employing the strand displacement technique (the interested reader is referred to the dedicated reviews on interlocked structures by Willner et al.¹³⁴ and Famulok et al.¹⁶³).

Famulok and co-workers created the first DNA-based rotaxanes, in which a double-stranded DNA ring was threaded onto a double-stranded axle with DNA-based “spherical” stoppers. By introducing gaps in the ring and the axle, the ring could be localized to a binding site on the axle by hybridization between the exposed single-stranded regions. Addition of a trigger oligonucleotide complementary to the gap on the axle could then be used to mobilize the ring. The same group later demonstrated light-switchable rotaxanes (involving azobenzene-modified oligonucleotides)¹⁶⁴ and also interlocked “daisy-chain” rotaxanes that could be reversibly switched between their various mechanical states via toehold-mediated strand displacement.¹⁶⁵ As a potential application, Famulok and co-workers recently demonstrated the allosteric control of oxidative catalysis with a DNA rotaxane containing a split DNAzyme.¹⁶⁶

Also a wide range of DNA catenane structures has been developed.¹⁶⁷ The Willner group created a variety of complicated DNA catenane structures composed of multiple single-stranded rings such as the olympiadane (containing 5 rings)¹⁶⁸ and even a seven-ring structure.¹⁶⁹ Using toehold-mediated strand displacement, the rings could be actuated and rotated with respect to each other. The resulting reconfigurable devices could be switched between multiple different states. As for the simple DNA devices and DNA walkers, incorporation of aptamers, ribozymes, or the i-motif can provide additional functionalities^{170–172} and make the switching process depend-

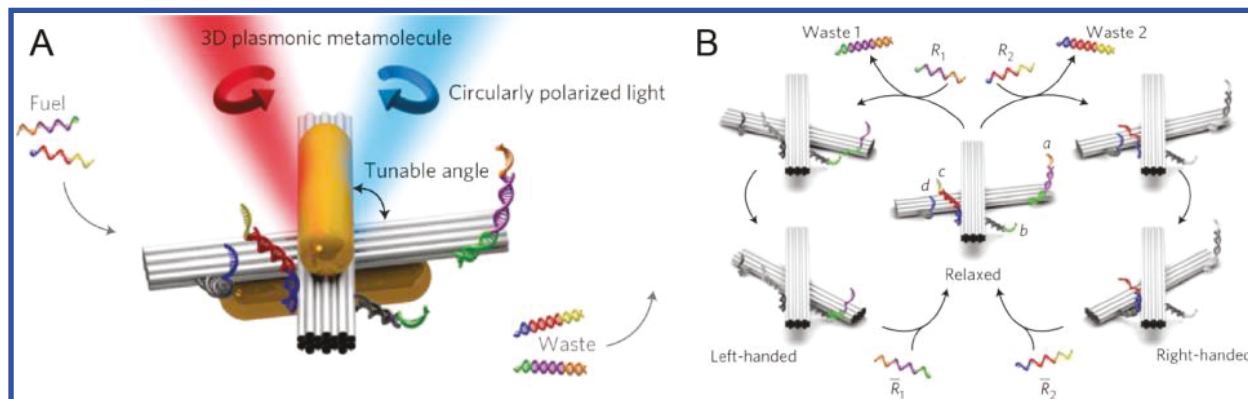


Figure 19. DNA origami-based nanomechanical device that can be used as a plasmonic switch.¹⁹⁰ (A) An origami cross-structure with movable arms carries two gold nanorods. Depending on the angle between the arms, the structure has a left-handed or right-handed chirality, which affects the plasmonic response to circularly polarized light. (B) Operation cycle of the devices, in which two sets of fuel/antifuel strands are used to switch between the two conformations. Reprinted with permission from ref 190. Copyright 2014 Nature Research.

ent on other trigger molecules than strand-displacing oligonucleotides. A series of DNA catenanes modified with metallic nanoparticles were generated to explore potential applications of such devices for switchable nanoplasmonics (Figure 18).¹⁷³

One of the main conceptual advantages of interlocked structures is their defining feature that the components are connected to each other via mechanical bonds. Thus, the release of the movable rings from their binding sites does not lead to a complete dissociation of the structures. An interesting application of this property was recently demonstrated by Famulok, Walter, and co-workers who created a hybrid biomolecular motor involving a DNA catenane structure.¹⁷⁴ One of the rings of the catenane included the promoter sequence for T7 RNA polymerase. Upon addition of T7RNAP, a highly processive rolling circle transcription process was started, resulting in a long RNA product with repetitive sequence. Importantly, the process was accompanied by a rotation of one of the catenane rings with respect to the other. Placed on a six-helix bundle origami substrate with periodically spaced footholds with a sequence complementary to the RNA product, the catenane motor then processively moved along the track.

As will be discussed further below, recently larger and more rigid rotaxane assemblies were created using the origami technique, which have been developed as molecular mechanical components that more closely resemble macroscopic machine parts.

4.2. Switchable and Reconfigurable Assembly of Nanomaterials

Rather than cycling DNA nanodevices through their mechanical states, an obvious application for strand displacement techniques is the control of assembly and disassembly reactions of DNA-based nanostructures, opening up the possibility to create reconfigurable nanoassemblies and, on a larger scale, even materials with switchable physical properties.

4.2.1. Reconfigurable Assembly of DNA Nanostructures. Obviously, the most direct application in this context is the reconfiguration of nanostructures that are made from DNA. Chen et al. demonstrated the realization of DNA origami-based tubes with reconfigurable chirality.¹⁷⁵ In this work DNA origami was used to create 30 nm short, cylindrical tube “monomers”, which could be stacked on top of each other to form long tubules. With the use of different sets of

connector staples, the monomers could be connected with each other to form structures with different chirality. Reconfiguration was achieved by replacing the connector staples using a strand-displacement process. The same group of researchers also studied the kinetics of folding and unfolding of flat DNA origami tiles into tubes in more detail, which further elucidated some of the mechanical properties of the origami.¹⁷⁵

Bryan Wei and co-workers demonstrated more complex reconfigurations of DNA nanostructures in the context of single-stranded tile (SST) assemblies.¹⁷⁶ In contrast to DNA origami, the SST technique does not require a scaffold strand but utilizes a large number of single-strands connected with each other via hybridization to build up arbitrarily shaped 2D or 3D objects.^{177,178} One approach is to create a rectangle (2D) or cuboid (3D) as a molecular “canvas” and selectively leave out some of the SST pixels/voxels to define the desired shape. Using DNA strand displacement, this can also be used to reconfigure the shape. For instance, Wei et al. showed that it is possible to “cut out” pieces from a DNA sheet or “carve” holes into a 3D block.

A different type of reconfiguration was achieved by Yan and co-workers who created a “Mobius strip” structure from DNA origami. By “cutting” the strip along its length at different positions using DNA strand displacement, the structure could be reconfigured into a larger ring or a catenane consisting of two small interlocked rings.¹⁷⁹

Sleiman and co-workers developed a wide variety of DNA structures, which could be reversibly switched in shape,¹⁸⁰ assembled into superstructures such as DNA nanotubes¹⁸¹ and selectively loaded with or emptied of molecular cargo^{182,183} (see also section 4.4 on molecular containers). Other groups have studied the reversible assembly and disassembly of DNA structures into multimeric structures. For instance, Peng et al. demonstrated strand displacement-mediated assembly and disassembly of DNA-based nanoprisms attached to giant liposomes.¹⁸⁴ We note in passing that reconfiguration of DNA nanostructures has also been achieved using a wide variety of other mechanisms than DNA strand displacement (e.g., light-switching using azobenzene-modified DNA molecules).¹⁸⁵

4.2.2. Reversible Assembly of Metallic Nanoparticles.

Since the first demonstration of DNA-directed assembly of gold nanoparticles by Mirkin, Alivisatos, and co-workers,^{186,187} a large body of work has been devoted to the study of such systems. Among the main interests here are the DNA-

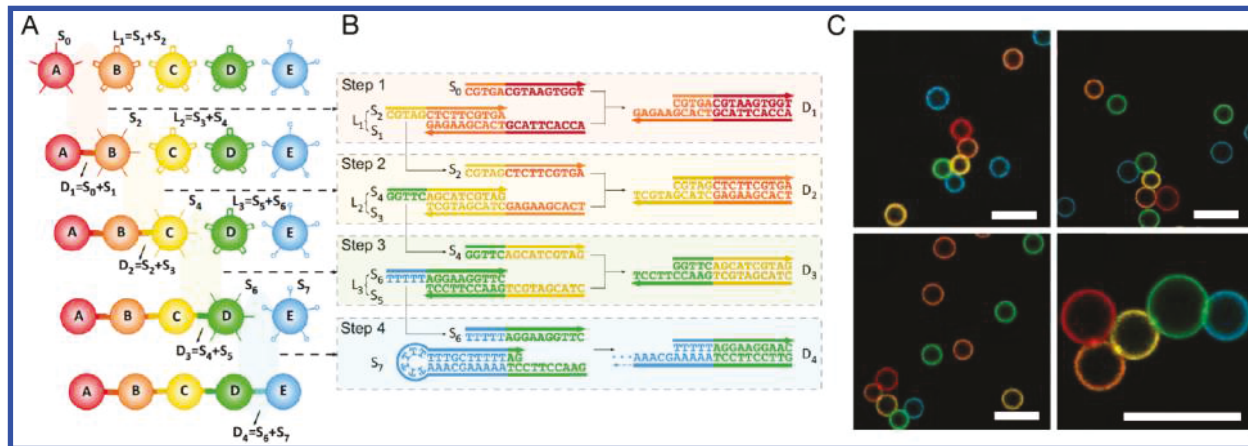


Figure 20. Sequential assembly of droplets.²⁰⁰ (A) Oil-in-water droplets encapsulated by a lipid monolayer are modified with different DNA tags. (B) Sequential addition of linker DNA molecules connects droplets involving a strand displacement process. (C) Examples for droplets assembled in the correct order. Scale bars: 10 μ m. Modified and reprinted from ref 200 under the license CC BY 4.0.

programmable crystallization of nanoparticles for the generation of new (meta-)materials, and the utilization of plasmonic effects that depend on the distance between the nanoparticles. One of the first examples of reversible aggregation and deaggregation of gold nanoparticles employing DNA strand displacement was demonstrated by Niemeyer and co-workers.¹⁸⁸ Due to plasmonic interactions between the particles in the aggregated state, the switching process was accompanied by a reversible change in the spectral properties of the gold nanoparticles. In a related approach, Song and Liang achieved control of gold nanoparticle aggregation via a hybridization catalysis scheme, in which the assembly of a DNA-modified gold particle onto a gold-labeled double-stranded DNA scaffold could be triggered by the addition of a catalyst oligonucleotide.¹⁸⁹

For advanced plasmonic applications, a more controlled variation of interparticle distance and orientation is desirable, which may be achieved using reconfigurable catenane structures¹⁷³ (see above) or switchable DNA origami nanostructures modified with metallic nanoparticles. The first origami device enabling such control was demonstrated by Kuzyk, Liu, et al.,¹⁹⁰ who created a reconfigurable plasmonic “cross structure”, in which the arms of the cross were decorated with gold nanorods (Figure 19). The cross could be switched between a left-handed and a right-handed configuration, resulting in a change in chirality of the nanorod assembly. This in turn created a large, reversible change in the plasmonic circular dichroism of the structure. Liu and co-workers further created a plasmonic walker system using a strand displacement scheme similar to the first DNA walkers created by Shin and Pierce.⁸⁰ In their system,¹⁹¹ a gold nanorod covered with DNA strands could be reversibly attached to DNA footholds extending from a DNA origami platform, which was modified with a second gold rod in perpendicular orientation on its other face. Using DNA strand displacement, the nanorod walker could be translocated across the platform, leading to a measurable change in circular dichroism. For a review dealing with concepts for dynamic DNA-based plasmonic nanodevices, the reader is further referred to the paper by Zhou et al.¹⁹²

Reversible assembly of gold nanoparticles was also utilized in the context of nanoparticle crystal assembly. Gang and co-workers utilized a DNA strand displacement mechanism to

control the interparticle distance between DNA-modified gold nanoparticles.¹⁹³ When assembled into a colloidal superlattice, the change in interparticle distance change translated into a contraction or expansion of the lattice, which could be directly monitored using *in situ* small-angle X-ray scattering (SAXS) measurements. Incorporation of chromophores into the lattices led to strong changes in their optical response upon reconfiguration.¹⁹⁴

4.2.3. Reversible Assembly of Biomolecules. DNA strand displacement has also been used to reversibly assemble biomolecules in various ways and for a wide range of different applications. For example, Flory et al. introduced toehold-mediated strand displacement as a gentle method for the purification of PNA-protein complexes, which they applied for the creation of protein-functionalized tetrahedral DNA nanocages.¹⁹⁵ In their purification method, the protein of interest is first conjugated to PNA and then hybridized to an auxiliary DNA structure which helps in the subsequent purification from unconjugated protein by size exclusion chromatography. The auxiliary DNA can be removed by strand displacement.

Using strand displacement, Song et al. achieved reversible immobilization of DNA-modified enzymes such as alkaline phosphatase, horseradish peroxidase, or trypsin to DNA-covered magnetic beads.¹⁹⁶ The immobilized enzymes displayed increased long-term stability and maintained their activity when exposed to elevated temperatures.

Chen et al. demonstrated various applications of reversible assembly of two conjugated proteins onto a linear DNA scaffold.¹⁹⁷ HaloTag-conjugated proteins were first loaded onto the scaffold using a strand displacement process and could also be removed from the scaffold using dedicated disassembly strands. Bringing two proteins into close proximity was used to create a FRET signal (using two fluorescent protein conjugates) but also to switch the catalytic activity of an “artificial cellulose”. For the latter application, conjugates of endoglucanase CelA and the cellulose-binding module CBM were used, which display an enhanced catalytic rate in cellulose degradation when in close proximity.

A different application involves the DNA-mediated aggregation of large unilamellar lipid vesicles (LUVs) of ≈ 0.4 μ m diameter, which can be sped up using a toehold exchange mechanism.¹⁹⁸ Parolini and co-workers modified

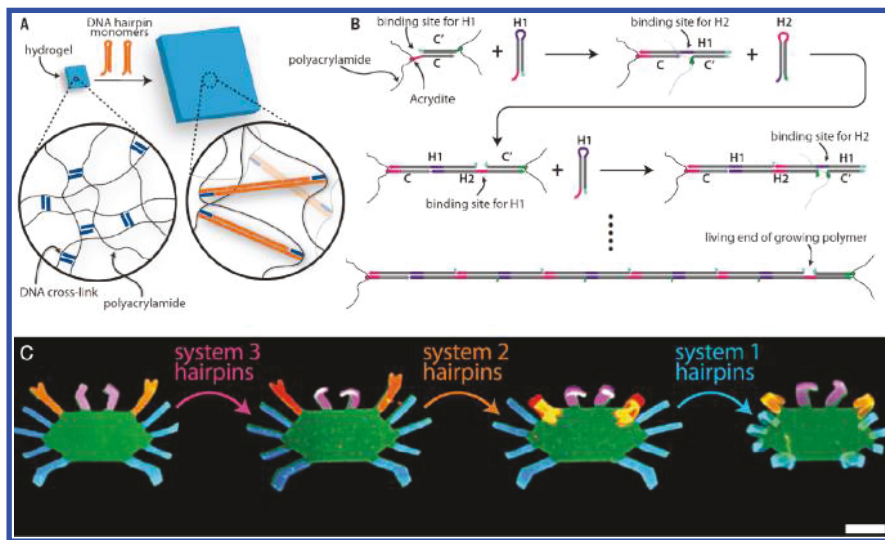


Figure 21. Hydrogel expansion via HCR.³⁷ (A) Schematic representation of a gel slab containing DNA cross-linkers. (B) With the use of hairpin fuels H1 and H2, the length of the cross-links can be expanded, leading to a swelling of the gel. (C) Lithographically structured gel containing regions with different DNA cross-linkers that can be specifically addressed with different sets of hairpin fuels. Swelling of selected layers in a multilayer gel leads to bending of the gel structures. Reprinted with permission from ref 37. Copyright 2017 AAAS.

UVs with cholesterol-conjugated DNA molecules bearing single-stranded sticky end extensions. These could either form loops by hybridization of two extensions on the surface of the same liposome or create a bridge between two separate vesicles. In the absence of a toehold, due to the high local concentration on the membrane, loop formation was favored. Introduction of a toehold sequence then led to much faster aggregation facilitated by toehold exchange.

Chaikin, Brujic, and co-workers demonstrated that it is also possible to assemble lipid-covered oil-in water droplets employing DNA molecules as connectors.¹⁹⁹ Using DNA strand displacement processes, they were able to direct sequential assembly of the droplets into various different arrangements²⁰⁰ (Figure 20).

An interesting application in the emerging field of molecular robotics of the ability to assemble and disassemble different types of biomolecules was demonstrated by Sato et al.²⁰¹

In their work, giant liposomes (GUVs) with diameter $>10\text{ }\mu\text{m}$ were loaded with microtubules and DNA-modified kinesin motors, while the lipid membrane itself was modified with cholesterol-functionalized DNA anchors. Using DNA connector strands, the motors could be attached to a membrane, resulting in a rolling motion of the GUVs caused by the motors acting on the artificial microtubule cytoskeleton. With the use of toehold-mediated strand displacement, this process could be switched off again via DNA “releaser” strands. Notably, the activation of DNA connectors and releasers could be controlled externally with UV light using photocleavable protecting strands.

4.2.4. DNA Switchable Gels. Apart from structurally well-defined nanodevices, soft and “amorphous” gel materials involving DNA components have become increasingly popular over the past years. While not providing nanometer-scale spatial resolution of DNA nanostructures, they provide a route toward the generation of macroscopic materials containing “DNA intelligence”.²⁰²

One of the earliest achievements in this area was the creation of DNA switchable polyacrylamide hydrogels. Using oligonucleotides modified with the commercially available

compound “acrydite”, which can be copolymerized with acrylamide, Langrana, Yurke, and co-workers were able to generate polyacrylamide gels which were cross-linked with DNA duplexes rather than bis(acrylamide). The mechanical properties of these gels could be controlled by the DNA modification density as well as the temperature; melting of the DNA cross-links resulted in a gel–sol transition of these hybrid gels.³⁰ As an alternative to melting, also toehold-mediated strand displacement could be used to dissolve these gels. In order to demonstrate this capability, Liedl and co-workers first trapped fluorescent nanoparticles inside of the gels and triggered their release from the gel by the addition of the corresponding strand-displacing release strands.³¹

Apart from DNA-cross-linked hybrid gels, various research groups have worked on the fabrication of hydrogels exclusively composed of DNA. DNA gels can be easily created at a bulk scale based on branched DNA motifs with sticky end extensions (sometimes termed “X-DNA”, “Y-DNA”, and “T-DNA” junctions^{203,204}). Compared to the fabrication of DNA crystals, the design criteria for the DNA motifs are relaxed, as gel formation does not require rigid building blocks or cross-links. Switching of gel structure was typically achieved by stimuli such as pH, small molecules, light, etc., which were coupled to aptamer recognition, enzyme action, or photo-sensitive compounds. For general reviews of smart and stimulus-responsive DNA hydrogels the reader is referred to, for example, refs 205 and 206.

Strand displacement switching mechanisms have not been extensively employed in the context of pure DNA hydrogels, however. One possible reason for this is that switching by branch migration is a relatively slow process, in particular on the macroscopic scale of the gels. DNA molecules employed for switching either have to diffuse into the gels, if this is permitted by the small pore size and the high charge of the DNA gel, or otherwise attack the DNA cross-links of the gel from its periphery.

A different application, which utilizes strand displacement processes inside of a DNA gel to control its mechanical properties was demonstrated by Romano and Sciortino.²⁰⁷ In

their work, DNA sequences with a weight fraction of a few percent were used to create four-way junctions with sticky end extensions, which formed a DNA gel when cross-linked with double-stranded “bridge molecules” containing complementary sticky ends. Importantly, free bridge molecules could displace other bridges inside of the gel via toehold-mediated strand displacement. As a result, the internal cross-links were highly dynamic and continuously reorganized without the network ever disintegrating. The authors note that in consequence this material represents an all-DNA vitrimer—a type of plastics, which is internally dynamic due to bond-exchange reactions and possesses stress releasing and self-healing properties. Indeed, the DNA vitrimer also was able to self-heal any internal fracture via toehold-mediated strand displacement.

An alternative way to control the mechanical properties of a hydrogel is to change the cross-linking density by gel swelling. In this context, Schulman, Gracias, and co-workers demonstrated that the length of the cross-links in a DNA hybrid gel can be expanded using a hairpin chain reaction mechanism (cf. section 3.2.1).³⁷ When the DNA cross-link contains a toehold sequence which can act as the trigger for an HCR process, the gel is correspondingly expanded at this point (Figure 21). Importantly, a multilayered gel, in which one of the layers is swollen via the addition of HCR hairpins, can be made to bend and change its shape. Employing photolithographic structuring of multilayered gels therefore allowed to create complex shapes, of which different parts could be bent in a sequence-addressable manner, opening up a new range of applications for strand displacement processes in soft robotics.

4.2.5. Control of Chemical Synthesis. An exciting application of strand displacement reactions is the control of DNA-directed chemical synthesis. It has been demonstrated that the efficiency of bimolecular reactions can be enhanced by colocalizing the reactants onto a DNA scaffold, which increases their local concentration.²⁰⁸ In this context, He and Liu demonstrated that a deoxyribozyme-based molecular walker carrying a reactive amine at its 5' end can react with and pick up several cargo molecules placed along a one-dimensional track.⁸¹

Turberfield and co-workers more recently developed an alternative scheme for an autonomous chemical assembler based on an ingeniously designed reaction cascade involving chemically functionalized DNA hairpins (“chemistry hairpins”) and additional hairpins that contain instructions for the assembly process (“instructor hairpins”).²⁰⁹ The process starts with an initiator molecule in which one of the DNA strands is modified with a functional group at its 3' end. During the assembly process, which is similar to the hybridization chain reaction, the initiator structure is extended by the addition of hairpin molecules to an elongated duplex structure. In this process, chemically reactive groups attached to the 5' end of chemistry hairpins are colocalized with the molecules already attached to the 3' end of the growing end of the polymer. Upon reaction, the incoming group is transferred to the 3' end of the chain. The instruction hairpins then supply the information of which chemistry hairpin to incorporate next. Depending on the mixture of instruction hairpins added to the reaction (the “assembly program”), well-defined oligomers, polymers, and also combinatorial reaction products of the reactants can be generated.

4.2.6. Other Reconfigurable Structures. Strand displacement techniques can be applied whenever controlled hybridization and dissociation between DNA-modified com-

ponents is desired, which can be applied in a wide variety of other contexts than discussed above. For instance, Feng Liu and co-workers utilized DNA strand displacement to regenerate the surface of a quartz crystal microbalance (QCM) DNA biosensor.²¹⁰ They immobilized DNA capture sequences on the gold-coated chip-surface of a QCM, which was then modified with a reporter DNA molecule, causing a measurable shift in the QCM frequency. The reporter was designed such that the DNA to be detected could displace the reporter from the capture strand in a toehold-mediated strand displacement process. This resulted in another frequency shift that served as the sensor signal and simultaneously recovered the chip-surface for repeated use.

Also using DNA strand displacement, Krissanaprasit and co-workers demonstrated switching of the conformation of a soft and bendable DNA-functionalized polymer (APPV-DNA) immobilized on a DNA origami platform.²¹¹ The conducting polymer could be forced into two bent conformations, connecting a fluorescent donor molecule with two alternative acceptors by either making a left or a right turn on the origami substrate. This resulted in two distinct fluorescence spectra indicating that Förster resonance energy transfer (FRET) took place between donors and acceptors and was mediated by the polymer.

A different application deals with the realization of a tunable FRET-based photonic nanowire.²¹² For this, Liang and co-workers used an amplification scheme similar to seesaw gate cycling to catalyze the binding of DNA molecules labeled with FRET acceptors to a DNA scaffold containing a FRET donor. With the use of two input strands labeled with two different acceptors, different fluorescence emission spectra are generated depending on the presence of the inputs.

Yet another application of strand displacement deals with the creation of a DNA “rewritable memory” based on changes in electrophoretic mobility of a long DNA molecule upon intramolecular cross-linking. Chandrasekaran, Halvorsen, and co-workers utilized the M13 scaffold commonly used for the assembly of DNA origami structures and hybridized it with a large number of short complementary strands, some of which were augmented with sequences serving as molecular “addresses”.²¹³ Cross-linking two addresses with a “set strand” resulted in the formation of a DNA structure with an internal loop, which had a distinctly different mobility in gel electrophoresis. By adding various set strands or removing them via strand displacement, different mobility patterns were achieved, which could be interpreted as information storage or erasure.

4.3. Origami-Based Nanomechanical Devices

The development of the DNA origami technique has enabled the creation of much larger discrete DNA nanostructures than previously achievable using other DNA assembly approaches. Naturally, also these larger structures can be switched by means of toehold-mediated strand displacement. Maybe the first example of such a system was the iconic “DNA origami box”, which was created by Andersen and co-workers in 2009.²¹⁴ In the DNA box, a single-layered origami structure composed of six connected rectangles was folded into an empty molecular cuboid box with dimensions $42 \times 36 \times 36$ nm³. One of the faces of the cuboid was attached to the rest of the box only via a flexible hinge, acting as the “lid” of the box. The lid could be closed via DNA hybridization and opened via a strand displacement mechanism similar as previously

employed for simpler DNA nanomachines. One of the goals of this work was the entrapment of molecules inside the box. For instance, enzymes could be made accessible or inaccessible for their substrates or drugs trapped and released. Later also a smaller version of the box with a volume of only $18 \times 18 \times 24 \text{ nm}^3$ or 4 zeploliters was demonstrated.²¹⁵ In a similar way, List and co-workers opened and closed a flat origami sheet using toehold-mediated strand displacement in conjunction with hydrophobic interactions, which were caused by cholesterol modifications of the structure.²¹⁶

Another switchable, container-like device was demonstrated with the “logic-gated nano robot” by Douglas, Bachelet, and Church.²¹⁸ The device consisted of a hollow cavity containing antibodies or other protein ligands that could specifically attach to certain cell surface epitopes. Composed of two parts connected by a hinge, the cavity could open in response to the presence of a trigger molecule. This was achieved by first clamping the cavity with a duplex formed by an aptamer sequence and its complement; in the presence of its ligand the aptamer refolded and thereby unbound from the complementary sequence, opening the cavity. The preparation of the loaded nanorobot structure was assisted by toehold-mediated strand displacement, which helped to assemble the cavity to high yield in its closed state. A conceptually similar device consisting of a rolled up DNA origami sheet was recently demonstrated to be capable of delivering thrombin specifically to tumor-associated blood vessels and thus lead to tumor necrosis and tumor growth inhibition *in vivo*.²¹⁹

Earlier, Sakai and co-workers described a couple of “tweezers-like” origami devices, which they termed “DNA origami pliers” and “DNA origami forceps”.²²⁰ These could be switched by various triggers and also closed and reset into an open state using toehold-mediated strand displacement. Kuzyk and co-workers demonstrated an application for a similar origami switch in the context of nanoplasmonics (cf. section 4.2.2).¹⁹⁰

An important contribution to the field of DNA origami nanomechanics came from the Castro group who approached the topic from the viewpoint of mechanical engineers.²¹⁷ In engineering, kinematic mechanisms are devices that transform an input motion into a defined output motion. They consist of interconnected components whose motion is constrained by kinematic joints such as hinges, sliders, and spherical joints. By combining several components and joints, complex 3D motion patterns can be generated. In their work, Castro et al. generated several origami implementations of joints for angular and linear motion and then connected them into devices such as a “crank slider” or a “Bennett linkage” (Figure 22). The devices could be switched between different possible configurations using toehold-mediated strand displacement.

Rotaxanes are molecular implementations of kinematic joints for linear motion and apart from the examples already mentioned above, also several origami rotaxanes were demonstrated recently, in which the origami axle and the ring were composed of separate origami structures.^{221,222} With the use of strand displacement, the ring could be attached to or displaced from docking sites on the axle and thus linear motion facilitated. Furthermore, a variety of devices were demonstrated, in which a “nanorobotic arm” attached to the center of an origami platform could be rotated between different positions.^{223,224} The arms could be addressably attached to or removed from the docking sites via strand displacement. For

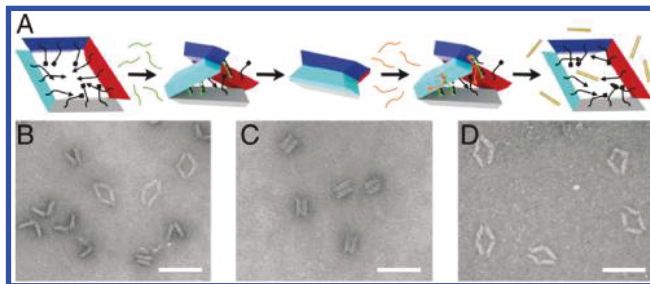


Figure 22. A DNA origami based “Bennett linkage”, which performs 3D motion with one degree of freedom.²¹⁷ (A) Scheme of the Bennett linkage with indicated DNA anchors. The structure can be fixed in one of the conformations using a set of linker strands, which can be displaced by complementary antilinker strands. (B–D) Corresponding electron microscopy images. Scale bars: 100 nm. Reprinted with permission from ref 217.

an interesting review focusing on the engineering aspects of origami-based mechanical devices, see ref 225.

Switchable origami devices also open up the possibility for the realization of reconfigurable nanostructures. One example for this was provided by Zhan et al., who created a DNA origami tripod, in which the angles between the three arms of the structure could be reversibly adjusted using different sets of DNA struts.²²⁶ The structure was functionalized with gold nanorods, which resulted in different dark field scattering spectra for the different tripod configurations.

Next to strand displacement, also other switching principles have been employed that utilize weak interactions such as hydrophobic forces²¹⁶ or DNA stacking interactions. In this context, an interesting reversible assembly scheme based on shape complementarity was developed by Woo and Rothemund²²⁷ and later generalized to 3D structures by Dietz and co-workers.²²⁸ Obviously such interactions can be used in conjunction with the strand displacement technique, which can, for example, support, activate, or deactivate the other switching modalities.

4.4. Switchable Cages and Containers

Switchable molecular cages and containers are a subclass of nucleic acid nanodevices, which may function as molecular machines for the controlled release of molecules. Ideally, the molecules of interest are entrapped or hidden inside of the containers and can be presented or released in response to a specific signal. The entrapped molecules could be drugs or other effectors (e.g., antibodies that activate a signaling cascade) or enzymes that convert prodrug molecules into drugs.

For a variety of the published DNA containers so far, the release mechanism was based on a toehold-mediated strand displacement scheme. This is based on the assumption that a meaningful nucleic acid trigger molecule would be available for the release process *in vivo*. Even though a series of publications have used micro-RNA sequences as the inputs, it is not clear how realistic such release scenarios in fact are; in a real application, the (often rather large) containers would have to be delivered inside of the target cells, where they would have to interact with these intracellular triggers. An alternative scheme could involve molecular transducers that sense a different type of molecular signal, translate it into a nucleic acid trigger molecule, and thereby cause the release of the payload. Other containers respond to extracellular signals (e.g., cell surface markers) via aptamer recognition but this does not necessarily

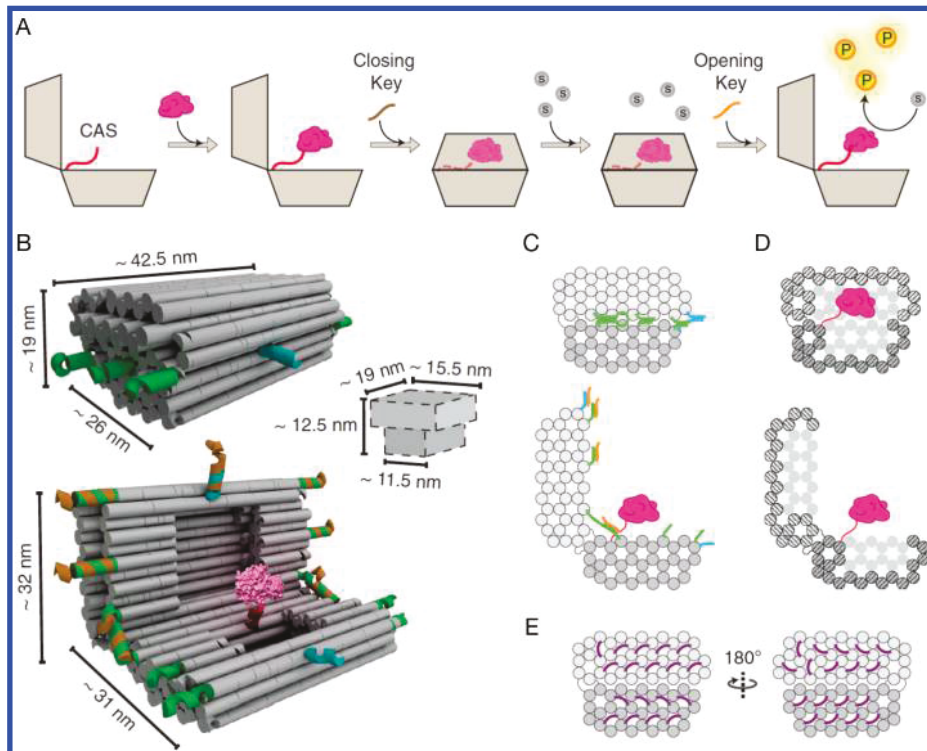


Figure 23. A DNA container for an enzyme.²²⁹ (A) Schematic representation of the container and its strand displacement-based switching mechanism. The encapsulated enzyme is bovine alpha-chymotrypsin and is anchored to the cargo anchoring site (CAS). Opening of the container allows substrate molecules (labeled peptides) to be cleaved by the enzyme, resulting in a measurable fluorescence signal. (B–E) show more detailed representations of the container in its closed and open form. Reprinted with permission from ref 229 under the license CC BY 4.0.

involve a strand displacement process. In any case, applications in controlled release involve a variety of technological challenges such as physiological stability of the structures, crossing of biological barriers, and efficient interaction with the trigger molecules, which are too complex to be discussed in the context of this review.²³⁰ For an overview of DNA-based delivery vehicles, see also ref 231.

4.4.1. Actuation of Origami Containers via Strand Displacement. Next to the DNA box,²¹⁴ the DNA nanorobot,²¹⁸ and the hydrophobically switchable DNA envelopes²¹⁶ introduced above, a variety of other DNA origami containers have been developed. With the creation of a more compact switchable DNA container than the original DNA box, termed “DNA nanovault” (Figure 23), Grossi and co-workers successfully demonstrated the control of enzyme activity.²²⁹ To this end, they placed the enzyme α -chymotrypsin into the 3 zeptoliter small inner cavity of the nanovault. In the closed state, the enzyme was unable to process its bulky substrate, fluorescein isothiocyanate (FITC)-casein, while in the open state the enzyme was accessible and active.

Saccà, Nienhaus, and Niemeyer demonstrated reversible reconfiguration of a single-layered origami structure containing a rectangular cavity in its center.²³² Later Saccà and co-workers demonstrated the encapsulation of the serine protease DegP inside of a 3D origami cavity with hexagonal cross-section. To this end, the inner surface of the hollow DNA origami structure was decorated with multiple peptide ligands that bind to DegP, facilitating the encapsulation of 6-mers, 12-mers, and even 24-mers with a molecular weight of up to 1 MDa. In this work, the peptide ligands were removed after binding of the DegP which, surprisingly, did not result in the release of the

protein complex. Apparently, the ligands were necessary to initially load the cargo into the cavity, but then also other molecular forces kept the DegP complexes in place.

4.4.2. Other Types of DNA Containers. Other cagelike DNA assemblies not based on the origami technique have been developed in parallel. An early example is given by a DNA tetrahedron with a 2.6 nm small inner cavity assembled from only four DNA strands,²³³ which could accommodate a small protein such as cytochrome c.²³⁴ By replacing one of the rigid edges of the tetrahedron by an extendable actuator comprising a DNA hairpin, the tetrahedron could be switched between several states using a strand-displacement mechanism.²³⁵

A wide variety of cagelike structures was also created by the Sleiman group, some of which also could be switched by DNA strand displacement. This involves switchable prismlike DNA assemblies whose vertices were defined by organic linker molecules¹⁸⁰ and also the extended hollow DNA nanotube structures¹⁸¹ already discussed above. An interesting application of the strand displacement process involved the use of hydrophobic alkyl-chain modifications of a DNA cube.¹⁸² Multiple modifications clustered inside of the cube’s cavity and could be used to sequester hydrophobic guest molecules (in this case Nile Red dyes). Removing the alkyl-modified strands from the cube via strand displacement resulted in the release of the molecules. A similar approach using hydrophobic drug molecules is conceivable.

4.5. Localized Strand Displacement Cascades on DNA Origami Platforms

As mentioned above, DNA origami structures have been multiply utilized to define the tracks for molecular walking devices. On a more general level, DNA origami provides an exquisite platform to program and spatially organize dynamic

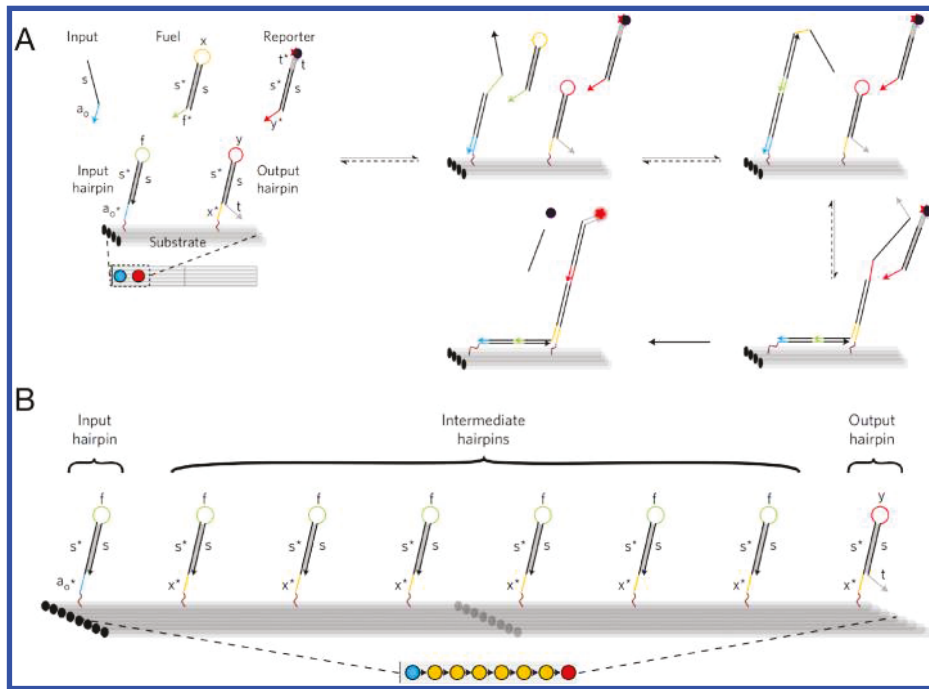


Figure 24. Localized HCR for signal transmission and computation on an origami substrate.²³⁹ (A) Scheme for making a connection between an input and an output node on the origami. A localized input hairpin is opened by an incoming input strand, which facilitates binding of a fuel strand that in turn opens the output hairpin. Output opening is read out by displacement of a quencher-labeled strand from the reporter duplex. (B) The same scheme can be used for communication along a chain of intermediate hairpins with identical sequence. Reprinted with permission from ref 239. Copyright 2017 Nature Research.

molecular processes. Spatial organization has several important ramifications. By colocalizing molecules onto an origami structure, their interaction volume is reduced to below $V \approx (10 \text{ nm})^3 = 10^{-21} \text{ L}$ (i.e., 1 zeptoliter), corresponding to an effective concentration of $1/(V \times NA) = 0.17 \text{ mM}$. This is 10^2 – 10^4 times larger than typical concentrations used for DNA-based reactions, and the speed of bimolecular reactions is increased accordingly. This has the consequence that a reaction between two colocalized molecules will take place much more likely than a competing reaction with a reactant in solution. Next to speeding up the reaction, the process should therefore become more robust with respect to external disturbances. What is important in the context of DNA nanotechnology and DNA computing, this also means that DNA sequences can be “re-used” on different origami platforms without interference, and molecular processes such as localized computations or walkers (or a combination thereof) can be isolated from each other and run in parallel. A theoretical proposal of localized strand displacement circuits has been given by Reif and co-workers,²³⁶ and the dynamics of such localized processes were analyzed in more detail by Dalchau et al.²³⁷

The effect of colocalization on the transfer of a DNA strand from one “docking site” on a single-layered origami platform to another was investigated experimentally by Teichmann et al.⁶⁰ In this work, a DNA strand initially attached to one docking site on the origami was displaced from this site by an incoming DNA strand via strand displacement. Upon release, the strand could attach to an alternative docking site. For close distances between the start and the end sites, a fraction of the strands was indeed transferred directly on the platform. For larger distance, most of the strands escaped from the platform by diffusion. In a similar study, Elezgaray and co-workers

demonstrated a localized amplification circuit, in which the presence of a single input strand led to the release of four output strands, consuming four fuel strands via localized strand transfers between different docking sites.²³⁸ These studies indicated that strand displacement reactions can indeed be sped up by colocalization, and that an efficient transfer of DNA strands on an origami platform requires a direct physical contact between the strand and the docking sites.

Briefly after that Chatterjee and co-workers experimentally demonstrated a viable approach for autonomous DNA signal propagation and computation on origami platforms, which utilized a localized version of the hybridization chain reaction.²³⁹ In this concept, tracks are laid out on an origami substrate by extending some of the staple strands with DNA hairpins (Figure 24). Although the hairpins are in close proximity ($\approx 10.9 \text{ nm}$), their size and secondary structure prevents unwanted interactions. However, when the hairpin at the start site is opened by an input strand, it can hybridize with a fuel hairpin molecule from solution, which then facilitates interaction with the neighboring hairpin. Strand displacement creates a double-stranded bridge between the two sites and activates the toehold region on the next hairpin. Importantly, all the hairpins along the track can have the same sequences and also use one generic fuel hairpin for signal propagation. The concentration of the fuel hairpins can be chosen high enough so that their hybridization with the track hairpins does not limit the speed of the cascade, resulting in a comparatively fast stepping time of only a few minutes. Next to linear signal propagation, the authors demonstrated signal crossings, localized logic gates, and even simple logic circuits. Using a similar reaction scheme, Chao et al. created a stochastic DNA “navigator” system, which autonomously explored paths through mazes defined on DNA origami structures.²⁴⁰

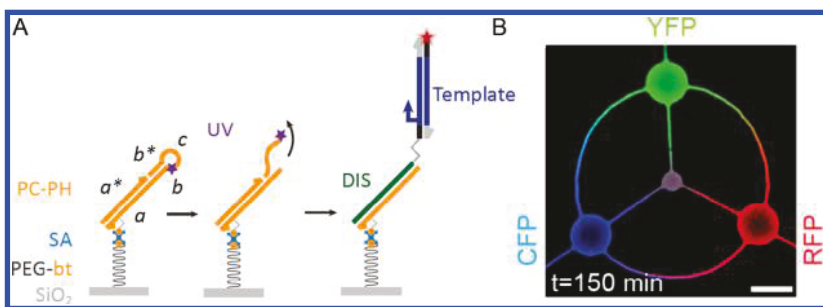


Figure 25. Biomolecular lithography employing strand displacement.²⁴⁴ (A) A DNA duplex comprising a hairpin loop with a photocleavable linker is immobilized on a substrate via a biocompatible PEG spacer. Upon UV irradiation, the loop dissociates, generating a toe hold for strand invasion by displacing strand DIS. This can be used to attach gene length DNA molecules on the substrate. (B) Fluorescence image of three connected microfluidic chambers containing immobilized genes for the fluorescent proteins CFP, YFP, RFP, which are expressed in a cell-free transcription/translation system. Adapted with permission from ref 244. Copyright 2018 Wiley-VCH.

Helmig and Gothelf also succeeded in directly imaging the progression of a HCR cascade localized on a DNA origami platform.²⁴¹ They could also demonstrate that the HCR process can cross from one origami structure to another, opening up the possibility to modularly create larger circuits on extended DNA origami assemblies.

An alternative approach toward origami-localized strand displacement processes, essentially diffusive motion based on a seesaw concept, was utilized in the cargo-sorting robot by Thubagere et al.,¹⁵⁹ which was already described in the context of DNA walker systems.

Rather than for signal propagation or computation, origami-localized strand displacement processes have also been utilized for the operation of molecular “robot arms” that could be rotated around a central pivot and switched between different docking sites.^{223,224}

4.6. Patterning and Lithography

A different field of application for strand displacement processes in nanotechnology was found in the context of biomolecular patterning on solid supports, either by adaptation of classical lithographic methods or through the utilization of reaction-diffusion processes for pattern formation. These applications typically utilize UV-cleavable DNA modifications which create a toehold for strand invasion upon irradiation.

4.6.1. Biocompatible Lithography Using DNA Strand Displacement. One of the first demonstrations of a strand invasion-based lithography process was provided by Huang et al.²⁴² who immobilized thiolated DNA molecules on a gold surface, which were hybridized to DNA molecules containing a photocleavable spacer. Upon irradiation with UV light through a photolithography mask, the exposed DNA molecules were cleaved, and thus a pattern could be transferred into the DNA layer on the surface. Importantly, this process could be utilized to create single-stranded toeholds in the exposed DNA molecules, which was then used to replace the cleavage product by another oligonucleotide via toehold-mediated strand displacement. This could be applied to demonstrate multicolor lithography via immobilization of oligos with different fluorescence labels, and also erasable lithography, in which the same DNA layer was repeatedly used to create and erase a pattern. The same approach was shown to be applicable to the creation of patchy microparticles by UV exposure of DNA-functionalized microspheres. A related technique was later used by the same authors to trigger a hybridization chain reaction at UV-exposed areas on a chip.²⁴³ Here, the photocleavable group was placed into the loop of a surface-

immobilized DNA hairpin. Upon irradiation, the loop region was cleaved, exposing a single-stranded DNA sequence complementary to the toe hold of one of the HCR hairpins.

More recently, Pardatscher and co-workers used a similar approach (termed “Bephore” for “Biocompatible electron beam and photo-resist”) to immobilize gene-length DNA molecules rather than oligos onto biocompatible glass surfaces.²⁴⁴ In their case, biotinylated, hairpin-forming DNA molecules were attached to the substrate via a long polyethylene glycol (PEG) spacer (Figure 25). Upon irradiation with UV light, the hairpin containing a photosensitive linker was cleaved, resulting in the dissociation of one of the cleavage products. This led to the exposure of a toe hold sequence, which could be used for immobilization of labeled dsDNA molecules up to several 1000 bp in length. Already in earlier studies, Bar-Ziv and co-workers had demonstrated that it is possible to express genes on a chip surface, which were immobilized through the biocompatible PEG spacer “Daisy”.²⁴⁵ Pardatscher et al. could demonstrate that also with the Bephore approach, which is based on the Daisy concept, it is possible to perform cell-free gene expression reactions from lithographically structured gene brushes. One of the advantages of the technique is that the high specificity of the strand displacement reaction allows for a relatively background-free implementation of multistep lithography.

4.6.2. Pattern Formation. An unconventional approach toward pattern generation using DNA strand displacement techniques was taken by Chirieleison and co-workers,²⁴⁶ which combined UV cleavable DNA strands with catalytic hairpin assembly (CHA, cf. section 3.2.2). The researchers designed a spatially distributed incoherent feed-forward network,²⁴⁷ comprising two photosensitive DNA species with activating and deactivating function, respectively. The activating species in the network was the CHA trigger sequence sequestered within the loop of a stable hairpin structure containing a photocleavable group. Upon irradiation, the trigger is released from the structure, potentially initiating a CHA reaction. One of the two hairpins of the CHA reaction, however, was modified with a UV cleavable group in the toe hold region, rendering the hairpin catalytically inactive under light. Chirieleison and co-workers embedded the components of their circuits in a spatially distributed gel matrix and irradiated the gel with light through a mask. As a result of the deactivation of the CHA hairpin, no reaction was started by the trigger molecules released in the bright regions. However, trigger molecules could diffuse from irradiated to neighboring dark regions within the gel and trigger a CHA cycle there,

which was further translated into a fluorescence signal. As a result, fluorescence was generated only at the boundary between irradiated and nonirradiated regions, effectively resulting in autonomous “edge detection” by the reaction circuit.

4.7. Super-Resolution Imaging and DNA-PAINT

While not explicitly using toehold-mediated strand displacement, the DNA-based superresolution microscopy method DNA-PAINT at least philosophically also rests on this process. For now more than a decade, researchers have developed various approaches to break the diffraction limit for the resolution of microscopic images. Next to more physical approaches such as the STED technique,²⁴⁸ a variety of stochastic single molecule approaches like STORM or PALM were developed that rely on fluorescence signals recorded from single molecules.²⁴⁹ The crucial conceptual insight of these approaches is the fact that while it is impossible to resolve two light emitters with a distance on the order of the wavelength of light, the position of a single emitter can be determined with a much greater position (depending on the number of photons that can be collected from it). Thus, determining the positions of many single fluorophore labels on a sample allows the reconstruction of a pixelated but super-resolved image. In a collaboration of the Tinnefeld and Simmel laboratories, these super-resolution techniques were utilized for the first time also for imaging of DNA origami structures.²⁵⁰ From previous work on DNA driven nanodevices, it was clear that one could tune the kinetics of binding of oligonucleotides to a complementary binding position through their concentration (controlling the on-rate) and length of complementarity (controlling the off-rate). By choosing short enough sequence domains, one could achieve fast and spontaneous duplex association and dissociation at room temperature, without strand displacement. It thus was an obvious step to utilize fluorescently labeled “imager” strands to artificially generate a blinking fluorescence signal, whose dynamics could be controlled by concentration and sequence length. On the basis of this concept (termed DNA-PAINT due to its similarity with a related super-resolution technique called PAINT (points accumulation for imaging in nanoscale topography),²⁵¹ in 2010 Jungmann, Tinnefeld, Simmel, and co-workers thus created the first super-resolved images of DNA origami structures.²⁵² In collaboration with Peng Yin’s lab, Jungmann later refined the technique and developed several variations such as Exchange-PAINT,²⁵³ which allows 3D multiplex imaging. More recently, Jungmann and co-workers achieved an impressive “super-resolution” of only 5 nm between two neighboring imager binding sites.²⁵⁴ DNA-PAINT can be easily combined with strand displacement processes. For instance, imager binding sites can be reversibly blocked by inhibitor strands and activated via toehold-mediated strand displacement.²⁵⁵ In principle DNA-PAINT can thus also be combined with simple molecular circuitry, and activation of docking sites can be made conditional on various molecular inputs.

4.8. Challenges and Future Directions for Dynamic DNA Nanotechnology

As pointed out in the preceding paragraphs, DNA strand displacement is the central concept of dynamic DNA nanotechnology. It has allowed the creation of a range of prototypic molecular machines and motors and has been utilized in a wide variety of reconfigurable DNA-based nanostructures, which can be programmably switched between

different mechanical, conformational, or configurational states. So far, however, there have only been few, if any, “real-world applications” of such devices, and most of the work performed in the field of dynamic DNA nanotechnology has been on a “proof of concept” level. In this context, two major challenges stand out: (i) the slow speed of strand displacement processes and (ii) the availability of DNA fuels.

4.8.1. Speed. As mentioned above, the speed of toehold-mediated DNA strand displacement processes can be controlled by the length of the toehold. But even in the best case (for long enough toeholds), the effective second-order strand displacement rate will be on the order of only a few $10^6 \text{ M}^{-1} \text{ s}^{-1}$. As typical fuel strand concentrations used are in the range of 1–100 nM, reaction times are on the order of minutes. While this probably is acceptable for some applications, for example the control of DNA assembly reactions, it is prohibitively slow for molecular motors and transport systems: if a single strand displacement reaction is associated with a movement over a few nanometers, the corresponding velocities inevitably are in the range of nanometers per minute rather than the hundreds of nanometers per second achieved by biological molecular motors.

We have discussed several attempts to increase the performance and speed of strand displacement processes. With the use of an improved theoretical understanding of toehold-mediated strand displacement, processes can be used to optimize DNA sequences to achieve maximum and reproducible speeds. This involves avoidance or optimization of secondary structures in toeholds, fuels, and other participating strands. A common strategy in the past few years has been to localize strand displacement systems on origami platforms, which increases the local concentrations of the strands and reduces unwanted cross-talk. Co-localizing interacting components at $\approx 10 \text{ nm}$ between neighboring sites on an origami roughly corresponds to a concentration of $\approx 1 \text{ mM}$. With the use of a second-order rate of $10^6 \text{ M}^{-1} \text{ s}^{-1}$ results in a typical reaction time of 1 ms. When the strand displacement process is coupled to motion between the two sites, this value corresponds to a velocity of $\approx 10 \text{ nm/s}$. This would be something like the “speed limit” for molecular motors that are exclusively driven by localized strand displacement processes. If higher speeds are required by an application, other means for driving the devices (e.g., by coupling to other chemical processes or by use of physical energy inputs) will become necessary.

4.8.2. DNA as a Fuel. The unconventional use of DNA as a “fuel” comes with several unique features: the thermodynamic driving force associated with a DNA fuel, the hybridization free energy, is as high or even higher than the free energy change associated with ATP hydrolysis and thus can be used to generate similar forces as biological motors (see discussion in section 2.3). Furthermore, DNA fuels are sequence specific fuels; a given DNA fuel only drives a specific process, which is in stark contrast to biology’s universal energy “currency” ATP, which is indifferently used by almost all energy-consuming processes in a cell.

Being able to use fuel strands simultaneously as “molecular addresses” can be extremely useful if the control of a specific group of devices among others is desired or when molecular assembly processes have to be carried out in a specific order. However, in other contexts sequence-specificity may be undesirable or useless. For instance, driving each step of a molecular motor with a separate fuel strand would be

cumbersome and uneconomic. In fact, recent work on substrate-localized strand displacement processes has already been performed with “universal” fuel sequences.^{239,240}

One of the biggest problems associated with DNA fuels, however, is their “availability”; they have to be synthesized, prepared in a high energy state (for instance, hairpins), externally supplied to a dynamic DNA system, and waste products have to be removed somehow. In other words, there is no artificial metabolism for dynamic DNA nanotechnology that generates DNA fuels and removes them from a system.

It is conceivable to address these issues with a technological solution: dynamic DNA systems could be operated in microfluidic reaction chambers, which could be continuously supplied with fuels to drive DNA strand displacement reactions.¹³⁵ In principle, these DNA fuels could be regenerated and resupplied in the same system, and microfluidic control could even be used to “program” such systems. While such an approach could be appropriate for nanotechnological applications such as molecular assembly lines and the control of chemical processes, it is less obvious how to implement and make use of “autonomous” DNA nanodevices in a biochemical or biological context.

Single-stranded DNA is typically not available in a biological context (even though it can be generated biochemically, for example, using strand displacement amplification²⁵⁶), and therefore RNA has been considered as an alternative, naturally single-stranded “fuel” for nucleic acid nanodevices.²⁵⁷ As discussed in section 5, natural RNAs such as mRNA or microRNAs have been frequently used as biological inputs for biosensors based on strand displacement. However, so far RNA has not been utilized for controlling assembly processes or conformational transitions inside of cells. Given the recent development of genetically encodable RNA-based nanostructures,^{258,259} it is conceivable that also dynamic RNA nano-systems can be realized in the near future, of which all the components can be genetically expressed and operated in living cells, thus piggy-backing on the cell’s metabolism for continuously driving nanotechnological processes.

4.8.3. Future Directions. In light of the challenges stated above, it seems most likely that in the near future toehold-mediated DNA strand displacement will be predominantly used as a useful methodology for the control of DNA-based self-assembly processes and for the realization of addressable and reconfigurable nanostructures. Thus, the future of strand displacement reactions will be intimately linked to the future success or failure of DNA nanotechnology itself.

Given the biophysical restrictions discussed above, it seems unlikely that we will develop molecular motors driven by DNA strand displacement that are as fast and powerful as biological motors, however. In order to achieve faster molecular movements, other driving forces will be implemented in the future instead; nevertheless, strand displacement will still be used for “programming” or controlling these faster processes. Speed is an issue when a certain time-scale is imposed from the outside (e.g., for the realization of responsive systems that have to quickly react to an external stimulus) or when a certain throughput (e.g., the production rate of a molecular assembly line) is required. In other cases, the speeds achievable with strand displacement processes may be sufficient, however.

In fact, dynamic DNA nanotechnology could turn out to be the ideal basis for the emerging discipline of molecular robotics; as seen with the manifold examples presented in this section, DNA plays the role of a structural material with built-

in information-processing capabilities that are also capable of sensing and actuation. Thus, dynamic DNA nanotechnological systems intrinsically are molecular robotic systems.

5. APPLICATIONS IN SENSING, DIAGNOSTICS, AND THERAPEUTICS

The basic task of a molecular sensor is to facilitate detection of a potentially tiny amount of analyte through the generation of a measurable physical readout signal. Amplification reactions therefore are essential components of most molecular detection schemes, as they chemically “pre-amplify” the concentration of the analyte before a physical detection mechanism such as a fluorescence measurement is utilized. In the context of nucleic acids, the most well-known and successful amplification scheme is the polymerase chain reaction (PCR). On the basis of a thermal cycling protocol and repeated copying of the analyte sequence using a thermostable polymerase, detection of very few, even only single, DNA molecules of a specific sequence is possible. Even though in this sense the PCR reaction is unbeatable in terms of sensitivity, the PCR scheme cannot be utilized in all applications. For instance, thermal cycling may be undesirable (due to heat sensitivity of the analyte sample) or technically impossible (e.g., in low-cost or field applications). To address this issue, a variety of isothermal amplification schemes have been developed [e.g., ligation chain reaction (LCR) loop mediated amplification reaction (LAMP), recombinase polymerase amplification (RPA), or nucleic acid sequence-based amplification (NASBA)]. However, all of these isothermal schemes still require the action of DNA modifying or amplifying enzymes.

In recent years, a variety of enzyme-free amplification processes have been developed, which are based on catalytic DNA reactions such as the hybridization chain reaction (HCR) or catalytic hairpin assembly (CHA) described in section 3. These have been utilized for the detection of nucleic acids both *in vitro* as well as *in vivo*. Notably, hybridization-based schemes can be directly coupled to DNA computing routines and molecular actuation schemes. This allows the implementation of not only sensors but also the subsequent evaluation of the sensory input by a diagnostic DNA computer. The output of the computer may further be used to trigger the release of a therapeutic agent. In combination, DNA strand displacement processes can therefore be used to realize theranostic systems (systems that combine diagnosis and therapy) or even nanorobotic systems for medical applications.

We note that sensors based on nucleic acid amplification schemes have been extensively reviewed by others in the recent past,^{40,133,260} and the interested reader is also referred to these publications.

5.1. Sensing Based on the Hybridization Chain Reaction

5.1.1. In Situ Detection of mRNA Using HCR. An exciting application of the hybridization chain reaction is its use for *in situ* detection of mRNA molecules inside of (fixed) cells. The low abundance of the molecules and the high background fluorescence in cells requires amplification of the signal “on the spot”. Choi et al. developed a method, in which several sequence probes are designed to bind to a single target mRNA sequence, which carry a common sequence extension that acts as a trigger for HCR.⁸⁵ For each mRNA molecule, thus multiple HCR processes are triggered, which can be detected by fluorescently labeling the H1 and H2 hairpins. In

order to reduce background fluorescence, *in situ* hybridization experiments are carried out under stringent conditions (using a low ionic strength citrate buffer and formamide), which prevents unspecific interaction between probes and non-cognate targets. Choi et al. found that the original HCR scheme was incompatible with stringent buffer conditions; instead of the original 18 bp stem hairpins with 6 nt loops/toeholds, they had to switch to RNA hairpins with a larger 10 nt loop size and 16 bp long stems (also utilizing the fact that bases in A-form RNA duplexes have stronger stacking interactions than bases in B-DNA). As fluorescently labeled RNA probes represented a considerable cost issue, a “second generation” HCR system for *in situ* hybridization amplification was established, which consisted of DNA hairpins with 12 nt toeholds/loops and 24 bp stems.²⁶¹ This new system also worked under permissive conditions (i.e., using a high ionic strength buffer at $T = 25\text{ }^{\circ}\text{C}$). More recently, the authors even further improved the system: using split initiator probes, triggering the HCR process becomes cooperatively dependent on the presence of the two mRNA subsequences, which are recognized by the probes.²⁶² This further reduces the background and thus improves signal-to-noise ratio and spatial resolution of the technique. *In situ* HCR v3.0 is now being commercialized by Molecular Instruments, Inc.²⁶³

One of the advantages of the HCR method for this application is that the labeled hairpins can easily diffuse into the cellular sample, and amplification by the chain reaction directly takes place *in situ*. Furthermore, in contrast to enzyme-mediated detection (such as chemiluminescence), which generates diffusing signals, the fluorescence probes are directly attached to the site of the mRNA, providing a higher spatial resolution.

5.1.2. Other Bioanalytical Applications of HCR. HCR reactions have been employed in a wide variety of other sensing applications. First and foremost, HCR schemes have been used for sensing and amplification of DNA or RNA analytes.^{85,110,264–279} HCR can be used, however, for the detection of other molecules by utilizing aptamer^{110,280,281} or antibody recognition. Aptamer-based detectors either utilize a structural rearrangement of the aptamer upon ligand-binding that triggers the HCR reaction or they simply use the aptamer as a tether for the trigger sequence. This has been utilized for detection of analytes such as ATP,¹¹⁰ interferon γ ,²⁸⁰ platelet-derived growth factor,²⁸¹ thrombin,²⁸² or cell surface epitopes.²⁸³

Antibodies have been utilized in approaches such as immuno-HCR,²⁸⁵ which are derived from typical antibody sandwich assays. Here an analyte first binds to an antibody-coated surface or particle. This allows binding of secondary antibodies to which the HCR trigger DNA is covalently attached. Addition of H1 and H2 hairpins then amplifies the detection event on the spot for readout either via fluorescence, plasmonic, or electrochemical effects. Antibody-coupled HCR reactions were used to detect a wide variety of proteins such as cytokines,²⁸⁵ carcinoembryonic antigen,²⁸⁶ thyroxine,²⁸⁷ and others.

Rather than using linear amplification via HCR, branched (Figure 26)²⁸⁴ and even “hyper-branched”²⁸⁸ HCR techniques have been developed. HCR branching can be achieved via the creation of two identical toeholds in one HCR step, which leads to the growth of DNA dendrimers rather than linear polymers, resulting in exponential instead of linear signal amplification in the early growth phase. Hyperbranched HCR

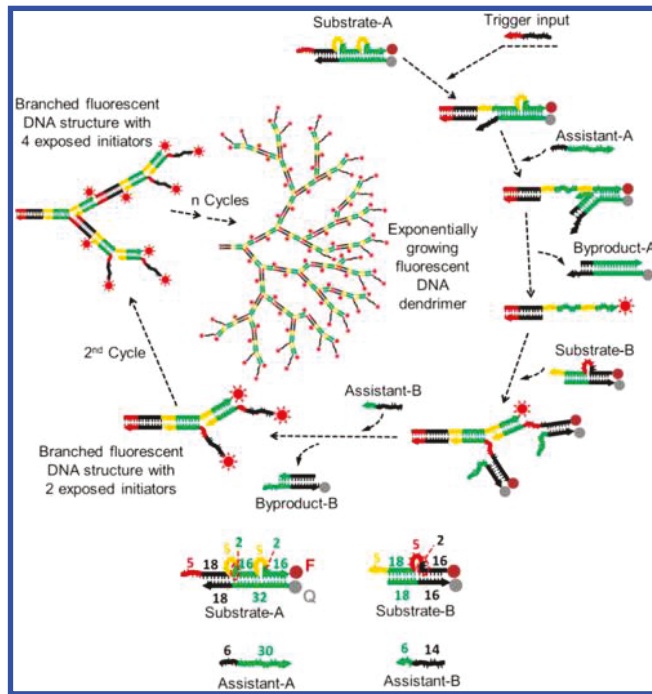


Figure 26. Branched HCR generates an exponentially growing dendrimer rather than a linear polymer.²⁸⁴ In contrast to HCR, the substrate A contains two toehold loops, and next to a trigger, two assistant strands are required. Reprinted with permission from ref 284. Copyright 2014 American Chemical Society.

(HB-HCR) utilizes two additional “super-hairpins” SH1 and SH2 next to the H1 and H2 hairpins, which expose two toeholds each upon hybridization to a growing dendrimer structure.

In several cases, HCR was combined with another amplification scheme such as circular strand displacement polymerase reaction²⁶⁹ or catalytic hairpin assembly^{270,276} (see next section), which resulted in limits of detection in the femtomolar range or lower. Instead of fluorescent probes, HCR processes were read out using various other detection schemes (e.g., excimer probes,²⁷⁴ bioluminescence,²⁷¹ chemiluminescence,^{264,268} electrochemiluminescence,²⁶⁶ electrochemical detection,^{267,270} colorimetric,²⁷⁹ or quartz crystal microbalance detection).²⁶⁵ For a more complete overview of HCR and its applications in sensing, imaging, and biomedicine, the reader is referred to the dedicated review by Bi, Yue, and Zhang.⁴⁰

5.2. Biosensors Based on Catalytic Hairpin Assembly

On the basis of catalytic hairpin assembly, a wide range of sensors has been developed over the past few years. With the use of similar principles as the HCR sensors discussed above, the CHA reaction has been applied to the detection of the same analyte classes (i.e., metal ions,^{289–295} DNA and DNA mismatches,^{296–305} mRNA,³⁰⁶ microRNAs,^{307–311,311–327} proteins,^{286,328–335} and cells).³³⁶ As for the HCR, analytes other than nucleic acids can be detected by coupling the CHA scheme to aptamer target recognition. CHA has also been used in more unconventional applications (e.g., for the detection of uracil-DNA glycosylase activity³³⁷ and in the context of food safety).^{338,339} For instance, CHA has been proposed for the detection of tetracycline-based antibiotics in milk samples.³³⁸ In this application, one of the CHA hairpins (H1, cf. Figure 14) is designed to contain an aptamer sequence for

tetracycline. In the presence of the drug, the aptamer restructures and hybridizes with H2. This releases the analyte and makes it available for another round of CHA. There have also been reports on intracellular detection of disease-associated mRNA molecules, which could have potential applications in theranostics.³⁴⁰ A good overview of diagnostic applications of nucleic acid circuits with emphasis on CHA is given in ref 260.

5.2.1. Reaction Cascades and Networks Based on Catalytic Hairpin Assembly. Rather than using CHA as a detection scheme, a variety of CHA-based reaction networks have been demonstrated, in which several CHA processes were linked together or were coupled to other dynamic processes. For instance, the output of enzymatic amplification schemes such as strand displacement amplification (SDA) or rolling circle amplification (RCA) was used as trigger for a subsequent CHA process, which increased both the specificity and sensitivity of the detection.^{341,342} Cascading CHA reactions into two-layer or even four-layer circuits led to signal amplification of up to 600,000 fold.³⁴³ A cross-catalytic network of two CHA amplification loops enabled exponential signal amplification and was also used to implement logic circuits.³⁴⁴

Bhadra and Ellington also demonstrated the realization of RNA-based CHA reactions.³⁴⁵ Using *in vitro* transcription from DNA templates, they synthesized RNA hairpins and trigger molecules for execution of various CHA circuits (e.g., signal amplifiers or OR logic gate processors). The circuits could be executed either with purified components or cotranscriptionally. Also more unconventional applications of CHA in reaction circuits have been described. For instance, a photosensitive CHA reaction was utilized for an *in vitro* reaction network capable of autonomous edge detection,²⁴⁶ which was already discussed in the paragraph on patterning and lithography above (section 4.6).

5.3. Other Sensor Schemes Based on Toehold-Mediated Strand Displacement

Apart from the HCR and CHA amplification schemes discussed in more detail above, a plethora of other ingenious sensor concepts have been developed over the past years that utilized toehold-mediated strand displacement in one way or another. In the following, we give a brief and probably nonexhaustive survey of the main applications in the detection of nucleic acids, proteins, small molecules, and metal ions, and in other sensor applications such as whole cell biosensors.

5.3.1. DNA and RNA Detection. **5.3.1.1. Mismatch Detection and Genotyping.** The detection of single nucleotide mismatches and single nucleotide polymorphisms (SNPs) are key applications of DNA strand displacement in identifying genetic variations and in disease diagnostics. As many genetic diseases are caused by single point mutations, the ability to detect these alleles is essential for their diagnosis. A large variety of detection schemes has been developed, and also first commercial applications are emerging.

One general approach is based on signal amplification by toehold-mediated strand displacement recycling of a nucleic acid sequence (i.e., hybridization catalysis). For instance, Wu et al. created a DNA probe containing a target specific region with an LNA base at the SNP position, which allows single-base discrimination between different SNPs. The sensor complex also comprises a fluorophore and a quencher labeled sequence. The latter is displaced by the analyte sequence with

the “correct” SNP, leading to an increase in fluorescence. Toehold-mediated strand displacement with two helper DNA strands is used to recycle the analyte, enabling recognition of a single nucleotide variant with a detection limit as low as 6 fM.³⁴⁶ A similar sensor scheme was combined with an electrochemical sensor platform by Gao et al.³⁴⁷

As the kinetics of strand displacement processes are highly sensitive to the presence of mismatches, this feature can also be utilized for single-base mismatch discrimination. An interesting approach toward SNP genotyping was developed by Khodakov and co-workers who first used PCR of the analyte DNA to generate dsDNA molecules with single-stranded overhangs (“toehold-PCR products”). The toeholds were introduced by using deoxyuracil-containing primers for PCR, followed by digestion of the primers with uracil-DNA glycosylase. The different kinetics of toehold-mediated strand transfer then allowed for a discrimination of different SNPs and was also used for sex genotyping³⁴⁸ or to discriminate single nucleotide polymorphisms in human mitochondrial DNA samples.³⁴⁹

A different approach for thermodynamic discrimination between target and nontarget strands (or mismatches) was taken by David Zhang and co-workers.³⁵⁰ One of the problems in discriminating long and very similar sequences is that even in the presence of mismatches, hybridization at low temperatures can be very efficient. In order to discriminate between matched and mismatched sequences, one approach is to analyze the DNA samples of interest at the melting temperature of the target strand. At this temperature, 50% of the strands are, by definition, in a duplex form, while nontarget strands have a much lower hybridization yield. On the basis of a thorough analysis of the thermodynamics of strand association, Zhang et al. came up with a new approach for mismatch detection using so-called “toehold exchange probes”. In this approach, the complement sequence C of the target sequence X is initially hybridized to a protector strand P. The complex PC contains a toehold for strand exchange with X. Upon formation of the complex XC, P can displace X again via a second toehold region (similar to the seesaw concept shown in Figure 7). It turns out that the standard free energy change for this toehold exchange reaction is close to zero, while that for a strand with only a single mismatch is markedly positive. This results in very different equilibrium concentrations of the strands and complexes involved, allowing a very good discrimination between very similar strands even at room temperature. The authors also show that these probes are robust with respect to changes in strand concentration (in contrast to a melting temperature based approach). Toehold exchange probes are currently being further developed by the company “Nuprobe”³⁵¹ and thus represent one of first commercial products based on toehold-mediated strand displacement.

Other approaches combined strand displacement with isothermal DNA amplification,³⁵² utilized lambda exonuclease activity,³⁵³ or PCR amplification.³⁵⁴ Enzyme-free SNP and mutation detection was achieved by several groups with a nanomolar detection range,^{355–357} and also DNA origami platforms were explored for SNP-genotyping.³⁵⁸

5.3.1.2. Specific Detection of Nucleic Acid Sequences. Rather than focusing on single base mismatches, a wide variety of sensors have been described for the specific detection of nucleic acid sequences. This involves toehold-mediated strand displacement combined with molecular beacons,³⁵⁹ dendritic assemblies from DNA and PNA,³⁶⁰ and various sensors based

on fluorogenic G quadruplexes.^{361,362} Strand displacement schemes were combined with surface enhanced Raman scattering (SERS),³⁶³ electrochemiluminescence,⁷⁴ or enzymatic amplification by acetylcholinesterase,³⁶⁴ to name but a few. Depending on the specific scheme and the number of amplification steps, limits of detection in the picomolar,³⁶⁵ femtomolar,^{72,76,77,366} or even attomolar range^{73,78,367} were reported.

5.3.1.3. Detection of Nucleic Acid Amplicons. Strand exchange reactions can also be utilized for real-time detection of nucleic acid amplification products.³⁶⁸ In this context, Ellington and co-workers demonstrated that products of a loop-mediated isothermal amplification (LAMP) reaction could be read out via a strand exchange reaction rather than using an intercalating dye. This allowed a better distinction of true amplicons from side products, SNP specificity, and also real-time detection of different genes in multiplex LAMP reactions.

5.3.1.4. RNA Detection. Direct detection of RNA can be useful in biomedical diagnostics. For instance, toehold-mediated strand displacement combined with a quantum dot readout has been utilized to detect tuberculosis-related mRNA biomarkers.⁶⁸ In another approach, RNA target molecules were used to trigger the formation of a Au-NP containing DNA network for colorimetric readout, which facilitated differentiation between the 16S rRNAs of closely related bacteria with a detection limit of $\geq 5 \times 10^5$ CFU.³⁶⁹ Similar as for the HCR and CHA discussed above, also a large number of miRNA sensors have been developed (Figure 27), which utilize strand displacement reactions in their sensing scheme, achieving detection of miRNA from the nanomolar down to the femtomolar range.^{109,370–385} Of note, Zhang et al.³⁸² achieved detection of miRNA at a concentration of 67 aM using a DNA walker scheme, and Shen et al. also used strand displacement techniques for sensitive miRNA imaging.³⁸³

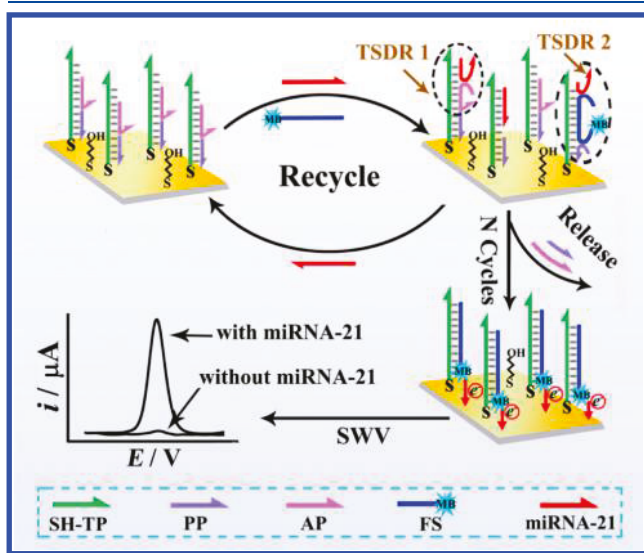


Figure 27. An miRNA sensor exemplifying the principle of strand displacement recycling.³⁷¹ In this scheme, the analyte (miRNA-21) displaces a protecting strand PP from a DNA molecule immobilized on a gold electrode. This enables hybridization of a methylene blue-labeled electrochemical probe strand, which recycles the miRNA-21 analyte. Thus, a single analyte molecule is translated into multiple labeled probe strands. Reprinted with permission from ref 371. Copyright 2015 American Chemical Society.

5.3.2. Protein Detection. Strand displacement techniques have also been widely used in the context of protein detection. Obviously, this requires a different type of interaction between analyte and DNA than the base-pairing interactions utilized for nucleic acid sensing. Most often, some kind of aptamer recognition is used to “translate” from the protein to the nucleic acid “language”, but also other interactions have been utilized.

Aptamers in combination with toehold-mediated strand displacement have been applied to sense cancer markers such as epithelial cell adhesion molecules (EpCAMs) via fluorescence (with a detection limit of 0.1 ng/mL³⁸⁶) or an electrochemical readout (LOD = 20 pg/mL³⁸⁷). Similar approaches were used to detect thrombin,^{388,389} prostate-specific antigen,³⁹⁰ vascular endothelial growth factor (VEGF),³⁹¹ or epidermal growth factor receptor-2 (HER2).³⁹² Huang et al. combined binding of a ligand-modified DNA probe to a protein with proximity induced photo-cross-linking followed by toehold-mediated strand displacement to generate specific probe complexes consisting of a protein tagged with two DNA sequences.³⁹³ With the use of graphene oxide (GO) as an amplifier for fluorescence anisotropy, the toxic protein ricin was detected with a linear range of detection between 1.0 and 13.3 μ g/mL and an LOD of 400 ng/mL (Figure 28).³⁹⁴

Implementing several steps of signal amplification is a general strategy to create ultrasensitive sensors. For instance, Yang et al. detected thrombin with a linear detection range from 100 fM to 10 nM and an LOD of only 30 fM³⁹⁵ by combining toehold-mediated target recycling, hybridization chain reaction, and electrochemical readout. A variety of strand displacement-based sensors were also developed for the assessment of enzyme activity; this is most naturally achieved for DNA-modifying enzymes such as T4 DNA ligase,³⁶¹ methyl transferase,³⁹⁶ uracil-DNA glycosylase (UDG),^{397,398} or telomerase.³⁹⁹

With the use of aptamer recognition combined with DNA strand displacement, also whole cell sensors have been developed. For instance, Guo and co-workers utilized an aptamer-functionalized chip surface to capture circulating tumor cells from blood samples. With the use of toehold-mediated strand displacement, the cells could be detached from the surface after washing and further characterized by analysis of additional aptamers bound to the cells’ surfaces.⁴⁰⁰

5.3.3. Sensing of Small Molecules and Ions. Coupling aptamer recognition to strand displacement also has been utilized for the detection of small organic compounds such as cocaine,⁴⁰¹ bisphenol A,⁴⁰² and aflatoxin B1.¹⁰⁶ In the approach by Chen et al.,⁴⁰² upon binding of bisphenol A to its DNA aptamer, a toehold sequence is exposed, which catalyzes the assembly of multiple DNA Y-junctions from DNA hairpins. The Y-junctions are resistant to Exo-III digestion and can be detected via Sybr Green I, resulting in a 5 fM LOD. Detection of aflatoxin B1 followed essentially the same approach.¹⁰⁶ Also the frequently utilized DNA aptamer for ATP was switched via a strand displacement process. For instance, Peng et al. created a three-arm junction assembled from three ATP binding aptamers,⁴⁰³ which could be switched between ATP-binding and ATP-releasing conformations.

Finally, even ions, typically those of heavy metals such as Hg^{2+} or Pb^{2+} , can be detected by utilizing the ion-dependent activity of deoxyribozymes or metal binding aptamers. Combining these with electrochemical detection,⁴⁰⁴ graphene

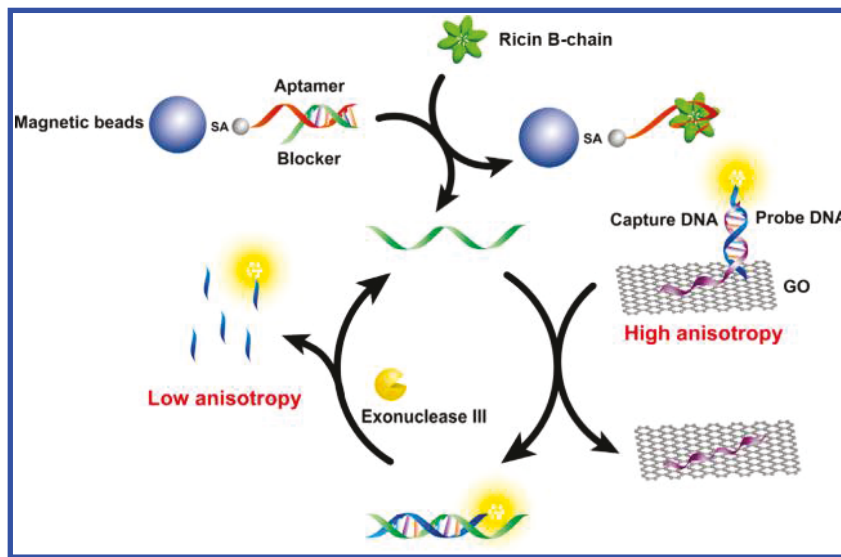


Figure 28. Detection of a protein (Ricin B-chain) by a combination of aptamer recognition and strand displacement recycling supported by exonuclease III.³⁹⁴ Upon binding of ricin to its aptamer, blocker DNA is released and displaces probe DNA from the graphene oxide (GO) sensor surface. Exo III (attacking blunt or recessed 3' ends) degrades only the fluorescently labeled probe, leading to a strong drop in fluorescence anisotropy of the fluorophore compared to the GO-bound state, while the blocker strand is recycled in this process. Reprinted with permission from ref 394. Copyright 2016 American Chemical Society.

oxide quenching,¹⁰⁸ exonuclease III-based target recycling, and HCR amplification,^{405,406} limits of detection in the picomolar range were achieved.

5.4. Autonomous Diagnosis and Therapy

With the use of switchable nucleic acid nanostructures, it is possible to directly couple biomedical sensor functions to the release of therapeutics, resulting in autonomous “theranostic nanodevices” or even biomedical “nanorobots”. A variety of switchable molecular containers for controlled release applications has already been described above.^{218,219} Delivery of therapeutics does not necessarily require a cagelike container, however.

You et al. designed DNA nanodevices (they termed “nanoclaws”) that combine aptamer recognition with strand displacement reactions to detect cancer cell surface markers and respond with targeted photodynamic therapy.⁷⁰ The devices consisted of Y- or X-shaped DNA nanoconstructs whose extensions carried the aptamers Sgc8c, Sgc4f, and TC01 which bind to three overexpressed markers on the surface of human acute lymphoblastic leukemia cells (CCRF-CEM). One of the extensions was modified with a quencher and an effector, either a fluorescent dye or drug. Importantly, the aptamer extensions were initially sequestered by complementary DNA containing a toehold region. Upon binding of the nanoclaw to a cancer cell surface, the complementary DNA was released and activated the effector molecule by displacing the quencher strand. With the use of the same implementation of strand displacement logic as in Seelig et al.,²⁶ this could be made conditionally dependent on several input signals. For photodynamic therapy, a porphyrin-based photosensitizer, chlorine e6 (Ce6), was employed to induce the generation of reactive oxygen species (ROS) upon light irradiation.⁶⁹

Rudchenko, Stojanovic, and co-workers demonstrated a similar molecular automaton that utilized antibodies for cell surface markers (Figure 29), in their case the “clusters of differentiation” CD45, CD20, CD3, and CD8, which allow distinction between B cells (CD45+CD20+) and T cells (CD45+CD3+).⁴⁰⁷ These antibodies were conjugated to DNA

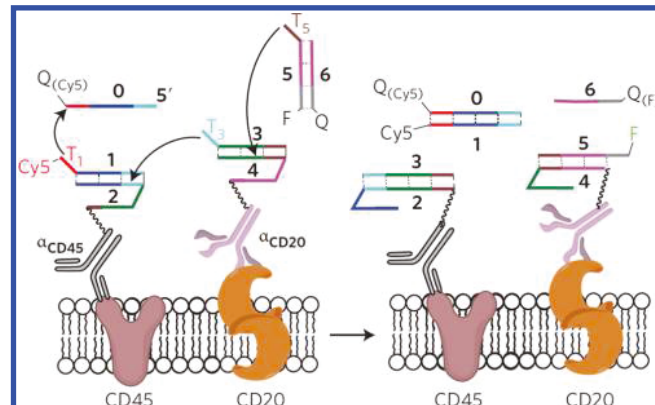


Figure 29. A strand displacement cascade proceeding on a cell membrane.⁴⁰⁷ The DNA strands comprising the cascade are attached to cell surface markers CD45 and CD20 via antibodies. In the process shown here, the fluorophore Cy5 is quenched, while the fluorophore F is unquenched. The reaction requires the presence of both CD45 and CD20 and can be read out via flow cytometry. Reprinted with permission from ref 407. Copyright 2013 SpringerNature.

strand displacement probes, which, when bound in close proximity onto a cell surface, executed a strand displacement cascade that generated a fluorescent readout for flow cytometry. Mixtures of automata strands could be used to distinguish between different cell types but also detect the absence of any marker.

Zhang et al. demonstrated smart nanocarriers consisting of gold nanorods decorated with Y-shaped DNA constructs and several shells of surface functionalization which allowed efficient penetration of biological barriers. Inside of the cell, the nanocarriers released the cancer therapeutic doxorubicin, while the Y-DNA molecules released siRNA in response to the presence of certain microRNAs. The nanocarriers were shown to synergistically inhibit tumor growth *in vivo* by silencing gene expression and inducing cell apoptosis.⁷¹

5.5. Challenges and Future Directions for Biosensors Based on Strand Displacement

A large variety of ingenious sensor schemes have been developed that utilize DNA strand displacement for the detection of DNA, RNA, proteins, or small molecules. Some schemes can discriminate single nucleotide mismatches while others have limits of detection down to the attomolar range (1 aM corresponds to only 600 molecules in a 1 mL sample!). Even though many schemes utilize strand displacement in conjunction with enzymatic amplification, strand displacement sensors in principle can be operated enzyme-free and isothermally. This makes such sensors potentially low-cost (when coupled to an inexpensive detection method) and robust, which should be of great interest for point-of-care testing and for applications in developing countries.

Strand displacement sensors are naturally best-suited for the detection of nucleic acid analytes. On the basis of our extensive knowledge of DNA hybridization thermodynamics and kinetics, our understanding of strand displacement processes, and the availability of computational prediction tools, it is possible to rationally design probes for a given target sequence. It is thus maybe not surprising that the first commercial applications of strand displacement techniques have emerged in this area (e.g., Nuprobe),³⁵¹ which develop isothermal DNA probes with single mismatch discrimination, and Molecular Instruments, Inc.²⁶³ commercializing *in situ* HCR for quantitative mRNA imaging. It can be expected that also other strand displacement-based detection schemes for nucleic acids will find their way into commercial applications in the near future.

As discussed, sensing of other analytes than nucleic acids requires the utilization of aptamers or antibodies for the primary detection event. The performance of such sensors is thus strongly dependent on the properties of the aptamer or antibody used. As a consequence, the details of the signal amplification scheme as well as buffer and potentially temperature requirements usually have to be adapted for each analyte in order to account for varying dissociation constants and specificities. This may be one of the reasons why there has not been widespread application of strand displacement-based protein or small molecule sensors yet. It is conceivable, however, that sensors could be developed in a modular fashion that consist of a variable aptamer-based input stage that transduces a given molecular input into a standard DNA signal, which is then amplified by a constant strand displacement-based amplification stage. Similar to nucleic acid detection, such sensors could potentially provide enzyme-free and robust detection of a wide range of analytes.

As already mentioned, future research in dynamic DNA nanotechnology will be directed toward the realization of molecular robotic systems that integrate sensing and actuation with information-processing. In this context, nucleic acid based *in vivo* sensors will play an important role for the realization of nanomedical robotic devices that couple molecular recognition events to diagnostics and therapeutic action. In fact, some of the first examples of such robotic devices were already equipped with “aptamer locks”, which were used to couple a sensing event to a conformational transition that led to the presentation of molecular cargo.^{218,219}

6. APPLICATIONS IN SYNTHETIC BIOLOGY

As discussed above, there have been a multitude of applications for branch migration in nanotechnology and biosensing. In a sense, DNA nanotechnology “traditionally” uses DNA in a nonbiological context; DNA serves as a building material or is utilized for the realization of molecular machines or computers. However, nucleic acids *do* have a biological function, and their sequence usually has a biological meaning.

This fact is already utilized for the DNA-based biosensors reviewed in the previous section, which aim at the detection of analytes of biomedical relevance. One can go even further and ask whether one can utilize concepts such as toehold-mediated strand displacement for the controlled interference with biological functions or even the creation of synthetic biological systems *de novo*, and this is where DNA nanotechnology enters the realm of synthetic biology.

One of the goals of synthetic biology is the creation of synthetic control circuits for biological functions in order to implement logical computation, decision-making, or pattern formation in biological systems. In contrast to other biological molecules that are employed for these goals, nucleic acid molecules again offer the unique possibility to rationally program molecular recognition interactions through the choice of their sequence.

The realization of strand displacement processes in the cellular context differs considerably depending on the cellular “chassis”, in particular whether their implementation is desired inside of bacteria or eukaryotes. Bacteria grow and divide relatively fast, and RNA degradation proceeds rapidly. Therefore, RNA-based circuits in bacteria require constant production of RNA species, and circuit operation has to consider their continuous build-up and degradation. By contrast, eukaryotic cells (most often mammalian cells in this context) do not grow and divide as quickly, and RNA degradation is slightly less of an issue. For applications in mammalian cells, the circuit components can therefore be delivered from the outside using transfection agents and then operated within an approximately static cellular environment. In addition, chemically stabilized nucleic acid species can be used as they are not diluted by cell growth and division.

6.1. Synthetic Riboregulators

6.1.1. First Generation Riboregulators. RNA-based gene regulatory processes are an obvious area of application for strand displacement techniques in synthetic biology. One interesting class of molecules in this context are the riboregulators, which are related to naturally occurring riboswitches. Riboswitches are aptamer-based regulatory regions present in the 5' untranslated region (UTR) of many bacterial mRNA molecules (some are also found in mRNAs of archaea, plants, and fungi), in which the accessibility of the ribosome binding site (RBS) is dependent on the binding of a small molecule metabolite. In the presence of the metabolite, the riboswitch undergoes a conformational change, which leads to either sequestration or release of the RBS (depending on whether this is negative or positive regulation).⁴⁰⁸

Synthetic riboregulators can be modeled after this scheme by making the conformational switch dependent on another RNA molecule instead of a metabolite. One of the first examples of a synthetic riboregulator controlling the expression of GFP in *E. coli* cells was provided by Isaacs et al. in 2004.⁴⁰⁹ They designed a “*cis*-repressing” RNA motif, which inhibited translation of an mRNA into GFP by sequestering the RBS

within the stem of a hairpin structure placed in the 5' UTR. Translation could be activated by the expression of a “trans-acting” RNA molecule, which was capable of binding to the hairpin of the cis-repressing RNA, breaking the secondary structure and thus releasing the RBS. For the best riboregulators, this scheme resulted in a \approx 20-fold change in gene expression upon activation. While not explicitly stated by Isaacs and co-workers, the riboregulator design utilized the loop region of the cis-repressing RNA as an internal toehold for nucleation of the cis-repressing/trans-acting RNA interaction and thus was also based on a strand invasion mechanism.

The design of the riboregulator switches was guided by thermodynamic calculations using the Mfold prediction tool. While such calculations are extremely important for the design process, one has to consider that intracellular conditions may differ strongly from the idealized experimental conditions under which the thermodynamic data underlying the predictions were generated. In this context, an interesting study by Lucks et al. using the SHAPE-Seq technique demonstrated that the riboregulator switches essentially folded and performed *in vivo* as designed but that there were also several deviations in the actually realized base-pairing patterns.⁴¹⁰

6.1.2. Toehold Riboregulators. The riboregulator design of the Isaacs paper was re-engineered in 2014 by explicitly using an external toehold for strand invasion into the regulatory hairpin.⁴¹¹ The mechanism of the “toehold switch riboregulator” is depicted in Figure 30. In the new design, the RBS is sequestered in the hairpin loop of the riboregulator,

while the start codon for translation (AUG) is placed into a bulge loop in the stem. As a result, the remaining sequence of the hairpin-stem loop can be freely chosen (i.e., it does not contain an anti-RBS sequence). In addition, the hairpin is extended at its 5' end with a 12 nt toehold sequence. In the folded state, the riboregulator is translationally inactive. Upon addition of a trigger RNA molecule, which is complementary to the toehold and (half of) the stem sequence, the hairpin structure is broken by strand invasion, exposing the RBS and AUG sequences. In this state, the ribosome can assemble on the mRNA molecule and translate its coding region into a protein. In a first round of rational design, a set of 168 toehold switches was investigated that exhibited ON/OFF gene expression ratios of up to 300. Thermodynamic analysis of the structures resulted in a number of thermodynamic “predictors” based on which the toehold switches could be further improved in a “forward-design” step, resulting in 13 more riboregulators with one exhibiting an ON/OFF ratio of more than 600!

Instead of synthetic trigger molecules, the authors were also able to use naturally occurring small RNAs as inputs and also mRNA molecules. For these natural RNA triggers, a secondary structure had to be taken into account, and this also required an extension of the toehold length to more than 24 nt. In contrast to the synthetically triggered switches, activation by natural RNAs resulted in reduced ON/OFF ratios in the range of 10–50.

The possibility for mRNA detection by toehold switches was then applied successfully by Pardee et al. for the realization of paper-based biosensors.⁴¹³ To this end, an *in vitro* transcription-translation mix was freeze-dried on paper and then used for the specific detection of disease-related mRNAs; for instance, the sensor could be used to distinguish mRNA from two different strains of Ebola virus.

More recently, Green et al. also demonstrated that toehold switches can be used for complex RNA-based input logic, which makes protein expression dependent on the presence of more than one trigger RNA.⁴¹² They showed multi-input AND and OR logic and also the evaluation of more complex circuits composed of AND, OR, and NOT components in disjunctive normal form (DNF) (cf. Figure 30B).

6.1.3. Translational Inhibitors and the YUNR Motif.

Rather than translational activation as realized in the toehold switches discussed in the previous paragraph, a similar scheme may be employed to inhibit translation by masking the ribosome binding site on an mRNA molecule. For instance, in the naturally occurring RNA-IN/RNA-OUT system in *E. coli*, the short noncoding RNA-OUT molecule binds to the complementary RNA-IN and regulates the expression level of insertion sequence IS10 both by masking its RBS and increasing RNA degradation. Interactions between RNA-IN and RNA-OUT are nucleated in the loop region of RNA-OUT, which contains a pyrimidine-uracil-nucleotide-purine (YUNR) motif, corresponding to an “internal” toehold in the hairpin loop. On the basis of the RNA-IN/RNA-OUT system, Mutualik and co-workers designed a library of 23 orthogonal regulator pairs, in which 5 nucleotides in the RNA-OUT recognition loop were mutated.⁴¹⁴ The library was tested experimentally *in vivo*, displaying strong variations in translational repression efficiency, ranging from less than 5% to more than 90%. Analysis of the results demonstrated that the YUNR motif was not essential for the performance of the artificial RNA regulators. The YUNR U-turn enforces a sharp bend in

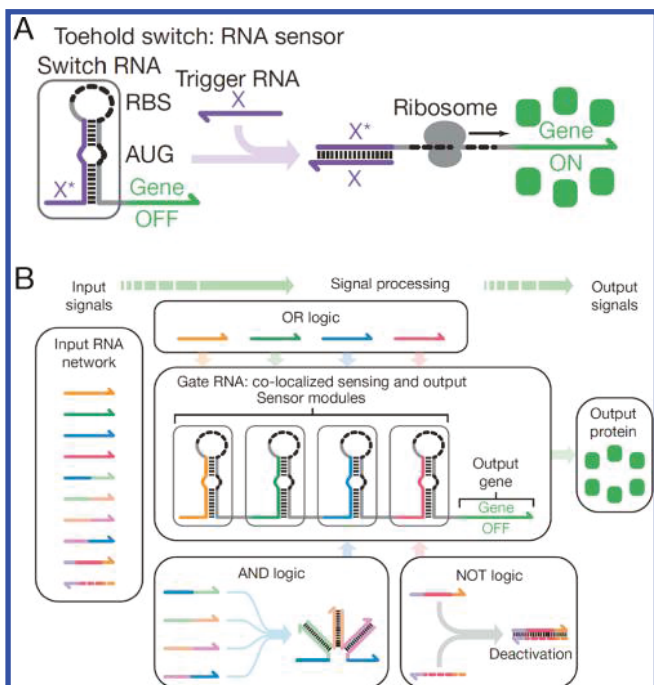


Figure 30. Principle of the toehold riboregulator switch⁴¹¹ and multi-input logic.⁴¹² (A) In the OFF state of the toehold switch RNA, the ribosome binding site (RBS) is sequestered in a hairpin loop as indicated. Hybridization with a trigger RNA X opens the hairpin and switches ON translation of the protein coding region of the RNA. (B) The toehold switch principle can be extended to multi-input AND and OR logic as indicated. Modified and reprinted with permission from ref 412. Copyright 2017 Nature Research.

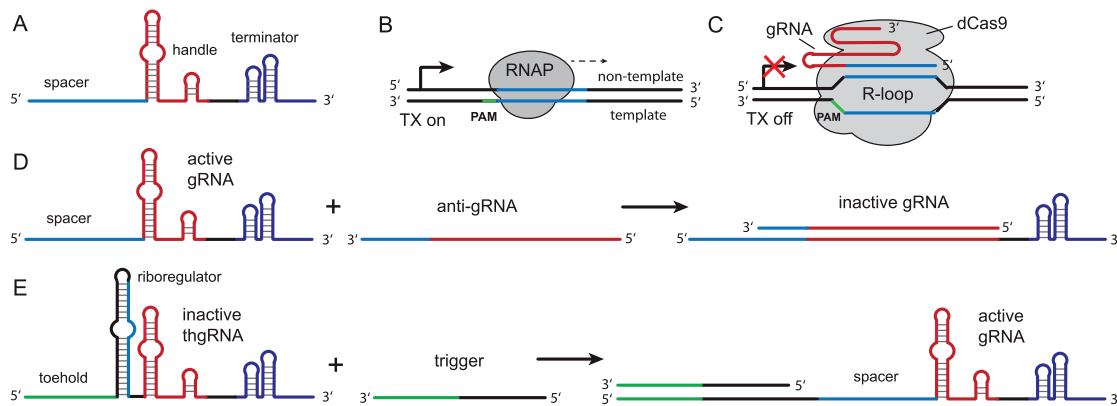


Figure 31. Controlling CRISPR interference via toehold-mediated strand invasion. (A) Structure of a guide RNA (gRNA) for Cas9, which binds to the handle of the molecule. (B) Transcription (TX) of a genetic template by RNA polymerase (RNAP). (C) In CRISPR interference, transcription is repressed by a catalytically inactive Cas protein (dCas9). gRNA directs dCas9 to bind to a sequence complementary to the spacer region, which must be flanked by a “protospacer adjacent motif” (PAM) as indicated. In the example shown, the non-template strand downstream of the promoter is targeted, which blocks transcriptional elongation by RNAP. (D) gRNA can be inactivated by disrupting the handle via strand invasion by an antisense RNA molecule, preventing dCas9 from binding to the gRNA (cf. ref 419). (E) The spacer region of the gRNA can also be sequestered in a riboregulator structure similar as in the toehold riboregulator described in Figure 30. The resulting “toehold” gRNA (thgRNA) can then be activated by an appropriate trigger RNA molecule (cf. ref 420).

phosphate backbone of a stem-loop structure. The bases following the bend are exposed to the solvent in a stacked configuration, making them available for base-pairing. In their study, Mutalik et al. found that also other 5 nt loop recognition sequences performed well, potentially because the A-U rich stem close to the loop provided enough flexibility for nucleation of the first base pairs.

6.2. Combining Strand Invasion with CRISPR Mechanisms

In the past years, life science research has been transformed by the development of new tools for genetic engineering based on CRISPR (“clustered regularly interspaced short palindromic repeats”) elements.^{415,416} In particular the CRISPR/Cas9 technology has enabled the precise cutting of double-stranded DNA molecules at arbitrary sequence locations, which can be freely programmed by the choice of an appropriate “guide RNA” (gRNA, see Figure 31A). Cas9 (CRISPR-associated protein 9) is a ≈ 160 kDa large protein, which comprises two distinct nuclease domains for cleavage of the target and nontarget DNA strand.⁴¹⁷ Cas9 binds to guide RNA molecules containing a specific handle sequence, and the sequence contained in the “protospacer” section of the gRNA directs the Cas9:gRNA complex to a sequence complementary region on a double-stranded DNA (in the natural CRISPR system, the gRNA is composed of two parts: the crRNA containing part of the handle and the tracrRNA containing the protospacer). In addition to sequence-complementarity of the protospacer, a short protospacer adjacent motif (PAM) is required on the 3' side adjacent to the binding sequence. Mechanistic studies have shown that the Cas9:gRNA complex actually first binds at the PAM sequence, where it melts open the adjacent double-stranded DNA and then displaces one of the DNA strands by the RNA protospacer loaded in the complex (which is also termed “R-loop formation”).⁴¹⁸ Thus, the PAM actually plays a role somewhat reminiscent of a “toehold” for strand invasion, which in this case is driven by the Cas9 protein.

In typical gene editing applications, Cas9:gRNA is used to cut at specific locations on the genome and thus create an artificial double-strand break, upon which a new gene sequence can be inserted via homology-directed repair. With the use of a catalytically inactive version of Cas9 (“dead Cas9” or dCas9),

CRISPR can also be used for gene regulation rather than gene editing (Figure 31, panels B and C). In this application (termed CRISPR interference, CRISPRi), dCas9:gRNA complexes are targeted toward the promoter region of genes, where they either inhibit transcription initiation or block transcriptional elongation.⁴²¹

As CRISPR mechanisms involve short RNA molecules as their central regulatory components, they are amenable for modulation via strand displacement or strand invasion processes. Several groups have already demonstrated the use of antisense RNA complementary to the gRNA to inhibit dCas9:gRNA action. In such applications, CRISPRi is used to suppress the expression of a gene, while anti-gRNA is used to sequester gRNA and promote its degradation. Tae Seok Moon and co-workers designed anti-gRNA molecules augmented by known binding sites for the RNA chaperone Hfq, which promotes interactions between the small RNAs.⁴²² They could show that anti-gRNA can be used to recover gene expression of initially dCas9:gRNA repressed genes and that several such processes could be operated in parallel. In related work, Mückl et al.⁴¹⁹ directly used a single-stranded section of the gRNA as a toehold for strand invasion by a complementary anti-gRNA, which disrupted the gRNA-handle and thus prevented dCas9 from binding (Figure 31 D). In this work, the antisense strand invasion concept was used to reversibly switch bacteria into a filamentous state and back to normal growth by first suppressing the expression of the cell division protein FtsZ via CRISPRi and then recovering its expression supported by anti-gRNAs. More recently, Siu and Chen demonstrated the related concept of “toehold-gated gRNAs” (thgRNAs), in which the activity of gRNAs was controlled via a toehold riboregulator (Figure 31E).⁴²⁰

Apart from Cas9/dCas9, there is a wide range of other CRISPR associated proteins, which are of interest in this context [e.g., Cpf1 (with similar function as Cas9),⁴²³ Cas13a (whose RNase activity has been used for biosensor applications⁴²⁴), or Cas1-Cas2 integrase for “storage” of dsDNA sequences],⁴²⁵ opening up many new opportunities for application of strand displacement techniques in synthetic biology.

6.3. Molecular Assembly and Computing via Strand Displacement in Mammalian Cells

Strand displacement reactions have been successfully employed for the activation and logical control of cellular processes inside of mammalian cells. As already mentioned above, in such applications, the required nucleic acid components can be delivered to the cells using transfection agents and do not have to be expressed *in vivo*. Afonin and co-workers demonstrated an interesting approach based on RNA-DNA hybrids^{426,427} with single-stranded DNA toeholds (Figure 32). Two of such hybrids could bind together via

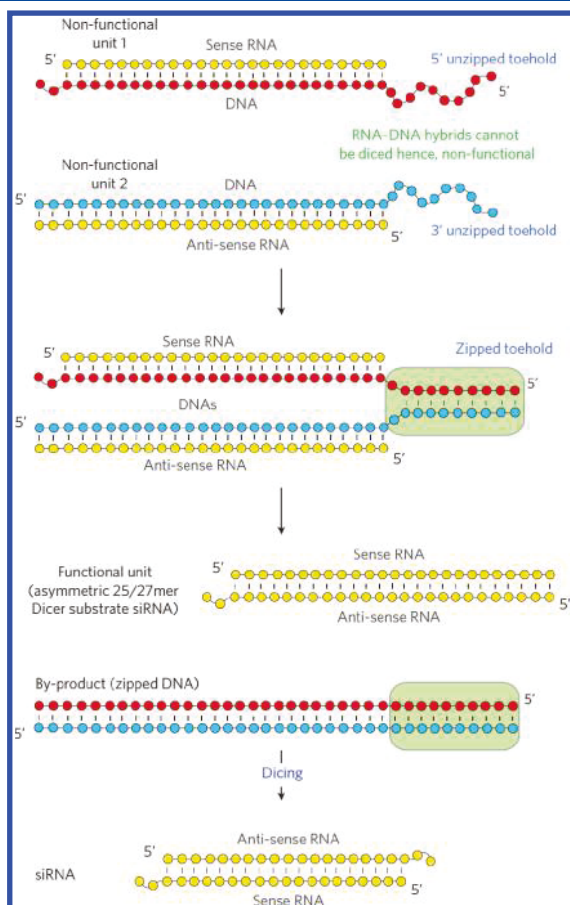


Figure 32. A strand displacement reaction generating siRNA duplexes in vivo.⁴²⁶ The DNARNA hybrid duplexes shown at the top are inactive with respect to RNA interference. Toehold-mediated strand exchange between the duplexes results in a double-stranded DNA product as well as a biologically functional siRNA duplex, which has gene silencing activity *in vivo*. Reprinted with permission from ref 426. Copyright 2013 SpringerNature.

the DNA toeholds, which initiated a four-stranded branch migration process that resulted in the formation of an RNA and a DNA duplex. In one application of this concept, they assembled siRNA molecules *in vivo* (consisting of a 21 bp duplex with 2 nt overhangs at the 3' ends), which then successfully silenced the expression of a target gene via RNA interference (RNAi). Gene silencing was only observed when the cells were transfected with both types of RNA-DNA hybrids necessary for formation of the siRNA. Using a slightly different approach, Groves et al. demonstrated four-way DNA-strand exchange reactions between double-stranded DNA species inside of mammalian cells, which could be utilized for

the execution of simple logical AND or OR gate operations.² They also demonstrated strand exchange between two RNA hybrids, which, similar as in the approach by Afonin et al., resulted in siRNA products that led to gene knockdown. Here, the highest efficacy was observed for RNA hybrids containing RNA strands with phosphorothioate bonds and 2'-O-methyl-ribonucleotides, which increased their stability with respect to nucleases.

6.4. Future Applications at the Interface of Dynamic DNA Nanotechnology and Synthetic Biology

As shown in the previous paragraphs, concepts initially developed in the context of dynamic DNA nanotechnology have been successfully utilized for the control of gene regulatory processes both in bacteria and in mammalian cells. Nucleic acid strand displacement processes are most naturally applied to RNA-based regulatory mechanisms such as riboregulators or riboswitches, CRISPR, or RNA interference. A more widespread application of RNA strand displacement *in vivo* is currently hindered by our lack of control of RNA degradation and RNA hybridization processes. Whereas for the realization of DNA strand displacement processes *in vitro* typically random sequences without any secondary structure are utilized, the design of dynamic RNA systems *in vivo* poses different challenges. On the one hand, RNA without any secondary structure is degraded rapidly, while on the other hand, secondary structure slows down hybridization and strand displacement reactions. Furthermore, undesired interactions with the plethora of other cellular RNA molecules have to be avoided, and also the intracellular localization of RNA molecules has to be considered. We anticipate that specifically for such applications new design rules can be established that will improve intracellular stability and hybridization of artificial RNA molecules and structures, which may also involve the utilization of RNA-protein interactions. It is also conceivable that *in vivo* dynamic RNA systems can be optimized by adopting molecular evolution techniques to balance hybridization and degradation techniques as well as intracellular crosstalk.

Apart from simple riboregulators, so far there have been no attempts to generate and operate RNA-based molecular machines inside of cells. However, based on recent advances in RNA origami,²⁵⁹ it is conceivable that more complex molecular devices can be generated by gene expression, which could further be actuated by RNA strand displacement or related processes. As also mentioned above, implementation of dynamic processes in fast-growing bacteria poses challenges such as a rapid dilution of components in the cell and the complex superimposition of bacterial growth effects with the dynamics of the artificial system. Slow-growing bacteria or eukaryotic cells may therefore turn out to be better chassis for dynamic RNA or DNA nanotechnology, as they represent a more constant biochemical background. It is then also possible to “transfect” all the components of a dynamic DNA or RNA system and to utilize chemically stabilized nucleic acids.

7. CONCLUSION

Nucleic acid strand displacement reactions are the key processes of dynamic DNA nanotechnology. Initially developed in the context of artificial DNA-based molecular machines,¹ the technique has found widespread application in various fields of research over the past 18 years. As extensively discussed in this review, toehold-mediated strand

displacement, strand exchange, and strand invasion processes enable sequence-programmable, reversible, isothermal switching of nucleic acid based or nucleic acid functionalized components between different functional states. This has been used for the operation of nanomachines, the realization of molecular computers and robots, and the assembly and actuation of a wide variety of nanomaterials. Remarkably, strand displacement processes have found particularly widespread application in biosensing. Ingenious sensor schemes based on the hybridization chain reaction (HCR), catalytic hairpin assembly, and a variety of strand displacement recycling schemes have led to the realization of a huge number of sensors for nucleic acids, proteins, and other analytes; approximately 40% of all references provided in this review are sensor-related!

Several emerging trends in dynamic DNA can be clearly discerned from the more recent publications. First, researchers attempt to integrate multiple functions, sensing, computation, actuation, into single devices, which will ultimately lead to the development of molecular robotics. As strand displacement processes play a key role in all of these functions, they will also have a major part to play in this context. Unfortunately, bimolecular hybridization and strand displacement can be relatively slow in solution, which may be undesirable for many applications. However, several strategies have been developed to speed up the operation of nucleic acid reactions and devices. This involves, most notably, the realization of substrate-localized strand-exchange processes, in which the DNA strands participating in the displacement reactions are at a much higher local concentration. Also strand displacement may be combined with other actuation mechanisms for better control and higher speed.

A major trend is the operation of nucleic acid based devices inside of biological systems; this comprises the realization of DNA-based drug delivery systems and containers and the evaluation of molecular patterns by molecular computers *in vivo*. Still, in this context issues like extra- and intracellular stability, toxicity, and immunogenicity have to be resolved, but considerable progress has been made in packaging and delivery of nucleic acid based devices and also the use of chemically modified nucleic acids. In the context of sensing and diagnostics, a variety of “real world” applications are emerging, and at least one strand displacement-based approach for genetic mismatch detection is being commercialized.

The omnipresence of RNA-based regulatory mechanisms in biology provides a wide range of opportunities for an application of strand invasion processes also in this context. Among others, this has already led to the rational design of artificial riboregulators with unprecedented ON/OFF ratios. We therefore anticipate a much more widespread application of dynamic DNA techniques in synthetic biology in the future.

AUTHOR INFORMATION

Corresponding Authors

*E-mail: simmel@tum.de.

*E-mail: bernard.yurke@boisestate.edu.

ORCID

Friedrich C. Simmel: [0000-0003-3829-3446](https://orcid.org/0000-0003-3829-3446)

Notes

The authors declare no competing financial interest.

Biographies

Friedrich C. Simmel received his diploma and Ph.D. degree in physics at Ludwig-Maximilians-Universität München. As a postdoc, he worked in the lab of Bernard Yurke at Bell Laboratories, Murray Hill, NJ, after which he returned to Germany as a DFG Emmy Noether fellow. He is currently Professor of physics at the Technical University Munich (TUM), where he holds the Chair of Physics of Synthetic Biological Systems. He also is the co-Coordinator of the Excellence Cluster Nanosystems Initiative Munich (NIM).

Bernard Yurke received his Ph.D. degree in physics at Cornell University. Upon completing of his Ph.D., he became employed as a research physicist at Bell Laboratories where he served for 25 years. After leaving Bell Laboratories, he joined the faculty at Boise State University where he is now a Distinguished Research Fellow in the Micron School of Materials Science and Engineering.

Hari Raj Singh obtained his BSc Honours in Biochemistry from the Aligarh Muslim University and his Masters degree in Biotechnology from the University of Pune. After a stint at JNCASR Bangalore, he did his Ph.D. at the Ludwig-Maximilians-Universität München on the allosteric activation mechanism of human oncogenic chromatin remodeler ALC1. Currently, he is working as a postdoc in the Simmel lab at the Technical University of Munich.

ACKNOWLEDGMENTS

The authors acknowledge financial support by the European Research Council (contract no. 694410/AEDNA), the National Science Foundation INSPIRE no. 1648655, and the Department of Energy LDRD no. 154754.

REFERENCES

- Yurke, B.; Turberfield, A. J.; Mills, A. P.; Simmel, F. C.; Neumann, J. L. A DNA-fuelled molecular machine made of DNA. *Nature* **2000**, *406*, 605–608.
- Groves, B.; Chen, Y.-J.; Zurla, C.; Pocheikilov, S.; Kirschman, J. L.; Santangelo, P. J.; Seelig, G. Computing in mammalian cells with nucleic acid strand exchange. *Nat. Nanotechnol.* **2016**, *11*, 287–294.
- Seeman, N. C.; Kallenbach, N. R. DNA branched junctions. *Annu. Rev. Biophys. Biomol. Struct.* **1994**, *23*, 53–86.
- Seeman, N. C. DNA nanotechnology: novel DNA constructions. *Annu. Rev. Biophys. Biomol. Struct.* **1998**, *27*, 225–248.
- Arora, A. A.; de Silva, C. Beyond the smiley face: applications of structural DNA nanotechnology. *Nano Rev. Exp.* **2018**, *9*, 1430976.
- Ke, Y.; Castro, C.; Choi, J. H. Structural DNA nanotechnology: artificial nanostructures for biomedical research. *Annu. Rev. Biomed. Eng.* **2018**, *20*, 375–401.
- Xavier, P. L.; Chandrasekaran, A. R. DNA-based construction at the nanoscale: emerging trends and application. *Nanotechnology* **2018**, *29*, No. 062001.
- Deaton, R.; Garzon, M.; Murphy, R. C.; Rose, J. A.; Franceschetti, D. R.; Stevens, S. E. J. Reliability and efficiency of DNA-based computation. *Phys. Rev. Lett.* **1998**, *80*, 417–420.
- Simmel, S. S.; Nickels, P. C.; Liedl, T. Wireframe and tensegrity DNA nanostructures. *Acc. Chem. Res.* **2014**, *47*, 1691–1699.
- Zhang, D. Y.; Seelig, G. Dynamic DNA nanotechnology using strand-displacement reactions. *Nat. Chem.* **2011**, *3*, 103–113.
- Mao, C.; Sun, W.; Shen, Z.; Seeman, N. C. A nanomechanical device based on the B-Z transition of DNA. *Nature* **1999**, *397*, 144–146.
- Kamiya, Y.; Asanuma, H. Light-driven DNA nanomachine with a photoresponsive molecular engine. *Acc. Chem. Res.* **2014**, *47*, 1663–1672.
- Yin, P.; Yan, H.; Daniell, X. G.; Turberfield, A. J.; Reif, J. H. A Unidirectional DNA Walker That Moves Autonomously along a Track. *Angew. Chem., Int. Ed.* **2004**, *43*, 4906–4911.

(14) Chen, Y.; Wang, M. S.; Mao, C. D. An autonomous DNA nanomotor powered by a DNA enzyme. *Angew. Chem., Int. Ed.* **2004**, *43*, 3554–3557.

(15) Beattie, K. L.; Wiegand, R. C.; Radding, C. M. Uptake of homologous single-stranded fragments by superhelical DNA ii. characterization of the reaction. *J. Mol. Biol.* **1977**, *116*, 783–803.

(16) Radding, C. M.; Beattie, K. L.; Holloman, W. K.; Wiegand, R. C. Uptake of homologous single-stranded fragments by superhelical DNA iv. branch migration. *J. Mol. Biol.* **1977**, *116*, 825–839.

(17) Sun, W.; Mao, C.; Liu, F.; Seeman, N. C. Sequence dependence of branch migratory minima. *J. Mol. Biol.* **1998**, *282*, 59–70.

(18) Morrison, L. E.; Stols, L. M. Sensitive fluorescence-based thermodynamic and kinetic measurements of DNA hybridization in solution. *Biochemistry* **1993**, *32*, 3095–3104.

(19) Panyutin, I. G.; Hsieh, P. The kinetics of spontaneous DNA branch migration. *Proc. Natl. Acad. Sci. U. S. A.* **1994**, *91*, 2021–2025.

(20) Simmel, F. C.; Yurke, B. Using DNA to construct and power a nanoactuator. *Phys. Rev. E: Stat. Phys., Plasmas, Fluids, Relat. Interdiscip. Top.* **2001**, *63*, No. 041913.

(21) Simmel, F. C.; Yurke, B.; Sanyala, R. J. Operation kinetics of a DNA-based molecular switch. *J. Nanosci. Nanotechnol.* **2002**, *2*, 383–390.

(22) Yan, H.; Zhang, X.; Shen, Z.; Seeman, N. C. A robust DNA mechanical device controlled by hybridization topology. *Nature* **2002**, *415*, 62–65.

(23) Li, J.; Tan, W. A single DNA molecule nanomotor. *Nano Lett.* **2002**, *2*, 315–318.

(24) Alberti, P.; Mergny, J.-L. DNA duplex-quadruplex exchange as the basis for a nanomolecular machine. *Proc. Natl. Acad. Sci. U. S. A.* **2003**, *100*, 1569–1573.

(25) Turberfield, A. J.; Mitchell, J. C.; Yurke, B.; Mills, A. P.; Blakey, M. I.; Simmel, F. C. DNA fuel for free-running nanomachines. *Phys. Rev. Lett.* **2003**, *90*, 118102.

(26) Seelig, G.; Yurke, B.; Winfree, E. Catalyzed relaxation of a metastable DNA fuel. *J. Am. Chem. Soc.* **2006**, *128*, 12211–12220.

(27) Niemeyer, C. M.; Adler, M. Nanomechanical devices based on DNA. *Angew. Chem., Int. Ed.* **2002**, *41*, 3779–3783.

(28) Beissenhirtz, M. K.; Willner, I. DNA-based machines. *Org. Biomol. Chem.* **2006**, *4*, 3392–3401.

(29) Wang, F.; Liu, X.; Willner, I. DNA Switches: From Principles to Applications. *Angew. Chem., Int. Ed.* **2015**, *54*, 1098–1129.

(30) Lin, D. C.; Yurke, B.; Langrana, N. A. Mechanical properties of a reversible, DNA-crosslinked polyacrylamide hydrogel. *J. Biochem. Eng.* **2004**, *126*, 104–110.

(31) Liedl, T.; Dietz, H.; Yurke, B.; Simmel, F. Controlled trapping and release of quantum dots in a DNA-switchable hydrogel. *Small* **2007**, *3*, 1688–1693.

(32) Guo, W.; Lu, C.-H.; Qi, X.-J.; Orbach, R.; Fadeev, M.; Yang, H.-H.; Willner, I. Switchable bifunctional stimuli-triggered poly-*N*-isopropylacrylamide/DNA hydrogels. *Angew. Chem., Int. Ed.* **2014**, *53*, 10134–10138.

(33) Sicilia, G.; Grainger-Boulby, C.; Francini, N.; Magnusson, J. P.; Saeed, A. O.; Fernández-Trillo, F.; Alexander, C.; Spain, S. G. Programmable polymer-DNA hydrogels with dual input and multi-scale responses. *Biomater. Sci.* **2014**, *2*, 203–211.

(34) Ren, J.; Hu, Y.; Lu, C.-H.; Guo, W.; Aleman-Garcia, M. A.; Ricci, F.; Willner, I. pH-responsive and switchable triplex-based DNA hydrogels. *Chem. Sci.* **2015**, *6*, 4190–4195.

(35) Lu, C.-H.; Guo, W.; Hu, Y.; Qi, X.-J.; Willner, I. Multitriggered shape-memory acrylamide-DNA hydrogels. *J. Am. Chem. Soc.* **2015**, *137*, 15723–15731.

(36) He, Y.; Yang, X.; Yuan, R.; Chai, Y. Switchable target-responsive 3D DNA hydrogels as a signal amplification strategy combining with SERS technique for ultrasensitive detection of miRNA 155. *Anal. Chem.* **2017**, *89*, 8538–8544.

(37) Cangialosi, A.; Yoon, C.; Liu, J.; Huang, Q.; Guo, J.; Nguyen, T. D.; Gracias, D. H.; Schulman, R. DNA sequence-directed shape change of photopatterned hydrogels via high-degree swelling. *Science* **2017**, *357*, 1126–1130.

(38) Fern, J.; Schulman, R. Modular DNA strand-displacement controllers for directing material expansion. *Nat. Commun.* **2018**, *9*, 3766.

(39) Iqbal, J.; Lim, G. S.; Gao, Z. The hybridization chain reaction in the development of ultrasensitive nucleic acid assays. *TrAC, Trends Anal. Chem.* **2015**, *64*, 86–99.

(40) Bi, S.; Yue, S.; Zhang, S. Hybridization chain reaction: a versatile molecular tool for biosensing, bioimaging, and biomedicine. *Chem. Soc. Rev.* **2017**, *46*, 4281–4298.

(41) Liu, N.; Huang, F.; Lou, X.; Xia, F. DNA hybridization chain reaction and DNA supersandwich self-assembly for ultrasensitive detection. *Sci. China: Chem.* **2017**, *60*, 311–318.

(42) Chen, J.; Tang, L.; Chu, X.; Jiang, J. Enzyme-free, signal-amplified nucleic acid circuits for biosensing and bioimaging analysis. *Analyst* **2017**, *142*, 3048–3061.

(43) Augspurger, E. E.; Rana, M.; Yigit, M. V. Chemical and biological sensing using hybridization chain reaction. *ACS Sens.* **2018**, *3*, 878–902.

(44) Huang, D.; Li, X.; Shen, B.; Li, J.; Ding, X.; Zhou, X.; Guo, B.; Cheng, W.; Ding, S. Enzyme-free dual-amplification strategy for the rapid, single-step detection of nucleic acids based on hybridization chain reaction initiated entropy-driven circuit reaction. *Sens. Actuators, B* **2018**, *273*, 393–399.

(45) Seelig, G.; Soloveichik, D.; Zhang, D. Y.; Winfree, E. Enzyme-free nucleic acid logic circuits. *Science* **2006**, *314*, 1585–1588.

(46) Soloveichik, D.; Seelig, G.; Winfree, E. DNA as a universal substrate for chemical kinetics. *Proc. Natl. Acad. Sci. U. S. A.* **2010**, *107*, 5393–5398.

(47) Srinivas, N.; Parkin, J.; Seelig, G.; Winfree, E.; Soloveichik, D. Enzyme-free nucleic acid dynamical systems. *Science* **2017**, *358*, No. eaal2052.

(48) Cherry, K. M.; Qian, L. Scaling up digital molecular pattern recognition with DNA-based winner-take-all neural networks. *Nature* **2018**, *559*, 370–376.

(49) Ouldridge, T. E.; Louis, A. A.; Doye, J. P. K. DNA nanotweezers studied with a coarse-grained model of DNA. *Phys. Rev. Lett.* **2010**, *104*, 178101.

(50) Ouldridge, T. E.; Louis, A. A.; Doye, J. P. K. Structural, mechanical and thermodynamic properties of a coarse-grained DNA model. *J. Chem. Phys.* **2011**, *134*, No. 085101.

(51) Srinivas, N.; Ouldridge, T. E.; Sulc, P.; Schaeffer, J. M.; Yurke, B.; Louis, A. A.; Doye, J. P. K.; Winfree, E. On the biophysics and kinetics of toehold-mediated DNA strand displacement. *Nucleic Acids Res.* **2013**, *41*, 10641–10658.

(52) Dirks, R. M.; Lin, M.; Winfree, E.; Pierce, N. A. Paradigms for computational nucleic acid design. *Nucleic Acids Res.* **2004**, *32*, 1392–1403.

(53) Zadeh, J. N.; Wolfe, B. R.; Pierce, N. A. Nucleic acid sequence design via efficient ensemble defect optimization. *J. Comput. Chem.* **2011**, *32*, 439–452.

(54) Cardelli, L. Two-domain DNA strand displacement. *Math. Struct. Comp. Science* **2013**, *23*, 247–271.

(55) Wolfe, B. R.; Pierce, N. A. Sequence design for a test tube of interacting nucleic acid strands. *ACS Synth. Biol.* **2015**, *4*, 1086–1100.

(56) Wolfe, B. R.; Porubsky, N. J.; Zadeh, J. N.; Dirks, R. M.; Pierce, N. A. Constrained multistate sequence design for nucleic acid reaction pathway engineering. *J. Am. Chem. Soc.* **2017**, *139*, 3134–3144.

(57) Yin, P.; Choi, H. M. T.; Calvert, C. R.; Pierce, N. A. Programming biomolecular self-assembly pathways. *Nature* **2008**, *451*, 318–322.

(58) Qian, L.; Winfree, E. Scaling up digital circuit computation with DNA strand displacement cascades. *Science* **2011**, *332*, 1196–1201.

(59) Chen, X.; Briggs, N.; McLain, J. R.; Ellington, A. Stacking nonenzymatic circuits for high signal gain. *Proc. Natl. Acad. Sci. U. S. A.* **2013**, *110*, 5386–5391.

(60) Teichmann, M.; Kopperger, E.; Simmel, F. C. Robustness of localized DNA strand displacement cascades. *ACS Nano* **2014**, *8*, 8487–8496.

(61) Jiang, Y. S.; Bhadra, S.; Li, B.; Ellington, A. D. Mismatches improve the performance of strand-displacement nucleic acid circuits. *Angew. Chem., Int. Ed.* **2014**, *53*, 1845–1848.

(62) Olson, X.; Kotani, S.; Padilla, J. E.; Hallstrom, N.; Goltry, S.; Lee, J.; Yurke, B.; Hughes, W. L.; Graugnard, E. Availability: a metric for nucleic acid strand displacement systems. *ACS Synth. Biol.* **2017**, *6*, 84–93.

(63) Olson, X.; Kotani, S.; Yurke, B.; Graugnard, E.; Hughes, W. L. Kinetics of DNA strand displacement systems with locked nucleic acids. *J. Phys. Chem. B* **2017**, *121*, 2594–2602.

(64) Kotani, S.; Hughes, W. L. Multi-arm junctions for dynamic DNA nanotechnology. *J. Am. Chem. Soc.* **2017**, *139*, 6363–6368.

(65) Wang, B.; Zhou, X.; Yao, D.; Sun, X.; He, M.; Wang, X.; Yin, X.; Liang, H. Contribution of gold nanoparticles to the catalytic DNA strand displacement in leakage reduction and signal amplification. *Chem. Commun.* **2017**, *53*, 10950–10953.

(66) Wang, B.; Thachuk, C.; Ellington, A. D.; Winfree, E.; Soloveichik, D. Effective design principles for leakless strand displacement systems. *Proc. Natl. Acad. Sci. U. S. A.* **2018**, *115*, E12182–E12191.

(67) Gao, M.; Daniel, D.; Zou, H.; Jiang, S.; Lin, S.; Huang, C.; Hecht, S. M.; Chen, S. Rapid detection of a dengue virus RNA sequence with single molecule sensitivity using tandem toehold-mediated displacement reactions. *Chem. Commun.* **2018**, *54*, 968–971.

(68) Gliddon, H. D.; Howes, P. D.; Kafourou, M.; Levin, M.; Stevens, M. M. A nucleic acid strand displacement system for the multiplexed detection of tuberculosis-specific mRNA using quantum dots. *Nanoscale* **2016**, *8*, 10087–10095.

(69) You, M.; Zhu, G.; Chen, T.; Donovan, M. J.; Tan, W. Programmable and multiparameter DNA-based logic platform for cancer recognition and targeted therapy. *J. Am. Chem. Soc.* **2015**, *137*, 667–674.

(70) You, M.; Peng, L.; Shao, N.; Zhang, L.; Qiu, L.; Cui, C.; Tan, W. DNA “nano-claw”: logic-based autonomous cancer targeting and therapy. *J. Am. Chem. Soc.* **2014**, *136*, 1256–1259.

(71) Zhang, P.; Wang, C.; Zhao, J.; Xiao, A.; Shen, Q.; Li, L.; Li, J.; Zhang, J.; Min, Q.; Chen, J.; Chen, H.-Y.; Zhu, J.-J. Near infrared-guided smart nanocarriers for microRNA-controlled release of doxorubicin/siRNA with intracellular ATP as fuel. *ACS Nano* **2016**, *10*, 3637–3647.

(72) Yang, F.; Wang, S.; Zhang, Y.; Tang, L.; Jin, D.; Ning, Y.; Zhang, G.-J. Toehold enabling stem-loop inspired hemiduplex probe with enhanced sensitivity and sequence-specific detection of tumor DNA in serum. *Biosens. Bioelectron.* **2016**, *82*, 32–39.

(73) Ravan, H.; Amandadi, M.; Esmaeili-Mahani, S. DNA domino-based nanoscale logic circuit: A versatile strategy for ultrasensitive multiplexed analysis of nucleic acids. *Anal. Chem.* **2017**, *89*, 6021–6028.

(74) Feng, Q.; Guo, Y.-H.; Xu, J.-J.; Chen, H.-Y. Self-assembled DNA tetrahedral scaffolds for the construction of electrochemiluminescence biosensor with programmable DNA cyclic amplification. *ACS Appl. Mater. Interfaces* **2017**, *9*, 17637–17644.

(75) Ling, Y.; Zhang, X. F.; Chen, X. H.; Liu, L.; Wang, X. H.; Wang, D. S.; Li, N. B.; Luo, H. Q. A dual-cycling biosensor for target DNA detection based on the toehold-mediated strand displacement reaction and exonuclease III assisted amplification. *New J. Chem.* **2018**, *42*, 4714–4718.

(76) Hun, X.; Liu, B.; Meng, Y. Ultrasensitive chemiluminescence assay for the lung cancer biomarker cytokeratin 21–1 via a dual amplification scheme based on the use of encoded gold nanoparticles and a toehold-mediated strand displacement reaction. *Microchim. Acta* **2017**, *184*, 3953–3959.

(77) Wang, S.; Yang, F.; Jin, D.; Dai, Q.; Tu, J.; Liu, Y.; Ning, Y.; Zhang, G.-J. Toehold mediated one-step conformation-switchable “signal-on” electrochemical DNA sensing enhanced with homogeneous enzymatic amplification. *Anal. Chem.* **2017**, *89*, 5349–5356.

(78) Liu, S.; Fang, L.; Tian, Y.; Wei, W.; Wang, L. Label-free, non-enzymatic and ultrasensitive electrochemical nucleic acid biosensing by tandem DNA-fueled target recycling and hybridization chain reaction. *Sens. Actuators, B* **2017**, *244*, 450–457.

(79) Sherman, W.; Seeman, N. C. A precisely controlled DNA biped walking device. *Nano Lett.* **2004**, *4*, 1203–1207.

(80) Shin, J.; Pierce, N. A synthetic DNA walker for molecular transport. *J. Am. Chem. Soc.* **2004**, *126*, 10834–10835.

(81) He, Y.; Liu, D. R. Autonomous multistep organic synthesis in a single isothermal solution mediated by a DNA walker. *Nat. Nanotechnol.* **2010**, *5*, 778–782.

(82) Gu, H.; Chao, J.; Xiao, S.-J.; Seeman, N. C. A proximity-based programmable DNA nanoscale assembly line. *Nature* **2010**, *465*, 202–205.

(83) Simmel, F. C. DNA-based assembly lines and nanofactories. *Curr. Opin. Biotechnol.* **2012**, *23*, 516–521.

(84) Venkataraman, S.; Dirks, R. M.; Rothemund, P. W. K.; Winfree, E.; Pierce, N. A. An autonomous polymerization motor powered by DNA hybridization. *Nat. Nanotechnol.* **2007**, *2*, 490–494.

(85) Choi, H. M. T.; Chang, J. Y.; Trinh, L. A.; Padilla, J. E.; Fraser, S. E.; Pierce, N. A. Programmable in situ amplification for multiplexed imaging of mRNA expression. *Nat. Biotechnol.* **2010**, *28*, 1208–U103.

(86) George, A. K.; Singh, H. Enzyme-free scalable DNA digital design techniques: a review. *IEEE Trans. Nanobiosci.* **2016**, *15*, 928–938.

(87) Santa Lucia, J. A unified view of polymer, dumbbell, and oligonucleotide DNA nearest-neighbor thermodynamics. *Proc. Natl. Acad. Sci. U. S. A.* **1998**, *95*, 1460–1465.

(88) Zhang, J. X.; Fang, J. Z.; Duan, W.; Wu, L. R.; Zhang, A. W.; Dalchau, N.; Yordanov, B.; Petersen, R.; Phillips, A.; Zhang, D. Y. Predicting DNA hybridization kinetics from sequence. *Nat. Chem.* **2017**, *10*, 91–98.

(89) Wetmur, J. G.; Davidson, N. Kinetics of renaturation of DNA. *J. Mol. Biol.* **1968**, *31*, 349–370.

(90) Yurke, B.; Mills, A. P., Jr. Using DNA to power nanostructures. *Genet. Progr. Evol. Machines* **2003**, *4*, 111–122.

(91) Reynaldo, L. P.; Vologodskii, A. V.; Neri, B. P.; Lyamichev, V. I. The kinetics of oligonucleotide replacements. *J. Mol. Biol.* **2000**, *297*, 511–520.

(92) Green, C.; Tibbets, C. Reassociation rate limited displacement of DNA strands by branch migration. *Nucleic Acids Res.* **1981**, *9*, 1905–1918.

(93) Zhang, D. Y.; Winfree, E. Control of DNA strand displacement kinetics using toehold exchange. *J. Am. Chem. Soc.* **2009**, *131*, 17303–17314.

(94) Ouldridge, T. E. Coarse-grained modeling of DNA and DNA nanotechnology. Ph.D. Thesis, University of Oxford, 2011.

(95) Li, M.-X.; Xu, C.-H.; Zhang, N.; Qian, G.-S.; Zhao, W.; Xu, J.-J.; Chen, H.-Y. Exploration of the kinetics of toehold-mediated strand displacement via plasmon rulers. *ACS Nano* **2018**, *12*, 3341–3350.

(96) Li, Q.; Tian, C.; Li, X.; Mao, C. Can strand displacement take place in DNA triplets? *Org. Biomol. Chem.* **2018**, *16*, 372–375.

(97) Kabza, A. M.; Young, B. E.; Szczepanski, J. T. Heterochiral DNA strand-displacement circuits. *J. Am. Chem. Soc.* **2017**, *139*, 17715–17718.

(98) Zhang, D. Y.; Turberfield, A. J.; Yurke, B.; Winfree, E. Engineering entropy-driven reactions and networks catalyzed by DNA. *Science* **2007**, *318*, 1121–1125.

(99) Qian, L.; Winfree, E. A simple DNA gate motif for synthesizing large-scale circuits. *J. R. Soc., Interface* **2011**, *8*, 1281–1297.

(100) Qian, L.; Winfree, E.; Bruck, J. Neural network computation with DNA strand displacement cascades. *Nature* **2011**, *475*, 368–372.

(101) Dittmer, W. U.; Reuter, A.; Simmel, F. C. A DNA-based machine that can cyclically bind and release thrombin. *Angew. Chem., Int. Ed.* **2004**, *43*, 3550–3553.

(102) Liu, M.; Fu, J.; Hejesen, C.; Yang, Y.; Woodbury, N. W.; Gothelf, K.; Liu, Y.; Yan, H. A DNA tweezer-actuated enzyme nanoreactor. *Nat. Commun.* **2013**, *4*, 2127.

(103) Bockelmann, U.; EssevazRoulet, B.; Heslot, F. Molecular stick-slip motion revealed by opening DNA with piconewton forces. *Phys. Rev. Lett.* **1997**, *79*, 4489–4492.

(104) Rief, M.; Clausen-Schaumann, H.; Gaub, H. Sequence-dependent mechanics of single DNA molecules. *Nat. Struct. Biol.* **1999**, *6*, 346–349.

(105) Smith, S. B.; Cui, Y.; Bustamante, C. Overstretching B-DNA: the elastic response of individual double-stranded and single-stranded DNA molecules. *Science* **1996**, *271*, 795–799.

(106) Chen, J.; Wen, J.; Zhuang, L.; Zhou, S. An enzyme-free catalytic DNA circuit for amplified detection of aflatoxin B1 using gold nanoparticles as colorimetric indicators. *Nanoscale* **2016**, *8*, 9791–9797.

(107) Yu, L.; Xu, H.; Chen, H.; Bai, L.; Wang, W. Exonuclease III assisted and label-free detection of mercury ion based on toehold strand displacement amplification strategy. *Anal. Methods* **2016**, *8*, 7054–7060.

(108) Meng, F.; Xu, H.; Yao, X.; Qin, X.; Jiang, T.; Gao, S.; Zhang, Y.; Yang, D.; Liu, X. Mercury detection based on label-free and isothermal enzyme-free amplified fluorescence platform. *Talanta* **2017**, *162*, 368–373.

(109) Oishi, M. Comparative study of DNA circuit system-based proportional and exponential amplification strategies for enzyme-free and rapid detection of miRNA at room temperature. *ACS Omega* **2018**, *3*, 3321–3329.

(110) Dirks, R. M.; Pierce, N. A. Triggered amplification by hybridization chain reaction. *Proc. Natl. Acad. Sci. U. S. A.* **2004**, *101*, 15275–15278.

(111) Li, B.; Ellington, A. D.; Chen, X. Rational, modular adaptation of enzyme-free DNA circuits to multiple detection methods. *Nucleic Acids Res.* **2011**, *39*, e110.

(112) Tyagi, S.; Kramer, F. Molecular beacons: Probes that fluoresce upon hybridization. *Nat. Biotechnol.* **1996**, *14*, 303–308.

(113) Green, S. J.; Lubrich, D.; Turberfield, A. J. DNA hairpins: fuel for autonomous DNA devices. *Biophys. J.* **2006**, *91*, 2966–2975.

(114) Amodio, A.; Zhao, B.; Porchetta, A.; Idili, A.; Castronovo, M.; Fan, C.; Ricci, F. Rational design of pH-controlled DNA strand displacement. *J. Am. Chem. Soc.* **2014**, *136*, 16469–16472.

(115) Idili, A.; Porchetta, A.; Amodio, A.; Vallée-Bélisle, A.; Ricci, F. Controlling hybridization chain reactions with pH. *Nano Lett.* **2015**, *15*, 5539–5544.

(116) Genot, A. J.; Zhang, D. Y.; Bath, J.; Turberfield, A. J. Remote toehold: a mechanism for flexible control of DNA hybridization kinetics. *J. Am. Chem. Soc.* **2011**, *133*, 2177–2182.

(117) Li, C.; Li, Y.; Chen, Y.; Lin, R.; Li, T.; Liu, F.; Li, N. Modulating the DNA strand-displacement kinetics with the one-sided remote toehold design for differentiation of single-base mismatched DNA. *RSC Adv.* **2016**, *6*, 74913–74916.

(118) Chen, X. Expanding the rule set of DNA circuitry with associative toehold activation. *J. Am. Chem. Soc.* **2012**, *134*, 263–271.

(119) Simmel, F. C.; Yurke, B. A DNA-based molecular device switchable between three distinct mechanical states. *Appl. Phys. Lett.* **2002**, *80*, 883–885.

(120) Elbaz, J.; Moshe, M.; Willner, I. Coherent activation of DNA tweezers: a “set-reset” logic system. *Angew. Chem., Int. Ed.* **2009**, *48*, 3834–3837.

(121) Li, X.-M.; Li, W.; Ge, A.-Q.; Chen, H.-Y. Logic-based dual-functional DNA tweezers with protein and small molecule as mechanical activators. *J. Phys. Chem. C* **2010**, *114*, 21948–21952.

(122) Zhou, C.; Yang, Z.; Liu, D. Reversible regulation of protein binding affinity by a DNA machine. *J. Am. Chem. Soc.* **2012**, *134*, 1416–1418.

(123) Shiu, S. C.-C.; Cheung, Y.-W.; Dirkzwager, R. M.; Liang, S.; Kinghorn, A. B.; Fraser, L. A.; Tang, M. S. L.; Tanner, J. A. Aptamer-mediated protein molecular recognition driving a DNA tweezer nanomachine. *Adv. Biosyst.* **2017**, *1*, 1600006–6.

(124) Liang, X.; Nishioka, H.; Takenaka, N.; Asanuma, H. A DNA nanomachine powered by light irradiation. *ChemBioChem* **2008**, *9*, 702–705.

(125) Asanuma, H.; Liang, X.; Yoshida, T.; Komiya, M. Photocontrol of DNA duplex formation by using azobenzene-bearing oligonucleotides. *ChemBioChem* **2001**, *2*, 39–44.

(126) Asanuma, H.; Liang, X.; Nishioka, H.; Matsunaga, D.; Liu, M.; Komiya, M. Synthesis of azobenzene-tethered DNA for reversible photo-regulation of DNA functions: hybridization and transcription. *Nat. Protoc.* **2007**, *2*, 203–212.

(127) Liu, D.; Balasubramanian, S. A proton-fuelled DNA nanomachine. *Angew. Chem., Int. Ed.* **2003**, *42*, 5734–5736.

(128) Chen, Y.; Lee, S.-H.; Mao, C. A DNA nanomachine based on a duplex-triplex transition. *Angew. Chem., Int. Ed.* **2004**, *43*, 5335–5338.

(129) Modi, S.; Swetha, M. G.; Goswami, D.; Gupta, G. D.; Mayor, S.; Krishnan, Y. A DNA nanomachine that maps spatial and temporal pH changes inside living cells. *Nat. Nanotechnol.* **2009**, *4*, 325–330.

(130) Surana, S.; Bhat, J. M.; Koushika, S. P.; Krishnan, Y. An autonomous DNA nanomachine maps spatiotemporal pH changes in a multicellular living organism. *Nat. Commun.* **2011**, *2*, 340–347.

(131) Modi, S.; Nizak, C.; Surana, S.; Halder, S.; Krishnan, Y. Two DNA nanomachines map pH changes along intersecting endocytic pathways inside the same cell. *Nat. Nanotechnol.* **2013**, *8*, 459–467.

(132) Krishnan, Y.; Simmel, F. C. Nucleic acid based molecular devices. *Angew. Chem., Int. Ed.* **2011**, *50*, 3124–3156.

(133) Wang, F.; Lu, C.-H.; Willner, I. From cascaded catalytic nucleic acids to enzyme–DNA nanostructures: controlling reactivity, sensing, logic operations, and assembly of complex structures. *Chem. Rev.* **2014**, *114*, 2881–2941.

(134) Lu, C.-H.; Ceccarello, A.; Willner, I. Recent advances in the synthesis and functions of reconfigurable interlocked dna nanostructures. *J. Am. Chem. Soc.* **2016**, *138*, 5172–5185.

(135) Tomov, T. E.; Tsukanov, R.; Glick, Y.; Berger, Y.; Liber, M.; Avrahami, D.; Gerber, D.; Nir, E. DNA bipedal motor achieves a large number of steps due to operation using microfluidics-based interface. *ACS Nano* **2017**, *11*, 4002–4008.

(136) Tomov, T. E.; Tsukanov, R.; Liber, M.; Masoud, R.; Plavner, N.; Nir, E. Rational design of DNA motors: fuel optimization through single-molecule fluorescence. *J. Am. Chem. Soc.* **2013**, *135*, 11935–11941.

(137) Tian, Y.; Mao, C. Molecular gears: a pair of DNA circles continuously rolls against each other. *J. Am. Chem. Soc.* **2004**, *126*, 11410–11411.

(138) Wang, Z.-G.; Elbaz, J.; Willner, I. A dynamically programmed DNA transporter. *Angew. Chem., Int. Ed.* **2012**, *51*, 4322–4326.

(139) Muscat, R. A.; Bath, J.; Turberfield, A. J. A programmable molecular robot. *Nano Lett.* **2011**, *11*, 982–987.

(140) Wang, Z.-G.; Elbaz, J.; Willner, I. DNA machines: bipedal walker and stepper. *Nano Lett.* **2011**, *11*, 304–309.

(141) Muscat, R. A.; Bath, J.; Turberfield, A. J. Small molecule signals that direct the route of a molecular cargo. *Small* **2012**, *8*, 3593–3597.

(142) Cheng, J.; Sreelatha, S.; Hou, R.; Efremov, A.; Liu, R.; van der Maarel, J. R. C.; Wang, Z. Bipedal nanowalker by pure physical mechanisms. *Phys. Rev. Lett.* **2012**, *109*, 238104.

(143) You, M.; Huang, F.; Chen, Z.; Wang, R.-W.; Tan, W. Building a nanostructure with reversible motions using photonic energy. *ACS Nano* **2012**, *6*, 7935–7941.

(144) You, M.; Chen, Y.; Zhang, X.; Liu, H.; Wang, R.; Wang, K.; Williams, K. R.; Tan, W. An autonomous and controllable light-driven DNA walking device. *Angew. Chem., Int. Ed.* **2012**, *51*, 2457–2460.

(145) Liu, M.; Hou, R.; Cheng, J.; Loh, I. Y.; Sreelatha, S.; Tey, J. N.; Wei, J.; Wang, Z. Autonomous synergic control of nanomotors. *ACS Nano* **2014**, *8*, 1792–1803.

(146) Loh, I. Y.; Cheng, J.; Tee, S. R.; Efremov, A.; Wang, Z. From bistate molecular switches to self-directed track-walking nanomotors. *ACS Nano* **2014**, *8*, 10293–10304.

(147) Yeo, Q. Y.; Loh, I. Y.; Tee, S. R.; Chiang, Y. H.; Cheng, J.; Liu, M. H.; Wang, Z. S. A DNA bipedal nanowalker with a piston-like expulsion stroke. *Nanoscale* **2017**, *9*, 12142–12149.

(148) Bath, J.; Green, S. J.; Turberfield, A. J. A free-running DNA motor powered by a nicking enzyme. *Angew. Chem., Int. Ed.* **2005**, *44*, 4358–4361.

(149) Wickham, S. F. J.; Endo, M.; Katsuda, Y.; Hidaka, K.; Bath, J.; Sugiyama, H.; Turberfield, A. J. Direct observation of stepwise movement of a synthetic molecular transporter. *Nat. Nanotechnol.* **2011**, *6*, 166–169.

(150) Wickham, S. F. J.; Bath, J.; Katsuda, Y.; Endo, M.; Hidaka, K.; Sugiyama, H.; Turberfield, A. J. A DNA-based molecular motor that can navigate a network of tracks. *Nat. Nanotechnol.* **2012**, *7*, 169–173.

(151) Lund, K.; Manzo, A. J.; Dabby, N.; Michelotti, N.; Johnson-Buck, A.; Nangreave, J.; Taylor, S.; Pei, R.; Stojanovic, M. N.; Walter, N. G.; Winfree, E.; Yan, H. Molecular robots guided by prescriptive landscapes. *Nature* **2010**, *465*, 206–210.

(152) Tian, Y.; He, Y.; Chen, Y.; Yin, P.; Mao, C. A DNAzyme that walks processively and autonomously along a one-dimensional track. *Angew. Chem., Int. Ed.* **2005**, *44*, 4355–4358.

(153) Pei, R.; Taylor, S.; Stefanovic, D.; Rudchenko, S.; Mitchell, T.; Stojanovic, M. N. Behavior of polycatalytic assemblies in a substrate-displaying matrix. *J. Am. Chem. Soc.* **2006**, *128*, 12693–12699.

(154) Green, S. J.; Bath, J.; Turberfield, A. J. Coordinated chemomechanical cycles: a mechanism for autonomous molecular motion. *Phys. Rev. Lett.* **2008**, *101*, 238101.

(155) Bath, J.; Green, S.; Allen, K.; Turberfield, A. Mechanism for a directional, processive, and reversible dna motor. *Small* **2009**, *5*, 1513–1516.

(156) Omabegho, T.; Sha, R.; Seeman, N. C. A bipedal DNA Brownian motor with coordinated legs. *Science* **2009**, *324*, 67–71.

(157) Simmel, F. C. Processive motion of bipedal DNA walkers. *ChemPhysChem* **2009**, *10*, 2593–2597.

(158) Pan, J.; Li, F.; Cha, T.-G.; Chen, H.; Choi, J. H. Recent progress on DNA based walkers. *Curr. Opin. Biotechnol.* **2015**, *34*, 56–64.

(159) Thubagere, A. J.; Li, W.; Johnson, R. F.; Chen, Z.; Doroudi, S.; Lee, Y. L.; Izatt, G.; Wittman, S.; Srinivas, N.; Woods, D.; Winfree, E.; Qian, L. A cargo-sorting DNA robot. *Science* **2017**, *357*, No. eaan6558.

(160) Li, J.; Johnson-Buck, A.; Yang, Y. R.; Shih, W. M.; Yan, H.; Walter, N. G. Exploring the speed limit of toehold exchange with a cartwheeling DNA acrobat. *Nat. Nanotechnol.* **2018**, *13*, 723.

(161) You, M.; Lyu, Y.; Han, D.; Qiu, L.; Liu, Q.; Chen, T.; Wu, C. S.; Peng, L.; Zhang, L.; Bao, G.; Tan, W. DNA probes for monitoring dynamic and transient molecular encounters on living cell membranes. *Nat. Nanotechnol.* **2017**, *12*, 453–459.

(162) Richards, V. 2016 Nobel Prize in Chemistry - Molecular machines. *Nat. Chem.* **2016**, *8*, 1090–1090.

(163) Valero, J.; Lohmann, F.; Famulok, M. Interlocked DNA topologies for nanotechnology. *Curr. Opin. Biotechnol.* **2017**, *48*, 159–167.

(164) Lohmann, F.; Ackermann, D.; Famulok, M. Reversible light switch for macrocycle mobility in a DNA rotaxane. *J. Am. Chem. Soc.* **2012**, *134*, 11884–11887.

(165) Weigandt, J.; Chung, C.-L.; Jester, S.-S.; Famulok, M. Daisy chain rotaxanes made from interlocked DNA nanostructures. *Angew. Chem., Int. Ed.* **2016**, *55*, 5512–5516.

(166) Centola, M.; Valero, J.; Famulok, M. Allosteric control of oxidative catalysis by a DNA rotaxane nanostructure. *J. Am. Chem. Soc.* **2017**, *139*, 16044–16047.

(167) Elbaz, J.; Wang, Z.-G.; Wang, F.; Willner, I. Programmed dynamic topologies in DNA catenanes. *Angew. Chem., Int. Ed.* **2012**, *51*, 2349–2353.

(168) Lu, C.-H.; Qi, X.-J.; Cecconello, A.; Jester, S.-S.; Famulok, M.; Willner, I. Switchable reconfiguration of an interlocked DNA olympiadane nanostructure. *Angew. Chem., Int. Ed.* **2014**, *53*, 7499–7503.

(169) Lu, C.-H.; Cecconello, A.; Qi, X.-J.; Wu, N.; Jester, S.-S.; Famulok, M.; Matthies, M.; Schmidt, T.-L.; Willner, I. Switchable reconfiguration of a seven-ring interlocked DNA catenane nanostructure. *Nano Lett.* **2015**, *15*, 7133–7137.

(170) Li, T.; Famulok, M. I-motif-programmed functionalization of DNA nanocircles. *J. Am. Chem. Soc.* **2013**, *135*, 1593–1599.

(171) Li, T.; Lohmann, F.; Famulok, M. Interlocked DNA nanostructures controlled by a reversible logic circuit. *Nat. Commun.* **2014**, *5*, 1–8.

(172) Hu, L.; Lu, C.-H.; Willner, I. Switchable catalytic DNA catenanes. *Nano Lett.* **2015**, *15*, 2099–2103.

(173) Elbaz, J.; Cecconello, A.; Fan, Z.; Govorov, A. O.; Willner, I. Powering the programmed nanostructure and function of gold nanoparticles with catenated DNA machines. *Nat. Commun.* **2013**, *4*, 1–7.

(174) Valero, J.; Pal, N.; Dhakal, S.; Walter, N. G.; Famulok, M. A bio-hybrid DNA rotor-stator nanoengine that moves along predefined tracks. *Nat. Nanotechnol.* **2018**, *13*, 496–503.

(175) Chen, H.; Weng, T.-W.; Riccitelli, M. M.; Cui, Y.; Irudayaraj, J.; Choi, J. H. Understanding the mechanical properties of DNA origami tiles and controlling the kinetics of their folding and unfolding reconfiguration. *J. Am. Chem. Soc.* **2014**, *136*, 6995–7005.

(176) Wei, B.; Ong, L. L.; Chen, J.; Jaffe, A. S.; Yin, P. Complex reconfiguration of DNA nanostructures. *Angew. Chem., Int. Ed.* **2014**, *53*, 7475–7479.

(177) Wei, B.; Dai, M.; Yin, P. Complex shapes self-assembled from single-stranded DNA tiles. *Nature* **2012**, *485*, 623–626.

(178) Ke, Y.; Ong, L. L.; Shih, W. M.; Yin, P. Three-dimensional structures self-assembled from DNA bricks. *Science* **2012**, *338*, 1177–1183.

(179) Han, D.; Pal, S.; Liu, Y.; Yan, H. Folding and cutting DNA into reconfigurable topological nanostructures. *Nat. Nanotechnol.* **2010**, *5*, 712–717.

(180) Aldaye, F. A.; Sleiman, H. F. Modular access to structurally switchable 3D discrete DNA assemblies. *J. Am. Chem. Soc.* **2007**, *129*, 13376–13377.

(181) Rahbani, J. F.; Hariri, A. A.; Cosa, G.; Sleiman, H. F. Dynamic DNA nanotubes: reversible switching between single and double-stranded forms, and effect of base deletions. *ACS Nano* **2015**, *9*, 11898–11908.

(182) Edwardson, T. G. W.; Carneiro, K. M. M.; McLaughlin, C. K.; Serpell, C. J.; Sleiman, H. F. Site-specific positioning of dendritic alkyl chains on DNA cages enables their geometry-dependent self-assembly. *Nat. Chem.* **2013**, *5*, 868–875.

(183) Bujold, K. E.; Hsu, J. C. C.; Sleiman, H. F. Optimized DNA “nanosuitcases” for encapsulation and conditional release of siRNA. *J. Am. Chem. Soc.* **2016**, *138*, 14030–14038.

(184) Peng, R.; Wang, H.; Lyu, Y.; Xu, L.; Liu, H.; Kuai, H.; Liu, Q.; Tan, W. Facile assembly/disassembly of DNA nanostructures anchored on cell-mimicking giant vesicles. *J. Am. Chem. Soc.* **2017**, *139*, 12410–12413.

(185) Suzuki, Y.; Endo, M.; Yang, Y.; Sugiyama, H. Dynamic assembly/disassembly processes of photoresponsive DNA origami nanostructures directly visualized on a lipid membrane surface. *J. Am. Chem. Soc.* **2014**, *136*, 1714–1717.

(186) Mirkin, C.; Letsinger, R.; Mucic, R.; Storhoff, J. A DNA-based method for rationally assembling nanoparticles into macroscopic materials. *Nature* **1996**, *382*, 607–609.

(187) Alivisatos, A.; Johnsson, K.; Peng, X.; Wilson, T.; Loweth, C.; Bruchez, M.; Schultz, P. Organization of ‘nanocrystal molecules’ using DNA. *Nature* **1996**, *382*, 609–611.

(188) Hazarika, P.; Ceyhan, B.; Niemeyer, C. Reversible switching of DNA-gold nanoparticle aggregation. *Angew. Chem., Int. Ed.* **2004**, *43*, 6469–6471.

(189) Song, T.; Liang, H. Synchronized assembly of gold nanoparticles drive by a dynamic DNA-fueled molecular machine. *J. Am. Chem. Soc.* **2012**, *134*, 10803–10806.

(190) Kuzyk, A.; Schreiber, R.; Zhang, H.; Govorov, A. O.; Liedl, T.; Liu, N. Reconfigurable 3D plasmonic metamolecules. *Nat. Mater.* **2014**, *13*, 862–866.

(191) Zhou, C.; Duan, X.; Liu, N. A plasmonic nanorod that walks on DNA origami. *Nat. Commun.* **2015**, *6*, 8102.

(192) Zhou, C.; Duan, X.; Liu, N. DNA-nanotechnology-enabled chiral plasmonics: from static to dynamic. *Acc. Chem. Res.* **2017**, *50*, 2906–2914.

(193) Maye, M. M.; Kumara, M. T.; Nykypanchuk, D.; Sherman, W. B.; Gang, O. Switching binary states of nanoparticle superlattices and dimer clusters by DNA strands. *Nat. Nanotechnol.* **2010**, *5*, 116–120.

(194) Xiong, H.; Sfeir, M. Y.; Gang, O. Assembly, structure and optical response of three-dimensional dynamically tunable multi-component superlattices. *Nano Lett.* **2010**, *10*, 4456–4462.

(195) Flory, J. D.; Simmons, C. R.; Lin, S.; Johnson, T.; Andreoni, A.; Zook, J.; Ghirlanda, G.; Liu, Y.; Yan, H.; Fromme, P. Low temperature assembly of functional 3D DNA-PNA-protein complexes. *J. Am. Chem. Soc.* **2014**, *136*, 8283–8295.

(196) Song, J.; Su, P.; Ma, R.; Yang, Y.; Yang, Y. Based on DNA strand displacement and functionalized magnetic nanoparticles: a promising strategy for enzyme immobilization. *Ind. Eng. Chem. Res.* **2017**, *56*, 5127–5137.

(197) Chen, R. P.; Blackstock, D.; Sun, Q.; Chen, W. Dynamic protein assembly by programmable DNA strand displacement. *Nat. Chem.* **2018**, *10*, 474–481.

(198) Parolini, L.; Kotar, J.; Di Michele, L.; Mognetti, B. M. Controlling self-assembly kinetics of DNA functionalized liposomes using toehold exchange mechanism. *ACS Nano* **2016**, *10*, 2392–2398.

(199) Feng, L.; Pontani, L.-L.; Dreyfus, R.; Chaikin, P.; Brujic, J. Specificity, flexibility and valence of DNA bonds guide emulsion architecture. *Soft Matter* **2013**, *9*, 9816–9818.

(200) Zhang, Y.; McMullen, A.; Pontani, L.-L.; He, X.; Sha, R.; Seeman, N. C.; Brujic, J.; Chaikin, P. M. Sequential self-assembly of DNA functionalized droplets. *Nat. Commun.* **2017**, *8*, 21.

(201) Sato, Y.; Hiratsuka, Y.; Kawamata, I.; Murata, S.; Nomura, S.-i. M. Micrometer-sized molecular robot changes its shape in response to signal molecules. *Sci. Robot.* **2017**, *2*, No. eaal3735.

(202) Simmel, F. C.; Schulman, R. Self-organizing materials built with DNA. *MRS Bull.* **2017**, *42*, 913–919.

(203) Li, Y.; Tseng, Y. D.; Kwon, S. Y.; D'espaux, L.; Bunch, J. S.; McEuen, P. L.; Luo, D. Controlled assembly of dendrimer-like DNA. *Nat. Mater.* **2004**, *3*, 38–42.

(204) Um, S. H.; Lee, J. B.; Park, N.; Kwon, S. Y.; Umbach, C. C.; Luo, D. Enzyme-catalysed assembly of DNA hydrogel. *Nat. Mater.* **2006**, *5*, 797–801.

(205) Liu, J. Oligonucleotide-functionalized hydrogels as stimuli responsive materials and biosensors. *Soft Matter* **2011**, *7*, 6757–11.

(206) Kahn, J. S.; Hu, Y.; Willner, I. Stimuli-responsive DNA-based hydrogels: from basic principles to applications. *Acc. Chem. Res.* **2017**, *50*, 680–690.

(207) Romano, F.; Sciortino, F. Switching bonds in a DNA gel: an all-DNA vitrimer. *Phys. Rev. Lett.* **2015**, *114*, No. 078104.

(208) Li, X.; Liu, D. R. DNA-templated organic synthesis: nature's strategy for controlling chemical reactivity applied to synthetic molecules. *Angew. Chem., Int. Ed.* **2004**, *43*, 4848–4870.

(209) Meng, W.; Muscat, R. A.; McKee, M. L.; Milnes, P. J.; El-Sagheer, A. H.; Bath, J.; Davis, B. G.; Brown, T.; O'Reilly, R. K.; Turberfield, A. J. An autonomous molecular assembler for programmable chemical synthesis. *Nat. Chem.* **2016**, *8*, 542–548.

(210) Wang, D.; Chen, G.; Wang, H.; Tang, W.; Pan, W.; Li, N.; Liu, F. Areusable quartz crystal microbalance biosensor for highly specific detection of single-base DNA mutation. *Biosens. Bioelectron.* **2013**, *48*, 276–280.

(211) Krissanaprasit, A.; Madsen, M.; Knudsen, J. B.; Gudnason, D.; Surareungchai, W.; Birkedal, V.; Gothelf, K. V. Programmed switching of single polymer conformation on DNA origami. *ACS Nano* **2016**, *10*, 2243–2250.

(212) Wang, B.; Wang, X.; Wei, B.; Huang, F.; Yao, D.; Liang, H. DNA photonic nanowires with tunable FRET signals on the basis of toehold-mediated DNA strand displacement reactions. *Nanoscale* **2017**, *9*, 2981–2985.

(213) Chandrasekaran, A. R.; Levchenko, O.; Patel, D. S.; MacIsaac, M.; Halvorsen, K. Addressable configurations of DNA nanostructures for rewritable memory. *Nucleic Acids Res.* **2017**, *45*, 11459–11465.

(214) Andersen, E. S.; Dong, M.; Nielsen, M. M.; Jahn, K.; Subramani, R.; Mamdouh, W.; Golas, M. M.; Sander, B.; Stark, H.; Oliveira, C. L. P.; Pedersen, J. S.; Birkedal, V.; Besenbacher, F.; Gothelf, K. V.; Kjems, J. Self-assembly of a nanoscale DNA box with a controllable lid. *Nature* **2009**, *459*, 73–76.

(215) Zadegan, R. M.; Jepsen, M. D. E.; Thomsen, K. E.; Okholm, A. H.; Schaffert, D. H.; Andersen, E. S.; Birkedal, V.; Kjems, J. Construction of a 4 zeptoliters switchable 3D DNA box origami. *ACS Nano* **2012**, *6*, 10050–10053.

(216) List, J.; Weber, M.; Simmel, F. C. Hydrophobic actuation of a DNA origami bilayer structure. *Angew. Chem., Int. Ed.* **2014**, *53*, 4236–4239.

(217) Marras, A. E.; Zhou, L.; Su, H.-J.; Castro, C. E. Programmable motion of DNA origami mechanisms. *Proc. Natl. Acad. Sci. U. S. A.* **2015**, *112*, 713–718.

(218) Douglas, S. M.; Bachelet, I.; Church, G. M. A logic-gated nanorobot for targeted transport of molecular payloads. *Science* **2012**, *335*, 831–834.

(219) Li, S.; et al. A DNA nanorobot functions as a cancer therapeutic in response to a molecular trigger *in vivo*. *Nat. Biotechnol.* **2018**, *36*, 258–264.

(220) Kuzuya, A.; Yamazaki, T.; Xu, Y.; Komiyama, M.; Sakai, Y. Nanomechanical DNA origami 'single-molecule beacons' directly imaged by atomic force microscopy. *Nat. Commun.* **2011**, *2*, 449–448.

(221) List, J.; Falgenhauer, E.; Kopperger, E.; Pardatscher, G. u. n.; Simmel, F. C. Long-range movement of large mechanically interlocked DNA nanostructures. *Nat. Commun.* **2016**, *7*, 1–7.

(222) Powell, J. T.; Akhuetie-Oni, B. O.; Zhang, Z.; Lin, C. DNA Origami Rotaxanes: Tailored Synthesis and Controlled Structure Switching. *Angew. Chem.* **2016**, *128*, 11584–11588.

(223) Kopperger, E.; Pirzer, T.; Simmel, F. C. Diffusive transport of molecular cargo tethered to a DNA origami platform. *Nano Lett.* **2015**, *15*, 2693–2699.

(224) Tomaru, T.; Suzuki, Y.; Kawamata, I.; Nomura, S.-I. M.; Murata, S. Stepping operation of a rotary DNA origami device. *Chem. Commun.* **2017**, *53*, 7716–7719.

(225) Castro, C. E.; Su, H.-J.; Marras, A. E.; Zhou, L.; Johnson, J. Mechanical design of DNA nanostructures. *Nanoscale* **2015**, *7*, 5913–5921.

(226) Zhan, P.; Dutta, P. K.; Wang, P.; Song, G.; Dai, M.; Zhao, S.-X.; Wang, Z.-G.; Yin, P.; Zhang, W.; Ding, B.; Ke, Y. Reconfigurable three-dimensional gold nanorod plasmonic nanostructures organized on DNA origami tripod. *ACS Nano* **2017**, *11*, 1172–1179.

(227) Woo, S.; Rothemund, P. W. K. Programmable molecular recognition based on the geometry of DNA nanostructures. *Nat. Chem.* **2011**, *3*, 620–627.

(228) Gerling, T.; Wagenbauer, K. F.; Neuner, A. M.; Dietz, H. Dynamic DNA devices and assemblies formed by shape-complementary, non-base pairing 3D components. *Science* **2015**, *347*, 1446–1452.

(229) Grossi, G.; Dalgaard Ebbesen Jepsen, M.; Kjems, J.; Andersen, E. S. Control of enzyme reactions by a reconfigurable DNA nanovault. *Nat. Commun.* **2017**, *8*, 992.

(230) Okholm, A. H.; Kjems, J. DNA nanovehicles and the biological barriers. *Adv. Drug Delivery Rev.* **2016**, *106*, 183–191 Biologically-inspired drug delivery systems. .

(231) Linko, V.; Ora, A.; Kostiainen, M. A. DNA nanostructures as smart drug-delivery vehicles and molecular devices. *Trends Biotechnol.* **2015**, *33*, 586–594.

(232) Saccà, B.; Ishitsuka, Y.; Meyer, R.; Sprengel, A.; Schöneweiß, E.-C.; Nienhaus, G. U.; Niemeyer, C. M. Reversible reconfiguration of DNA origami nanochambers monitored by single-molecule FRET. *Angew. Chem., Int. Ed.* **2015**, *54*, 3592–3597.

(233) Goodman, R. P.; Schaap, I. A. T.; Tardin, C. F.; Erben, C. M.; Berry, R. M.; Schmidt, C. F.; Turberfield, A. J. Rapid chiral assembly of rigid DNA building blocks for molecular nanofabrication. *Science* **2005**, *310*, 1661–1665.

(234) Erben, C.; Goodman, R.; Turberfield, A. J. Single-molecule protein encapsulation in a rigid DNA cage. *Angew. Chem., Int. Ed.* **2006**, *45*, 7414–7417.

(235) Goodman, R. P.; Heilemann, M.; Doose, S.; Erben, C. M.; Kapanidis, A. N.; Turberfield, A. J. Reconfigurable, braced, three-dimensional DNA nanostructures. *Nat. Nanotechnol.* **2008**, *3*, 93–96.

(236) Chandran, H.; Gopalkrishnan, N.; Phillips, A.; Reif, J. Localized hybridization circuits. In *DNA Computing and Molecular Programming*; Lecture Notes in Computer Science; Springer: Berlin, 2011; Vol. 6937, p 64.

(237) Dalchau, N.; Chandran, H.; Gopalkrishnan, N.; Phillips, A.; Reif, J. Probabilistic analysis of localized DNA hybridization circuits. *ACS Synth. Biol.* **2015**, *4*, 898–913.

(238) Mullor Ruiz, I.; Arbona, J. M.; Lad, A.; Mendoza, O.; Aimé, J.-P.; Elezgaray, J. Connecting localized DNA strand displacement reactions. *Nanoscale* **2015**, *7*, 12970–12978.

(239) Chatterjee, G.; Dalchau, N.; Muscat, R. A.; Phillips, A.; Seelig, G. A spatially localized architecture for fast and modular DNA computing. *Nat. Nanotechnol.* **2017**, *12*, 920–927.

(240) Chao, J.; Wang, J.; Wang, F.; Ouyang, X.; Kopperger, E.; Liu, H.; Li, Q.; Shi, J.; Wang, L.; Hu, J.; Wang, L.; Huang, W.; Simmel, F. C.; Fan, C. Solving mazes with single-molecule DNA navigators. *Nat. Mater.* **2018**, *17*, 479, 208.

(241) Helmig, S.; Gothelf, K. V. AFM imaging of hybridization chain reaction mediated signal transmission between two DNA origami structures. *Angew. Chem., Int. Ed.* **2017**, *56*, 13633–13636.

(242) Huang, F.; Xu, H.; Tan, W.; Liang, H. Multicolor and erasable DNA photolithography. *ACS Nano* **2014**, *8*, 6849–6855.

(243) Huang, F.; Zhou, X.; Yao, D.; Xiao, S.; Liang, H. DNA Polymer Brush Patterning through Photocontrollable Surface-Initiated DNA Hybridization Chain Reaction. *Small* **2015**, *11*, 5800–5806.

(244) Pardatscher, G.; Schwarz-Schilling, M.; Daube, S. S.; Bar-Ziv, R. H.; Simmel, F. C. Gene expression on DNA biochips patterned with strand-displacement lithography. *Angew. Chem., Int. Ed.* **2018**, *57*, 4783–4786.

(245) Buxboim, A.; Bar-Dagan, M.; Frydman, V.; Zbaida, D.; Morpurgo, M.; Bar-Ziv, R. A single-step photolithographic interface for cell-free gene expression and active biochips. *Small* **2007**, *3*, 500–510.

(246) Chirieleison, S. M.; Allen, P. B.; Simpson, Z. B.; Ellington, A. D.; Chen, X. Pattern transformation with DNA circuits. *Nat. Chem.* **2013**, *5*, 1000–1005.

(247) Alon, U. Network motifs: theory and experimental approaches. *Nat. Rev. Genet.* **2007**, *8*, 450–461.

(248) Hell, S. W. Microscopy and its focal switch. *Nat. Methods* **2009**, *6*, 24–32.

(249) Huang, B.; Bates, M.; Zhuang, X. Super-resolution fluorescence microscopy. *Annu. Rev. Biochem.* **2009**, *78*, 993–1016.

(250) Steinhauer, C.; Jungmann, R.; Sobey, T. L.; Simmel, F. C.; Tinnefeld, P. DNA Origami as a Nanoscopic Ruler for Super-Resolution Microscopy. *Angew. Chem., Int. Ed.* **2009**, *48*, 8870–8873.

(251) Sharonov, A.; Hochstrasser, R. M. Wide-field subdiffraction imaging by accumulated binding of diffusing probes. *Proc. Natl. Acad. Sci. U. S. A.* **2006**, *103*, 18911–18916.

(252) Jungmann, R.; Steinhauer, C.; Scheible, M.; Kuzyk, A.; Tinnefeld, P.; Simmel, F. C. Single-molecule kinetics and super-resolution microscopy by fluorescence imaging of transient binding on DNA origami. *Nano Lett.* **2010**, *10*, 4756–4761.

(253) Jungmann, R.; Avendaño, M. S.; Woehrstein, J. B.; Dai, M.; Shih, W. M.; Yin, P. Multiplexed 3D Cellular super-resolution imaging with DNA-PAINT and Exchange-PAINT. *Nat. Methods* **2014**, *11*, 313.

(254) Dai, M.; Jungmann, R.; Yin, P. Optical imaging of individual biomolecules in densely packed clusters. *Nat. Nanotechnol.* **2016**, *11*, 798–807.

(255) Scheible, M. B.; Pardatscher, G.; Kuzyk, A.; Simmel, F. C. Single molecule characterization of DNA binding and strand displacement reactions on lithographic DNA origami microarrays. *Nano Lett.* **2014**, *14*, 1627–33.

(256) Walker, G. T.; Little, M. C.; Nadeau, J. G.; Shank, D. D. Isothermal invitro amplification of DNA by a restriction enzyme DNA-polymerase system. *Proc. Natl. Acad. Sci. U. S. A.* **1992**, *89*, 392–396.

(257) Franco, E.; Friedrichs, E.; Kim, J.; Murray, R.; Winfree, E.; Simmel, F. C.; Jungmann, R. Timing molecular motion and production with a synthetic transcriptional clock. *Proc. Natl. Acad. Sci. U. S. A.* **2011**, *108*, E784–E793.

(258) Afonin, K. A.; Bindewald, E.; Yaghoubian, A. J.; Voss, N.; Jacovetty, E.; Shapiro, B. A.; Jaeger, L. In vitro assembly of cubic RNA-based scaffolds designed in silico. *Nat. Nanotechnol.* **2010**, *5*, 676–682.

(259) Geary, C.; Rothmund, P. W. K.; Andersen, E. S. A single-stranded architecture for cotranscriptional folding of RNA nanostructures. *Science* **2014**, *345*, 799–804.

(260) Jung, C.; Ellington, A. D. Diagnostic applications of nucleic acid circuits. *Acc. Chem. Res.* **2014**, *47*, 1825–1835.

(261) Choi, H. M. T.; Beck, V. A.; Pierce, N. A. Next-generation in situ hybridization chain reaction: higher gain, lower cost, greater durability. *ACS Nano* **2014**, *8*, 4284–4294.

(262) Choi, H. M. T.; Schwarzkopf, M.; Fornace, M. E.; Acharya, A.; Artavanis, G.; Stegmaier, J.; Cunha, A.; Pierce, N. A. Third-generation in situ hybridization chain reaction: multiplexed, quantitative, sensitive, versatile, robust. *Development* **2018**, *145*, dev165753.

(263) Molecular Instruments by scientists for scientists. <https://www.molecularinstruments.com/> (accessed January 1, 2019).

(264) Shimron, S.; Wang, F.; Orbach, R.; Willner, I. Amplified detection of DNA through the enzyme-free autonomous assembly of hemin/G-quadruplex DNAzyme nanowires. *Anal. Chem.* **2012**, *84*, 1042–1048.

(265) Tang, W.; Wang, D.; Xu, Y.; Li, N.; Liu, F. A self-assembled DNA nanostructure-amplified quartz crystal microbalance with dissipation biosensing platform for nucleic acids. *Chem. Commun.* **2012**, *48*, 6678–3.

(266) Chen, Y.; Xu, J.; Su, J.; Xiang, Y.; Yuan, R.; Chai, Y. In situ hybridization chain reaction amplification for universal and highly sensitive electrochemiluminescent detection of DNA. *Anal. Chem.* **2012**, *84*, 7750–7755.

(267) Zhuang, J.; Fu, L.; Xu, M.; Yang, H.; Chen, G.; Tang, D. Sensitive electrochemical monitoring of nucleic acids coupling DNA nanostructures with hybridization chain reaction. *Anal. Chim. Acta* **2013**, *783*, 17–23.

(268) Wang, X.; Lau, C.; Kai, M.; Lu, J. Hybridization chain reaction-based instantaneous derivatization technology for chemiluminescence detection of specific DNA sequences. *Analyst* **2013**, *138*, 2691–2697.

(269) Wang, C.; Zhou, H.; Zhu, W.; Li, H.; Jiang, J.; Shen, G.; Yu, R. Ultrasensitive electrochemical DNA detection based on dual amplification of circular strand-displacement polymerase reaction and hybridization chain reaction. *Biosens. Bioelectron.* **2013**, *47*, 324–328.

(270) Liu, S.; Wang, Y.; Ming, J.; Lin, Y.; Cheng, C.; Li, F. Enzyme-free and ultrasensitive electrochemical detection of nucleic acids by target catalyzed hairpin assembly followed with hybridization chain reaction. *Biosens. Bioelectron.* **2013**, *49*, 472–477.

(271) Xu, Q.; Zhu, G.; Zhang, C.-y. Homogeneous bioluminescence detection of biomolecules using target-triggered hybridization chain reaction-mediated ligation without luciferase label. *Anal. Chem.* **2013**, *85*, 6915–6921.

(272) Chemeris, D. A.; Nikonorov, Y. M.; Vakhitov, V. A. Real-time hybridization chain reaction. *Dokl. Biochem. Biophys.* **2008**, *419*, 53–55.

(273) Niu, S.; Jiang, Y.; Zhang, S. Fluorescence detection for DNA using hybridization chain reaction with enzyme-amplification. *Chem. Commun.* **2010**, *46*, 3089–3091.

(274) Huang, J.; Wu, Y.; Chen, Y.; Zhu, Z.; Yang, X.; Yang, C. J.; Wang, K.; Tan, W. Pyrene-eximer probes based on the hybridization chain reaction for the detection of nucleic acids in complex biological fluids. *Angew. Chem., Int. Ed.* **2011**, *50*, 401–404.

(275) Dong, J.; Cui, X.; Deng, Y.; Tang, Z. Amplified detection of nucleic acid by G-quadruplex based hybridization chain reaction. *Biosens. Bioelectron.* **2012**, *38*, 258–263.

(276) Jiang, Y.; Li, B.; Chen, X.; Ellington, D. A. Coupling two different nucleic acid circuits in an enzyme-free amplifier. *Molecules* **2012**, *17*, 13211–13220.

(277) Yang, L.; Liu, C.; Ren, W.; Li, Z. Graphene surface-anchored fluorescence sensor for sensitive detection of microRNA coupled with enzyme-free signal amplification of hybridization chain reaction. *ACS Appl. Mater. Interfaces* **2012**, *4*, 6450–6453.

(278) Ren, W.; Liu, H.; Yang, W.; Fan, Y.; Yang, L.; Wang, Y.; Liu, C.; Li, Z. A cytometric bead assay for sensitive DNA detection based on enzyme-free signal amplification of hybridization chain reaction. *Biosens. Bioelectron.* **2013**, *49*, 380–386.

(279) Liu, P.; Yang, X.; Sun, S.; Wang, Q.; Wang, K.; Huang, J.; Liu, J.; He, L. Enzyme-free colorimetric detection of dna by using gold nanoparticles and hybridization chain reaction amplification. *Anal. Chem.* **2013**, *85*, 7689–7695.

(280) Zhao, J.; Chen, C.; Zhang, L.; Jiang, J.; Yu, R. An electrochemical aptasensor based on hybridization chain reaction with enzyme-signal amplification for interferon-gamma detection. *Biosens. Bioelectron.* **2012**, *36*, 129–134.

(281) Song, W.; Zhu, K.; Cao, Z.; Lau, C.; Lu, J. Hybridization chain reaction-based aptameric system for the highly selective and sensitive detection of protein. *Analyst* **2012**, *137*, 1396–1401.

(282) Bai, L.; Chai, Y.; Yuan, R.; Yuan, Y.; Xie, S.; Jiang, L. Amperometric aptasensor for thrombin detection using enzyme-mediated direct electrochemistry and DNA-based signal amplification strategy. *Biosens. Bioelectron.* **2013**, *50*, 325–330.

(283) Zhu, G.; Zhang, S.; Song, E.; Zheng, J.; Hu, R.; Fang, X.; Tan, W. Building fluorescent DNA nanodevices on target living cell surfaces. *Angew. Chem. Int. Ed.* **2013**, *52*, 5490–5496.

(284) Xuan, F.; Hsing, I.-M. Triggering hairpin-free chain-branching growth of fluorescent DNA dendrimers for nonlinear hybridization chain reaction. *J. Am. Chem. Soc.* **2014**, *136*, 9810–9813.

(285) Choi, J.; Routenberg Love, K.; Gong, Y.; Gierahn, T. M.; Love, J. C. Immuno-hybridization chain reaction for enhancing detection of individual cytokine-secreting human peripheral mononuclear cells. *Anal. Chem.* **2011**, *83*, 6890–6895.

(286) Zhou, F. Y.; Yao, Y.; Luo, J. J.; Zhang, X.; Zhang, Y.; Yin, D. Y.; Gao, F. L.; Wang, P. Proximity hybridization-regulated catalytic DNA hairpin assembly for electrochemical immunoassay based on in situ DNA template-synthesized Pd nanoparticles. *Anal. Chim. Acta* **2017**, *969*, 8–17.

(287) Han, J.; Zhuo, Y.; Chai, Y.; Yu, Y.; Liao, N.; Yuan, R. Electrochemical immunoassay for thyroxine detection using cascade catalysis as signal amplified enhancer and multi-functionalized magnetic graphene sphere as signal tag. *Anal. Chim. Acta* **2013**, *790*, 24–30.

(288) Bi, S.; Chen, M.; Jia, X.; Dong, Y.; Wang, Z. Hyperbranched hybridization chain reaction for triggered signal amplification and concatenated logic circuits. *Angew. Chem.* **2015**, *127*, 8262–8266.

(289) Li, D. X.; Zhou, W. J.; Chai, Y. Q.; Yuan, R.; Xiang, Y. Click chemistry-mediated catalytic hairpin self-assembly for amplified and sensitive fluorescence detection of Cu²⁺ in human serum. *Chem. Commun.* **2015**, *51*, 12637–12640.

(290) Yang, L. Z.; Yun, W.; Chen, Y. L.; Wu, H.; Liu, X. Y.; Fu, M.; Huang, Y. Ultrasensitive colorimetric and fluorometric detection of Hg(II) based on the use of gold nanoparticles and a catalytic hairpin assembly. *Microchim. Acta* **2017**, *184*, 4741–4747.

(291) Li, X.; Xie, J. Q.; Jiang, B. Y.; Yuan, R.; Xiang, Y. Metallo-toehold-activated catalytic hairpin assembly formation of three-way DNAzyme junctions for amplified fluorescent detection of Hg²⁺. *ACS Appl. Mater. Interfaces* **2017**, *9*, 5733–5738.

(292) Wu, Z. K.; Fan, H. H.; Satyavolu, N. S. R.; Wang, W. J.; Lake, R.; Jiang, J. H.; Lu, Y. Imaging endogenous metal ions in living cells using a DNAzyme-catalytic hairpin assembly probe. *Angew. Chem. Int. Ed.* **2017**, *56*, 8721–8725.

(293) Yun, W.; Xiong, W.; Wu, H.; Fu, M.; Huang, Y.; Liu, X. Y.; Yang, L. Z. Graphene oxide-based fluorescent “turn-on” strategy for Hg²⁺ detection by using catalytic hairpin assembly for amplification. *Sens. Actuators, B* **2017**, *249*, 493–498.

(294) Zhao, J. M.; Jing, P.; Xue, S. Y.; Xu, W. J. Dendritic structure DNA for specific metal ion biosensor based on catalytic hairpin assembly and a sensitive synergistic amplification strategy. *Biosens. Bioelectron.* **2017**, *87*, 157–163.

(295) Huang, X. Y.; Li, J. L.; Zhang, Q. Y.; Chen, S.; Xu, W.; Wu, J. Y.; Niu, W. C.; Xue, J. J.; Li, C. R. A protease-free and signal-on electrochemical biosensor for ultrasensitive detection of lead ion based on GR-5 DNAzyme and catalytic hairpin assembly. *J. Electronanal. Chem.* **2018**, *816*, 75–82.

(296) Ma, C. P.; Wang, W. S.; Li, Z. X.; Cao, L. J.; Wang, Q. Y. Simple colorimetric DNA detection based on hairpin assembly reaction and target-catalytic circuits for signal amplification. *Anal. Biochem.* **2012**, *429*, 99–102.

(297) Li, C. X.; Li, Y. X.; Xu, X.; Wang, X. Y.; Chen, Y.; Yang, X. D.; Liu, F.; Li, N. Fast and quantitative differentiation of single-base mismatched DNA by initial reaction rate of catalytic hairpin assembly. *Biosens. Bioelectron.* **2014**, *60*, 57–63.

(298) Song, W. L.; Zhang, Q.; Sun, W. B. Ultrasensitive detection of nucleic acids by template enhanced hybridization followed by rolling circle amplification and catalytic hairpin assembly. *Chem. Commun.* **2015**, *51*, 2392–2395.

(299) Hun, X.; Xie, G. L.; Luo, X. L. Scaling up an electrochemical signal with a catalytic hairpin assembly coupling nanocatalyst label for DNA detection. *Chem. Commun.* **2015**, *51*, 7100–7103.

(300) Zang, Y.; Lei, J. P.; Ling, P. H.; Ju, H. X. Catalytic hairpin assembly-programmed porphyrin-DNA complex as photoelectrochemical initiator for dna biosensing. *Anal. Chem.* **2015**, *87*, 5430–5436.

(301) Liu, S. F.; Wei, W. J.; Liu, T.; Wang, L. Catalytic hairpin assembly-programmed DNA three-way junction for enzyme-free and amplified electrochemical detection of target dna. *Chem. - Asian J.* **2015**, *10*, 1903–1908.

(302) Tao, C. Y.; Yan, Y. R.; Xiang, H.; Zhu, D.; Cheng, W.; Ju, H. X.; Ding, S. J. A new mode for highly sensitive and specific detection of DNA based on exonuclease III-assisted target recycling amplification and mismatched catalytic hairpin assembly. *Chem. Commun.* **2015**, *51*, 4220–4222.

(303) Chen, C. H.; Li, N. X.; Lan, J. W.; Ji, X. H.; He, Z. K. A label-free colorimetric platform for DNA via target-catalyzed hairpin assembly and the peroxidase-like catalytic of graphene/Au-NPs hybrids. *Anal. Chim. Acta* **2016**, *902*, 154–159.

(304) Park, C.; Song, Y.; Jang, K.; Choi, C. H.; Na, S. Target switching catalytic hairpin assembly and gold nanoparticle colorimetric for EGFR mutant detection. *Sens. Actuators, B* **2018**, *261*, 497–504.

(305) Hun, X.; Meng, Y.; Wang, S. S.; Zhang, H.; Luo, X. L. Mismatched catalytic hairpin assembly coupling hydroxylamine-O-sulfonic acid as oxide for DNA assay. *Sens. Actuators, B* **2018**, *254*, 347–353.

(306) Xu, Y.; Zheng, Z. Direct RNA detection without nucleic acid purification and PCR: Combining sandwich hybridization with singnal amplification based on branched hybridization chain reaction. *Biosens. Bioelectron.* **2016**, *79*, 593–599.

(307) Zhuang, J. Y.; Lai, W. Q.; Chen, G. N.; Tang, D. P. A rolling circle amplification-based DNA machine for miRNA screening coupling catalytic hairpin assembly with DNAzyme formation. *Chem. Commun.* **2014**, *50*, 2935–2938.

(308) Zhang, Y.; Yan, Y. R.; Chen, W. H.; Cheng, W.; Li, S. Q.; Ding, X. J.; Li, D. D.; Wang, H.; Ju, H. X.; Ding, S. J. A simple electrochemical biosensor for highly sensitive and specific detection of microRNA based on mismatched catalytic hairpin assembly. *Biosens. Bioelectron.* **2015**, *68*, 343–349.

(309) Yan, Y. R.; Shen, B.; Wang, H.; Sun, X.; Cheng, W.; Zhao, H.; Ju, H. X.; Ding, S. J. A novel and versatile nanomachine for ultrasensitive and specific detection of microRNAs based on

molecular beacon initiated strand displacement amplification coupled with catalytic hairpin assembly with DNAzyme formation. *Analyst* **2015**, *140*, 5469–5474.

(310) Hao, N.; Dai, P. P.; Yu, T.; Xu, J. J.; Chen, H. Y. A dual target-recycling amplification strategy for sensitive detection of microRNAs based on duplex-specific nuclease and catalytic hairpin assembly. *Chem. Commun.* **2015**, *51*, 13504–13507.

(311) Li, D. D.; Cheng, W.; Li, Y. J.; Xu, Y. J.; Li, X. M.; Yin, Y. B.; Ju, H. X.; Ding, S. J. Catalytic hairpin assembly actuated DNA nanotweezer for logic gate building and sensitive enzyme-free biosensing of microRNAs. *Anal. Chem.* **2016**, *88*, 7500–7506.

(312) Zhang, C. H.; Tang, Y.; Sheng, Y. Y.; Wang, H.; Wu, Z.; Jiang, J. H. Ultrasensitive detection of microRNAs using catalytic hairpin assembly coupled with enzymatic repairing amplification. *Chem. Commun.* **2016**, *52*, 13584–13587.

(313) Wei, Y. L.; Zhou, W. J.; Li, X.; Chai, Y. Q.; Yuan, R.; Xiang, Y. Coupling hybridization chain reaction with catalytic hairpin assembly enables non-enzymatic and sensitive fluorescent detection of microRNA cancer biomarkers. *Biosens. Bioelectron.* **2016**, *77*, 416–420.

(314) Ouyang, W. J.; Liu, Z. H.; Zhang, G. F.; Chen, Z.; Guo, L. H.; Lin, Z. Y.; Qiu, B.; Chen, G. N. Enzyme-free fluorescent biosensor for miRNA-21 detection based on MnO₂ nanosheets and catalytic hairpin assembly amplification. *Anal. Methods* **2016**, *8*, 8492–8497.

(315) Li, J. B.; Lei, P. H.; Ding, S. J.; Zhang, Y.; Yang, J. R.; Cheng, Q.; Yan, Y. R. An enzyme-free surface plasmon resonance biosensor for real-time detecting microRNA based on allosteric effect of mismatched catalytic hairpin assembly. *Biosens. Bioelectron.* **2016**, *77*, 435–441.

(316) Zhang, H.; Wang, Q.; Yang, X. H.; Wang, K. M.; Li, Q.; Li, Z. P.; Gao, L.; Nie, W. Y.; Zheng, Y. An isothermal electrochemical biosensor for the sensitive detection of microRNA based on a catalytic hairpin assembly and supersandwich amplification. *Analyst* **2017**, *142*, 389–396.

(317) Yao, J.; Zhang, Z.; Deng, Z. H.; Wang, Y. Q.; Guo, Y. C. An enzyme free electrochemical biosensor for sensitive detection of miRNA with a high discrimination factor by coupling the strand displacement reaction and catalytic hairpin assembly recycling. *Analyst* **2017**, *142*, 4116–4123.

(318) Cai, W.; Xie, S. B.; Tang, Y.; Chai, Y. Q.; Yuan, R.; Zhang, J. A label-free electrochemical biosensor for microRNA detection based on catalytic hairpin assembly and in situ formation of molybdocephosphate. *Talanta* **2017**, *163*, 65–71.

(319) Zhang, K. Y.; Zhang, N.; Zhang, L.; Wang, H. Y.; Shi, H. W.; Liu, Q. Label-free impedimetric sensing platform for microRNA-21 based on ZrO₂-reduced graphene oxide nanohybrids coupled with catalytic hairpin assembly amplification. *RSC Adv.* **2018**, *8*, 16146–16151.

(320) Zhang, H. M.; Wang, K. Y.; Bu, S. J.; Li, Z. Y.; Ju, C. J.; Wan, J. Y. Colorimetric detection of microRNA based on DNAzyme and nuclease-assisted catalytic hairpin assembly signal amplification. *Mol. Cell. Probes* **2018**, *38*, 13–18.

(321) Tang, S. S.; Gu, Y.; Lu, H. T.; Dong, H. F.; Zhang, K.; Dai, W. H.; Meng, X. D.; Yang, F.; Zhang, X. J. Highly-sensitive microRNA detection based on bio-bar-code assay and catalytic hairpin assembly two-stage amplification. *Anal. Chim. Acta* **2018**, *1004*, 1–9.

(322) Luo, J.; Xu, Y. J.; Huang, J.; Zhang, S.; Xu, Q.; He, J. Enzyme-free amplified detection of circulating microRNA by making use of DNA circuits, a DNAzyme, and a catalytic hairpin assembly. *Microchim. Acta* **2018**, *185*, 38.

(323) Liu, J. T.; Du, P.; Zhang, J.; Shen, H.; Lei, J. P. Sensitive detection of intracellular microRNA based on a flowerlike vector with catalytic hairpin assembly. *Chem. Commun.* **2018**, *54*, 2550–2553.

(324) Li, Q.; Zeng, F. P.; Lyu, N.; Liang, J. Highly sensitive and specific electrochemical biosensor for microRNA-21 detection by coupling catalytic hairpin assembly with rolling circle amplification. *Analyst* **2018**, *143*, 2304–2309.

(325) Liao, X. J.; Li, L. Q.; Pan, J. B.; Peng, T. T.; Ge, B.; Tang, Q. L. In situ biosensor for detection miRNA in living cells based on carbon nitride nanosheets with catalytic hairpin assembly amplification. *Luminescence* **2018**, *33*, 190–195.

(326) Kim, H.; Kang, S.; Park, K. S.; Park, H. G. Enzyme-free and label-free miRNA detection based on target-triggered catalytic hairpin assembly and fluorescence enhancement of DNA-silver nanoclusters. *Sens. Actuators, B* **2018**, *260*, 140–145.

(327) Dai, W. H.; Zhang, J.; Meng, X. D.; He, J.; Zhang, K.; Cao, Y.; Wang, D. D.; Dong, H. F.; Zhang, X. J. Catalytic hairpin assembly gel assay for multiple and sensitive microRNA detection. *Theranostics* **2018**, *8*, 2646–2656.

(328) Tang, Y. N.; Lin, Y. W.; Yang, X. L.; Wang, Z. X.; Le, X. C.; Li, F. Universal strategy to engineer catalytic DNA hairpin assemblies for protein analysis. *Anal. Chem.* **2015**, *87*, 8063–8066.

(329) Liu, S. F.; Cheng, C. B.; Gong, H. W.; Wang, L. Programmable Mg²⁺-dependent DNAzyme switch by the catalytic hairpin DNA assembly for dual-signal amplification toward homogeneous analysis of protein and DNA. *Chem. Commun.* **2015**, *51*, 7364–7367.

(330) Chang, C. C.; Chen, C. P.; Chen, C. Y.; Lin, C. W. DNA base-stacking assay utilizing catalytic hairpin assembly-induced gold nanoparticle aggregation for colorimetric protein sensing. *Chem. Commun.* **2016**, *52*, 4167–4170.

(331) Shi, K.; Dou, B. T.; Yang, J. M.; Yuan, R.; Xiang, Y. Target-triggered catalytic hairpin assembly and TdT-catalyzed DNA polymerization for amplified electronic detection of thrombin in human serums. *Biosens. Bioelectron.* **2017**, *87*, 495–500.

(332) Jiang, B. Y.; Li, F. Z.; Yang, C. Y.; Xie, J. Q.; Xiang, Y.; Yuan, R. Target-induced catalytic hairpin assembly formation of functional Y-junction DNA structures for label-free and sensitive electrochemical detection of human serum proteins. *Sens. Actuators, B* **2017**, *244*, 61–66.

(333) Zhao, J. C.; Ma, Z. F. Ultrasensitive detection of prostate specific antigen by electrochemical aptasensor using enzyme-free recycling amplification via target-induced catalytic hairpin assembly. *Biosens. Bioelectron.* **2018**, *102*, 316–320.

(334) Yang, W. T.; Zhou, X. X.; Zhao, J. M.; Xu, W. J. A cascade amplification strategy of catalytic hairpin assembly and hybridization chain reaction for the sensitive fluorescent assay of the model protein carcinoembryonic antigen. *Microchim. Acta* **2018**, *185*, DOI: 10.1007/s00604-017-2620-6.

(335) Cui, H. Y.; Bo, B.; Ma, J.; Tang, Y. Y.; Zhao, J.; Xiao, H. P. A target-responsive liposome activated by catalytic hairpin assembly enables highly sensitive detection of tuberculosis-related cytokine. *Chem. Commun.* **2018**, *54*, 4870–4873.

(336) Zhang, Y.; Luo, S. H.; Situ, B.; Chai, Z. X.; Li, B.; Liu, J. M.; Zheng, L. A novel electrochemical cytosensor for selective and highly sensitive detection of cancer cells using binding-induced dual catalytic hairpin assembly. *Biosens. Bioelectron.* **2018**, *102*, 568–573.

(337) Xu, X. W.; Wang, L.; Wu, Y. S.; Jiang, W. Uracil removal-inhibited ligase reaction in combination with catalytic hairpin assembly for the sensitive and specific detection of uracil-DNA glycosylase activity. *Analyst* **2017**, *142*, 4655–4660.

(338) Zhou, C.; Zou, H. M.; Sun, C. J.; Ren, D. X.; Xiong, W.; Li, Y. X. Fluorescent aptasensor for detection of four tetracycline veterinary drugs in milk based on catalytic hairpin assembly reaction and displacement of G-quadruplex. *Anal. Bioanal. Chem.* **2018**, *410*, 2981–2989.

(339) Zhou, C.; Sun, C. J.; Luo, Z. W.; Liu, K. P.; Yang, X. J.; Zou, H. M.; Li, Y. X.; Duan, Y. X. Fiber optic biosensor for detection of genetically modified food based on catalytic hairpin assembly reaction and nanocomposites assisted signal amplification. *Sens. Actuators, B* **2018**, *254*, 956–965.

(340) Su, F. X.; Yang, C. X.; Yan, X. P. Intracellular messenger RNA triggered catalytic hairpin assembly for fluorescence imaging guided photothermal therapy. *Anal. Chem.* **2017**, *89*, 7277–7281.

(341) Jiang, Y.; Li, B. L.; Milligan, J. N.; Bhadra, S.; Ellington, A. D. Real-time detection of isothermal amplification reactions with thermostable catalytic hairpin assembly. *J. Am. Chem. Soc.* **2013**, *135*, 7430–7433.

(342) Bi, S.; Yue, S.; Wu, Q.; Ye, J. Initiator-catalyzed self-assembly of duplex-looped DNA hairpin motif based on strand displacement reaction for logic operations and amplified biosensing. *Biosens. Bioelectron.* **2016**, *83*, 281–286.

(343) Chen, X.; Briggs, N.; McLain, J. R.; Ellington, A. D. Stacking nonenzymatic circuits for high signal gain. *Proc. Natl. Acad. Sci. U. S. A.* **2013**, *110*, 5386–5391.

(344) Yue, S.; Zhao, T.; Qi, H.; Yan, Y.; Bi, S. Cross-catalytic hairpin assembly-based exponential signal amplification for CRET assay with low background noise. *Biosens. Bioelectron.* **2017**, *94*, 671–676.

(345) Bhadra, S.; Ellington, A. D. Design and application of cotranscriptional non-enzymatic RNA circuits and signal transducers. *Nucleic Acids Res.* **2014**, *42*, No. e58.

(346) Wu, F.; Chen, M.; Lan, J.; Xia, Y.; Liu, M.; He, W.; Li, C.; Chen, X.; Chen, J. A universal locked nucleic acid-integration X-shaped DNA probe design for amplified fluorescence detection of single-nucleotide variant. *Sens. Actuators, B* **2017**, *241*, 123–128.

(347) Gao, Z. F.; Ling, Y.; Lu, L.; Chen, N. Y.; Luo, H. Q.; Li, H. B. Detection of single-nucleotide polymorphisms using an ON-OFF switching of regenerated biosensor based on a locked nucleic acid-integrated and toehold-mediated strand displacement reaction. *Anal. Chem.* **2014**, *86*, 2543–2548.

(348) Khodakov, D. A.; Khodakova, A. S.; Linacre, A.; Ellis, A. V. Toehold-mediated nonenzymatic DNA strand displacement as a platform for DNA genotyping. *J. Am. Chem. Soc.* **2013**, *135*, 5612–5619.

(349) Khodakov, D. A.; Khodakova, A. S.; Huang, D. M.; Linacre, A.; Ellis, A. V. Protected DNA strand displacement for enhanced single nucleotide discrimination in double-stranded DNA. *Sci. Rep.* **2015**, *5*, 8721.

(350) Zhang, D. Y.; Chen, S. X.; Yin, P. Optimizing the specificity of nucleic acid hybridization. *Nat. Chem.* **2012**, *4*, 208–214.

(351) NuProbe. <https://www.nuprobe.com/> (accessed January 1, 2019)..

(352) Zhu, J.; Ding, Y.; Liu, X.; Wang, L.; Jiang, W. Toehold-mediated strand displacement reaction triggered isothermal DNA amplification for highly sensitive and selective fluorescent detection of single-base mutation. *Biosens. Bioelectron.* **2014**, *59*, 276–281.

(353) Yu, Y.; Wu, T.; Johnson-Buck, A.; Li, L.; Su, X. A two-layer assay for single-nucleotide variants utilizing strand displacement and selective digestion. *Biosens. Bioelectron.* **2016**, *82*, 248–254.

(354) Fenati, R. A.; Connolly, A. R.; Ellis, A. V. Single nucleotide polymorphism discrimination with and without an ethidium bromide intercalator. *Anal. Chim. Acta* **2017**, *954*, 121–128.

(355) Wang, X.; Zou, M.; Huang, H.; Ren, Y.; Li, L.; Yang, X.; Li, N. Gold nanoparticle enhanced fluorescence anisotropy for the assay of single nucleotide polymorphisms (SNPs) based on toehold-mediated strand-displacement reactions. *Biosens. Bioelectron.* **2013**, *41*, 569–575.

(356) Long, J.-B.; Liu, Y.-X.; Cao, Q.-F.; Guo, Q.-P.; Yan, S.-Y.; Meng, X.-X. Sensitive and enzyme-free detection for single nucleotide polymorphism using microbead-assisted toehold-mediated strand displacement reaction. *Chin. Chem. Lett.* **2015**, *26*, 1031–1035.

(357) Zhang, Z.; Li, J. L.; Yao, J.; Wang, T.; Yin, D.; Xiang, Y.; Chen, Z.; Xie, G. Energy driven cascade recognition for selective detection of nucleic acids with high discrimination factor at room temperature. *Biosens. Bioelectron.* **2016**, *79*, 488–494.

(358) Zhang, Z.; Zeng, D.; Ma, H.; Feng, G.; Hu, J.; He, L.; Li, C.; Fan, C. A DNA-origami chip platform for label-free SNP genotyping using toehold-mediated strand displacement. *Small* **2010**, *6*, 1854–1858.

(359) Massey, M.; Ancona, M. G.; Medintz, I. L.; Algar, W. R. Time-resolved nucleic acid hybridization beacons utilizing unimolecular and toehold-mediated strand displacement designs. *Anal. Chem.* **2015**, *87*, 11923–11931.

(360) Xuan, F.; Fan, T. W.; Hsing, I.-M. Electrochemical interrogation of kinetically-controlled dendritic DNA/PNA assembly for immobilization-free and enzyme-free nucleic acids sensing. *ACS Nano* **2015**, *9*, 5027–5033.

(361) Guo, Y.; Wang, Q.; Wang, Z.; Chen, X.; Xu, L.; Hu, J.; Pei, R. Label-free detection of T4 DNA ligase and polynucleotide kinase activity based on toehold-mediated strand displacement and split G-quadruplex probes. *Sens. Actuators, B* **2015**, *214*, 50–55.

(362) Guo, Y.; Yao, W.; Xie, Y.; Zhou, X.; Hu, J.; Pei, R. Logic gates based on G-quadruplexes: principles and sensor applications. *Microchim. Acta* **2016**, *183*, 21–34.

(363) Kim, S.; Huan, T. N.; Kim, J.; Yoo, S. Y.; Chung, H. Toehold-mediated DNA displacement-based surface-enhanced Raman scattering DNA sensor utilizing and Au-Ag bimetallic nanodendrite substrate. *Anal. Chim. Acta* **2015**, *885*, 132–139.

(364) Guo, Y.; Yang, K.; Sun, J.; Wu, J.; Ju, H. A pH-responsive colorimetric strategy for DNA detection by acetylcholinesterase catalyzed hydrolysis and cascade amplification. *Biosens. Bioelectron.* **2017**, *94*, 651–656.

(365) Chen, H. G.; Ren, W.; Jia, J.; Feng, J.; Gao, Z. F.; Li, N. B.; Luo, H. Q. Fluorometric detection of mutant DNA oligonucleotide based on toehold strand displacement-driven target recycling strategy and exonuclease III-assisted suppression. *Biosens. Bioelectron.* **2016**, *77*, 40–45.

(366) Yin, D.; Tao, Y.; Tang, L.; Li, W.; Zhang, Z.; Li, J.; Xie, G. Cascade toehold-mediated strand displacement along with non-enzymatic target recycling amplification for the electrochemical determination of the HIV-1 related gene. *Microchim. Acta* **2017**, *184*, 3721–3728.

(367) Feng, Q.; Zhao, X.; Guo, Y.; Liu, M.; Wang, P. Stochastic DNA walker for electrochemical biosensing sensitized with gold nanocages@graphene nanoribbons. *Biosens. Bioelectron.* **2018**, *108*, 97–102.

(368) Jiang, Y. S.; Bhadra, S.; Li, B.; Wu, Y. R.; Milligan, J. N.; Ellington, A. D. Robust strand exchange reactions for the sequence-specific, real-time detection of nucleic acid amplicons. *Anal. Chem.* **2015**, *87*, 3314–3320.

(369) Ravan, H. Isothermal RNA detection through the formation of DNA concatemers containing HRP-mimicking DNAzymes on the surface of gold nanoparticles. *Biosens. Bioelectron.* **2016**, *80*, 67–73.

(370) Deng, R.; Tang, L.; Tian, Q.; Wang, Y.; Lin, L.; Li, J. Toehold-initiated rolling circle amplification for visualizing individual microRNAs *in situ* in single cells. *Angew. Chem., Int. Ed.* **2014**, *53*, 2389–2393.

(371) Shi, K.; Dou, B.; Yang, C.; Chai, Y.; Yuan, R.; Xiang, Y. DNA-fueled molecular machine enables enzyme-free target recycling amplification for electronic detection of microRNA from cancer cells with highly minimized background noise. *Anal. Chem.* **2015**, *87*, 8578–8583.

(372) Li, W.; Jiang, W.; Ding, Y.; Wang, L. Highly selective and sensitive detection of miRNA based on toehold-mediated strand displacement reaction and DNA tetrahedron substrate. *Biosens. Bioelectron.* **2015**, *71*, 401–406.

(373) Bi, S.; Xiu, B.; Ye, J.; Dong, Y. Target-catalyzed DNA four-way junctions for CRET imaging of microRNA, concatenated logic operations, and self-assembly of DNA nanohydrogels for targeted drug delivery. *ACS Appl. Mater. Interfaces* **2015**, *7*, 23310–23319.

(374) Zhu, Y.; Qiu, D.; Yang, G.; Wang, M.; Zhang, Q.; Wang, P.; Ming, H.; Zhang, D.; Yu, Y.; Zou, G.; Badugu, R.; Lakowicz, J. R. Selective and sensitive detection of MiRNA-21 based on gold-nanorod functionalized polydiacetylene microtube waveguide. *Biosens. Bioelectron.* **2016**, *85*, 198–204.

(375) Wang, R.; Wang, L.; Zhao, H.; Jiang, W. A split recognition mode combined with cascade signal amplification strategy for highly specific, sensitive detection of microRNA. *Biosens. Bioelectron.* **2016**, *86*, 834–839.

(376) Shi, K.; Dou, B.; Yang, J.; Yuan, R.; Xiang, Y. Cascaded strand displacement for non-enzymatic target recycling amplification and label-free electronic detection of microRNA from tumor cells. *Anal. Chim. Acta* **2016**, *916*, 1–7.

(377) Oishi, M.; Sugiyama, S. An efficient particle-based DNA circuit system: catalytic disassembly of DNA/PEG-modified gold

nanoparticle-magnetic bead composites for colorimetric detection of mirna. *Small* 2016, 12, 5153–5158.

(378) Miao, J.; Wang, J.; Guo, J.; Gao, H.; Han, K.; Jiang, C.; Miao, P. A plasmonic colorimetric strategy for visual miRNA detection based on hybridization chain reaction. *Sci. Rep.* 2016, 6, 32219.

(379) Liu, W.; Zhu, M.; Liu, H.; Wei, J.; Zhou, X.; Xing, D. Invading stacking primer: A trigger for high-efficiency isothermal amplification reaction with superior selectivity for detecting microRNA variants. *Biosens. Bioelectron.* 2016, 81, 309–316.

(380) Li, D.; Cheng, W.; Yan, Y.; Zhang, Y.; Yin, Y.; Ju, H.; Ding, S. A colorimetric biosensor for detection of attomolar microRNA with a functional nucleic acid-based amplification machine. *Talanta* 2016, 146, 470–476.

(381) Yue, S.; Zhao, T.; Bi, S.; Zhang, Z. Programmable strand displacement-based magnetic separation for simultaneous amplified detection of multiplex microRNAs by chemiluminescence imaging array. *Biosens. Bioelectron.* 2017, 98, 234–239.

(382) Zhang, J.; Wang, L.-L.; Hou, M.-F.; Xia, Y.-K.; He, W.-H.; Yan, A.; Weng, Y.-P.; Zeng, L.-P.; Chen, J.-H. A radiometric electrochemical biosensor for the exosomal microRNAs detection based on bipedal DNA walkers propelled by locked nucleic acid modified toehold mediated strand displacement reaction. *Biosens. Bioelectron.* 2018, 102, 33–40.

(383) Shen, Y.; Li, Z.; Wang, G.; Ma, N. Photocaged nanoparticle sensor for sensitive microRNA imaging in living cancer cells with temporal control. *ACS Sens.* 2018, 3, 494–503.

(384) Peng, Y.; Zhou, W.; Yuan, R.; Xiang, Y. Dual-input molecular logic circuits for sensitive and simultaneous sensing of multiple microRNAs from tumor cells. *Sens. Actuators, B* 2018, 264, 202–207.

(385) Park, Y.; Lee, C. Y.; Kang, S.; Kim, H.; Park, K. S.; Park, H. G. Universal, colorimetric microRNA detection strategy based on target-catalyzed toehold-mediated strand displacement reaction. *Nanotechnology* 2018, 29, No. 085501.

(386) Chen, J.; Shang, B.; Zhang, H.; Zhu, Z.; Chen, L.; Wang, H.; Ran, F.; Chen, Q.; Chen, J. Enzyme-free ultrasensitive fluorescence detection of epithelial cell adhesion molecules based on a toehold-aided DNA recycling amplification strategy. *RSC Adv.* 2018, 8, 14798–14805.

(387) Chen, Q.; Hu, W.; Shang, B.; Wei, J.; Chen, L.; Guo, X.; Ran, F.; Chen, W.; Ding, X.; Xu, Y.; Wu, Y. Ultrasensitive amperometric aptasensor for the epithelial cell adhesion molecule by using target-driven toehold-mediated DNA recycling amplification. *Microchim. Acta* 2018, 185, 202.

(388) Yang, J.; Dou, B.; Yuan, R.; Xiang, Y. Aptamer/protein proximity binding-triggered molecular machine for amplified electrochemical sensing of thrombin. *Anal. Chem.* 2017, 89, 5138–5143.

(389) Zhu, J.; Gan, H.; Wu, J.; Ju, H. Molecular machine powered surface programmatic chain reaction for highly sensitive electrochemical detection of protein. *Anal. Chem.* 2018, 90, 5503–5508.

(390) Li, F.; Lin, Y.; Le, X. C. Binding-induced formation of DNA three-way junctions and its application to protein detection and DNA strand displacement. *Anal. Chem.* 2013, 85, 10835–10841.

(391) Li, J.; Sun, K.; Chen, Z.; Shi, J.; Zhou, D.; Xie, G. A fluorescence biosensor for VEGF detection based on DNA assembly structure switching and isothermal amplification. *Biosens. Bioelectron.* 2017, 89, 964–969.

(392) Tang, Y.; Wang, Z.; Yang, X.; Chen, J.; Liu, L.; Zhao, W.; Le, X. C.; Li, F. Constructing real-time, wash-free, and reiterative sensors for cell surface proteins using binding-induced dynamic DNA assembly. *Chem. Sci.* 2015, 6, 5729–5733.

(393) Huang, Y.; Zheng, W.; Li, X. Detection of protein targets with a single binding epitope using DNA-templated photo-crosslinking and strand displacement. *Anal. Biochem.* 2018, 545, 84–90.

(394) Xiao, X.; Tao, J.; Zhang, H. Z.; Huang, C. Z.; Zhen, S. J. Exonuclease III-assisted graphene oxide amplified fluorescence anisotropy strategy for ricin detection. *Biosens. Bioelectron.* 2016, 85, 822–827.

(395) Yang, D.; Ning, L.; Gao, T.; Ye, Z.; Li, G. Enzyme-free dual amplification strategy for protein assay by coupling toehold-mediated DNA strand displacement reaction with hybridization chain reaction. *Electrochim. Commun.* 2015, 58, 33–36.

(396) Chen, S.; Ma, H.; Li, W.; Nie, Z.; Yao, S. An entropy-driven signal amplification strategy for real-time monitoring of DNA methylation process and high-throughput screening of methyltransferase inhibitors. *Anal. Chim. Acta* 2017, 970, 57–63.

(397) Wu, Y.; Wang, L.; Jiang, W. Toehold-mediated strand displacement reaction-dependent fluorescent strategy for sensitive detection of uracil-DNA glycosylase activity. *Biosens. Bioelectron.* 2017, 89, 984–988.

(398) Ren, R.; Shi, K.; Yang, J.; Yuan, R.; Xiang, Y. DNA three way junction-mediated recycling amplification for sensitive electrochemical monitoring of uracil-DNA glycosylase activity and inhibition. *Sens. Actuators, B* 2018, 258, 783–788.

(399) Xu, X.; Wang, L.; Li, K.; Huang, Q.; Jiang, W. A smart DNA tweezer for detection of human telomerase activity. *Anal. Chem.* 2018, 90, 3521–3530.

(400) Guo, S.; Huang, H.; Deng, X.; Chen, Y.; Jiang, Z.; Xie, M.; Liu, S.; Huang, W.; Zhou, X. Programmable DNA-responsive microchip for the capture and release of circulating tumor cells by nucleic acid hybridization. *Nano Res.* 2018, 11, 2592–2604.

(401) Shlyahovsky, B.; Li, D.; Weizmann, Y.; Nowarski, R.; Kotler, M.; Willner, I. Spotlighting of cocaine by an autonomous aptamer-based machine. *J. Am. Chem. Soc.* 2007, 129, 3814–3815.

(402) Chen, J.; Zhou, S. Label-free DNA Y junction for bisphenol A monitoring using exonuclease III-based signal protection strategy. *Biosens. Bioelectron.* 2016, 77, 277–283.

(403) Peng, P.; Shi, L.; Wang, H.; Li, T. A DNA nanoswitch-controlled reversible nanosensor. *Nucleic Acids Res.* 2017, 45, 541–546.

(404) Zhao, J.; Zheng, T.; Gao, J.; Xu, W. Toehold-mediated strand displacement reaction triggered by nicked DNAzymes substrate for amplified electrochemical detection of lead ion. *Electrochim. Acta* 2018, 274, 16–22.

(405) Yu, L.; Lan, W.; Chen, H.; Bai, L.; Wang, W.; Xu, H. Label-free detection of Hg^{2+} based on Hg^{2+} -triggered toehold binding, Exonuclease III assisted target recycling and hybridization chain reaction. *Sens. Actuators, B* 2017, 248, 411–418.

(406) Chen, J.; Zhou, S.; Wen, J. Disposable strip biosensor for visual detection of Hg^{2+} based on Hg^{2+} -triggered toehold binding and exonuclease III-assisted signal amplification. *Anal. Chem.* 2014, 86, 3108–3114.

(407) Rudchenko, M.; Taylor, S.; Pallavi, P.; Dechkovskaia, A.; Khan, S.; Butler, V. P.; Rudchenko, S.; Stojanovic, M. N. Autonomous molecular cascades for evaluation of cell surfaces. *Nat. Nanotechnol.* 2013, 8, 580–586.

(408) Mandal, M.; Breaker, R. R. Gene regulation by riboswitches. *Nat. Rev. Mol. Cell Biol.* 2004, 5, 451–463.

(409) Isaacs, F. J.; Dwyer, D. J.; Ding, C. M.; Pervouchine, D. D.; Cantor, C. R.; Collins, J. J. Engineered riboregulators enable post-transcriptional control of gene expression. *Nat. Biotechnol.* 2004, 22, 841–847.

(410) Watters, K. E.; Abbott, T. R.; Lucks, J. B. Simultaneous characterization of cellular RNA structure and function with in-cell SHAPE-Seq. *Nucleic Acids Res.* 2016, 44, No. e12.

(411) Green, A. A.; Silver, P. A.; Collins, J. J.; Yin, P. Toehold switches: de-novo-designed regulators of gene expression. *Cell* 2014, 159, 925–939.

(412) Green, A. A.; Kim, J.; Ma, D.; Silver, P. A.; Collins, J. J.; Yin, P. Complex cellular logic computation using ribocomputing devices. *Nature* 2017, 548, 117–121.

(413) Pardee, K.; Green, A. A.; Ferrante, T.; Cameron, D. E.; Daleykeyser, A.; Yin, P.; Collins, J. J. Paper-based synthetic gene networks. *Cell* 2014, 159, 940–954.

(414) Mutualik, V. K.; Qi, L.; Guimaraes, J. C.; Lucks, J. B.; Arkin, A. P. Rationally designed families of orthogonal RNA regulators of translation. *Nat. Chem. Biol.* 2012, 8, 447–454.

(415) Makarova, K. S.; Haft, D. H.; Barrangou, R.; Brouns, S. J. J.; Charpentier, E.; Horvath, P.; Moineau, S.; Mojica, F. J. M.; Wolf, Y. I.;

Yakunin, A. F.; van der Oost, J.; Koonin, E. V. Evolution and classification of the CRISPR–Cas systems. *Nat. Rev. Microbiol.* **2011**, *9*, 467–477.

(416) Wiedenheft, B.; Sternberg, S. H.; Doudna, J. A. RNA-guided genetic silencing systems in bacteria and archaea. *Nature* **2012**, *482*, 331–338.

(417) Anders, C.; Niewohner, O.; Duerst, A.; Jinek, M. Structural basis of PAM-dependent target DNA recognition by the Cas9 endonuclease. *Nature* **2014**, *513*, 569–573.

(418) Szczelkun, M. D.; Tikhomirova, M. S.; Sinkunas, T.; Gasiunas, G.; Karvelis, T.; Pschera, P.; Siksnys, V.; Seidel, R. Direct observation of R-loop formation by single RNA-guided Cas9 and Cascade effector complexes. *Proc. Natl. Acad. Sci. U. S. A.* **2014**, *111*, 9798–9803.

(419) Mückl, A.; Schwarz-Schilling, M.; Fischer, K.; Simmel, F. C. Filamentation and restoration of normal growth in *Escherichia coli* using a combined CRISPRi sgRNA/antisense RNA approach. *PLoS One* **2018**, *13*, No. e0198058.

(420) Siu, K.-H.; Chen, W. Riboregulated toehold-gated gRNA for programmable CRISPR–Cas9 function. *Nat. Chem. Biol.* **2018**, DOI: 10.1038/s41589-018-0186-1.

(421) Qi, L. S.; Larson, M. H.; Gilbert, L. A.; Doudna, J. A.; Weissman, J. S.; Arkin, A. P.; Lim, W. A. Repurposing CRISPR as an RNA-guided platform for sequence-specific control of gene expression. *Cell* **2013**, *152*, 1173–1183.

(422) Lee, Y. J.; Hoynes-O'connor, A.; Leong, M. C.; Moon, T. S. Programmable control of bacterial gene expression with the combined CRISPR and antisense RNA system. *Nucleic Acids Res.* **2016**, *44*, 2462–2473.

(423) Zetsche, B.; Gootenberg, J. S.; Abudayyeh, O. O.; Slaymaker, I. M.; Makarova, K. S.; Essletzbichler, P.; Volz, S. E.; Joung, J.; van der Oost, J.; Regev, A.; Koonin, E. V.; Zhang, F. Cpf1 is a single RNA-guided endonuclease of a Class 2 CRISPR-Cas system. *Cell* **2015**, *163*, 759–771.

(424) Gootenberg, J. S.; et al. Nucleic acid detection with CRISPR-Cas13a/C2c2. *Science* **2017**, *356*, 438–442.

(425) Shipman, S. L.; Nivala, J.; Macklis, J. D.; Church, G. M. CRISPR–Cas encoding of a digital movie into the genomes of a population of living bacteria. *Nature* **2017**, *547*, 345–349.

(426) Afonin, K. A.; Viard, M.; Martins, A. N.; Lockett, S. J.; Maciag, A. E.; Freed, E. O.; Heldman, E.; Jaeger, L.; Blumenthal, R.; Shapiro, B. A. Activation of different split functionalities on re-association of RNA-DNA hybrids. *Nat. Nanotechnol.* **2013**, *8*, 296–304.

(427) Afonin, K. A.; Desai, R.; Viard, M.; Kireeva, M. L.; Bindewald, E.; Case, C. L.; Maciag, A. E.; Kasprzak, W. K.; Kim, T.; Sappe, A.; Stepler, M.; Kewalramani, V. N.; Kashlev, M.; Blumenthal, R.; Shapiro, B. A. Co-transcriptional production of RNA-DNA hybrids for simultaneous release of multiple split functionalities. *Nucleic Acids Res.* **2014**, *42*, 2085–2097.